Estimation of site index and soil properties using the topographic depth-to-water index

by

Gabriel Simion Oltean

A thesis submitted in partial fulfillment of the requirements for the degree of

Master of Science

in

Forest Biology and Management

Department of Renewable Resources
University of Alberta

Abstract

Site index is widely used as a measure of forest site productivity, and is an essential input into growth and yield models forecasting forest stand development. However, accurate estimates of site index are frequently difficult or even impossible to obtain, particularly in the boreal mixedwoods of trembling aspen (*Populus tremuloides* Michx.) and white spruce [*Picea glauca* (Moench) Voss]. Topographic indices derived from remotely sensed digital elevation models have become increasingly available and can provide information about site and soil characteristics. The depth-to-water (DTW) index measures the hydrological connectivity of any cell in the landscape with the nearest flow channel by integrating the horizontal and vertical distance between them. The central objective of this thesis was to evaluate the potential to use the DTW index to estimate site index of aspen. The first component of this study was aimed to understand the capabilities and limitations of the DTW index to map site and soil properties. The DTW index was related with soil moisture regime, drainage and depth to mottles, attributes that are closely controlled by water movement in the soil. Important edaphic characteristics, such as nutrient availability or texture, were not associated with the DTW index. The second component of this thesis examined the linkage between the DTW index and drought stress. Carbon isotope ratio, as a measure of water stress in trees, of both aspen and spruce increased with DTW until a certain point after which it levelled off, indicating that large DTW values reflect site conditions that cause water stress. Tree height and diameter followed a similar pattern with the DTW index. These first two components provided the necessary foundations to address the central objective of this thesis. Site index of aspen was significantly associated with the DTW index but model fit

statistics indicated that predictions of aspen site index based solely on the DTW index are not reliable. Throughout the thesis I also investigated the effects of flow initiation area assumptions on relationships between DTW and other variables. For the relatively flat topography of the boreal landscape a catchment area of 2 or 4 ha is recommended, whereas a threshold value of 12 or 16 ha is suggested for the stronger topographic gradients found in the foothills region. This thesis has shown that the DTW index can capture site and soil properties closely influenced by water in the soil but fails to represent nutrient availability, which limits the extent to which the DTW index can be used to estimate site index.

Preface

The digital elevation models were provided by the Government of Alberta. The geospatial data (i.e., flow direction, flow accumulation, flow channels and depth-to-water rasters) were prepared by Jae Ogilvie of the University of New Brunswick.

Chapter 2 of this thesis has been submitted and is currently under review by *Forest Science* as Oltean G.S., Comeau P.G. and White B., "Linking the depth-to-water topographic index to soil moisture on boreal forest sites in Alberta". Comeau P.G. was the supervising author and assisted with the design of the study, analysis of the data and manuscript editing. White B. contributed to manuscript edits.

To my father, Andrei Oltean

Acknowledgements

This dissertation would not be in your hands now (or on your computer screen) without the help of some great people I had the opportunity to learn from and work with during my MSc program. I will always be grateful to my supervisor, Prof. Phil Comeau, for putting his trust in me and allowing me to develop into an independent individual. Phil patiently provided support and guidance when I needed them most but also gave me the so necessary freedom and encouragement to explore various ideas and get involved in different projects. In the summer of 2013, Phil took me on an incredible trip throughout Alberta and British Columbia, teaching us about forestry and showing us the beauty of western Canada. For all these and many more, thank you, Phil!

I am very thankful to Dr. Barry White, who has been a close collaborator, suggesting the idea behind Chapter 2 and providing valuable insights at all stages of this project. He was also a key factor in securing the financial support for this project from the Government of Alberta. The statistical knowledge I gained over this period and employed in this thesis was possible thanks to Prof. Fangliang He, who also carefully reviewed my thesis. Along with Fang, I was able to explore and learn how to teach a subject loved by everyone—statistics. I would also like to thank Dr. Mike Bokalo and Prof. Ellen Macdonald who agreed to be on my committee and thoroughly evaluated my thesis.

Obviously, no data means no thesis, so I greatly appreciate the help provided by Barbora Smerekova digging all those soil pits. The geospatial data was supplied by Jae Ogilvie through

Alberta Agriculture and Forestry, while the Western Boreal Growth and Yield Association granted me access to their data and research sites. Shujie Ren and Allan Harms provided assistance with laboratory analyses for Chapter 2.

My colleagues and friends within the Forest Stand Dynamics Lab—Kirk, Derek, Valerie, Ivan, Kyu and Felix—have created a dynamic and supportive environment while being great company during the long days spent in the lab. Our group became even more active with the arrival of Vlad, who helped me with work in the field and made it possible to enjoy an entire summer spent in the office. Discussions with Erik about visual exploration of data pushed me to find more graphically expressive ways to convey the results of my statistical analyses. These are just some of the great people who have made the time I spent in the Department of Renewable Resources beneficial and enjoyable.

I deeply acknowledge the support I received from Horatiu and Raluca Muresan and their sons who accepted me in their family making it easier for me to adapt to a new place so far from home. Alina Botis was my guide in exploring Edmonton and always warmly welcomed me to her home for joyful discussions.

Finally, I would have not reached this step in my life without the moral support and understanding of my family. My parents have helped and encouraged me to pursue my dreams, even if that meant travelling across an ocean. They were the ones who bore the burden of my long time away from home. Despite the distance, my brothers kept me close and encouraged me when I was down. Thank you for your unconditional love and support.

Table of Contents

List of Tables

List of Figures

Chapter 1

General introduction

1. Introduction

Estimating the potential productivity of a forest site is important in management planning and in yield estimation. However, obtaining such estimates is not always straightforward since field measurements of tree size or assessments of soil properties are necessary. Advances in remote sensing technologies have increased the availability of accurate data and facilitated the widening of applications to forestry. This is of even greater importance when considering the vast extent of the boreal landscape, where remotely sensed data could potentially provide information about site and soil characteristics, as well as individual tree or stand level attributes.

Site productivity refers to the amount of plant biomass (i.e., wood in a forestry context) that a specific site can produce (Husch et al. 2003). It is important to distinguish between site productivity and *site quality*, the latter being an intrinsic property of the site while productivity depends on the species present on the site. Environmental factors defining site quality set an upper limit on productivity, termed potential site productivity, while species composition and management practices control the proportion that is actually achieved, realized site productivity (Skovsgaard and Vanclay 2008). Substantial alterations of resource availability (e.g., fertilization, drainage, and irrigation, or erosion, nutrient depletion, and climate change) can have strong impacts on potential, and further on realized site productivity (Burger 2009).

Assessment methods of site productivity can be grouped into geo- and phyto-centric approaches (Skovsgaard and Vanclay 2008). Geocentric methods require information about important environmental factors including, edaphic (e.g., moisture and nutrient regime, texture, temperature, pH), topographic (e.g., slope, aspect, elevation), and climatic (e.g., air temperature, precipitation, length of growing season) factors (Husch et al. 2003). The costs and difficulties associated with obtaining accurate and detailed data about these factors has limited the use of geocentric methods in practice. On the other hand, phytocentric approaches are indirect relying on measurements of trees (e.g., volume, site index) or ground vegetation (e.g., indicator species). Quantifying net primary productivity or even maximum mean annual volume increment can provide direct and appropriate estimates of realized site productivity (Husch et al. 2003). However, these data are not directly measured in the field, being frequently estimated using growth and yield models that use site index as an indicator of site productivity.

Site index (SI) is defined as the average height of dominant and codominant trees at a reference age (i.e., 50 years in Alberta). Ease of measurement, a strong correlation between volume increment and height growth and the general assumption that height of top trees is independent of stand structure (Lanner 1985) has made SI the most commonly used measure of site productivity (Skovsgaard and Vanclay 2008). SI has been employed to generate yield tables (Barnes et al. 1998) and is the key input into the growth functions of the Mixedwood Growth Model used in the boreal forest of western Canada (Bokalo et al. 2013).

Despite its wide acceptance, there are several deficiencies associated with SI. Clearly SI cannot be determined for sites which currently lack trees, or grow a species different from that for which SI was determined (Ung et al. 2001). Further, SI estimates from trees that are now dominant but have been suppressed in the past can grossly underestimate real site productivity.

This is of particular importance in the boreal mixedwoods where naturally regenerated white spruce (*Picea glauca* (Moench.) Voss.) seedlings are suppressed by trembling aspen (*Populus tremuloides* Minchx.) and other vegetation until 60 or 80 years after stand initiation (Chen and Popadiouk 2002), leading to lower estimates of spruce SI (Osika et al. 2013). Forecasting the yield of young stands requires an SI estimate of the harvested stands, which is often difficult to determine in old aspen forests where stem decay does not permit accurate determination of stand age. To overcome these limitations, numerous studies have sought to establish relationships between SI and environmental factors defining site quality (Bontemps and Bouriaud 2014).

Consistent with basic physiological theory, indicators of soil moisture and nutrient availability have been found to strongly relate with SI across species and different forest ecosystems. Soil moisture regime (SMR) was the strongest predictor of white spruce SI in British Columbia, but the model fit improved when aeration and soil nutrient regime (SNR) were added (Wang and Klinka 1996). Similarly, SMR and SNR were the factors controlling SI of coastal Douglas-fir (*Pseudotsuga menziesii* (Mirb.) Franco) (Klinka and Carter 1990). The availability of these soil attributes is partly controlled by climate, thus it is expected that climate factors will also be related to SI. A biophysical SI model integrating degree-days, water holding capacity, and an aridity index was used to predict productivity of aspen and three other species in the boreal forest of eastern Canada (Ung et al. 2001). These studies emphasize the importance of detailed and accurate soil and climate data to predict SI, but the use of such models has been restricted by the high costs associated with collecting these data (Bontemps and Bouriaud 2014).

Accurate digital elevation models (DEM) are becoming increasingly available, providing data about the morphology of the terrain, enabling calculation of topographic indices. Soil formation processes are controlled by the interactions between climate, geology, topography and

vegetation over time (Jenny 1941), creating the opportunity to use topographic indices to map soil properties. Simple indices such as slope, aspect, profile curvature were related with organic matter depth, or soil texture, but model fits were improved when a more complex index was included (Moore et al. 1993). The most widely used index is the topographic wetness index (TWI), defined as the ratio of the contributing upslope area to the local slope (Beven and Kirkby 1979). Results from use of TWI differ between applications. Linear features such as flow channels are better determined under flow routing algorithms with greater convergence (Sorensen et al. 2006), while more distributed flow worked better for broad features (Kopecky and Cizkova 2010).

Soil properties determined from terrain attributes can be used to predict site productivity, but topographic indices have also been directly employed to map SI. Iverson et al. (1997) tested, with some success, an integrated moisture index which accounts for slope, aspect, upslope area, and profile curvature to predict SI and tree species composition in hardwood stands from the US Midwest. However, this cannot be readily generalized because the relationships between SI and topographic indices can vary with species, as found in Sweden (Holmgren 1994).

The depth-to-water (DTW) index is a topographic index developed by Murphy et al. (2007) that has not been extensively studied, particularly in relationship to site productivity. Moreover, studies have shown that it can perform better than TWI when modeling soil moisture conditions (Murphy et al. 2009). The DTW index is defined as the sum of slopes along the least cost path from any cell in the raster to the nearest channel, thus it integrates both the horizontal and vertical distance from a source of water to the receiving areas downslope. The algorithm requires delineation of a flow channel network, which is obtained by calculating a flow direction and a flow accumulation area for each cell of the DEM. The extent of the flow channel network

can be controlled by the flow initiation area, which represents the catchment area necessary to form a channel. The Government of Alberta purchased highly accurate DEMs based on LiDAR (Light Detection And Ranging) point clouds, which were then used to calculate DTW rasters. Currently, these and related layers are available for 30 million ha of forested land in Alberta and are used for operational planning by the forest industry and energy sector.

2. Objectives

The central objective of this thesis was to evaluate the potential to use the extensive DTW rasters available in Alberta to estimate site index of trembling aspen in the boreal forest, which will lead to improved predictions of future yield of these stands. However, the first natural step was to explore the relationships between soil properties and DTW, and understand the limits of this index. The second step was to test the extent to which DTW can explain physiological responses of individual trees to soil conditions. These two outcomes can then be assembled to support an expected relationship between DTW and site index. Based on this rationale, I organized this thesis around three main objectives with several sub-objectives for each.

1. Explore the relationship between site and soil properties and the DTW index.
    1.1. Determine which site and soil properties are related with DTW
    1.2. Find the optimal flow initiation area
    1.3. Build models to map site and soil attributes based on topography
2. Investigate the capacity of the DTW index to explain responses of individual trees.
    2.1. Examine the relationship between carbon isotope ratio and DTW
    2.2. Find the optimal flow initiation area
    2.3. Assess the association between tree size and DTW

3. Evaluate the potential to use the DTW index to estimate site index of trembling aspen.
    3.1. Explore the response of aspen site index to site and soil attributes
    3.2. Find the optimal flow initiation area
    3.3. Develop models to predict aspen site index using topographic data

3. Thesis outline

The thesis is structured around the three main objectives, with a separate chapter devoted to each, forming the body of the thesis. These three chapters were designed as stand-alone pieces of writing, thus some points are repeated in each chapter (e.g., the DTW algorithm).

The first chapter provides the context for this study, giving a general introduction of the main topics encountered throughout the thesis. The concept and measurement of site productivity is presented, highlighting the limitations of site index as the most widely used indicator of site productivity. Some topographic indices are briefly reviewed to show how this remotely sensed information can be used to obtain information about soil properties or directly site productivity. Lastly, the main steps of the depth-to-water algorithm are briefly introduced.

The second chapter provides a description of the methods and results relevant to objective 1. The findings are discussed in the context of soil formation processes, emphasizing the limitations of the DTW index. The third chapter is focused on individual tree characteristics measured at two sites with contrasting terrain morphology and how they relate to the DTW index. Carbon isotope ratio was measured on wood samples from trembling aspen and white spruce being used as an indicator of water stress in trees. The fourth chapter addresses the central objective of my thesis, showing which site and soil properties are most closely related to SI of trembling aspen and then evaluating the potential to use topographic indices to predict SI.

The fifth chapter provides a synthesis of the main results in the context of the objectives delineated in Chapter 1, trying to pull together the findings of the three analysis chapters to identify a common theme. I formulate some general conclusions based on my results and identify major gaps in our understanding that require further work.

Literature cited

Barnes, B.V., Zak, D.R., Denton, S.R., and Spurr, S.H. 1998. Forest ecology. 4th ed. John Wiley & Sons, Inc.

Beven, K.J., and Kirkby, M.J. 1979. A physically based, variable contributing area model of basin hydrology. Hydrol. Sci. Bul. **24**(1): 43-69. doi: 10.1080/02626667909491834.

Bokalo, M., Stadt, K.J., Comeau, P.G., and Titus, S.J. 2013. The validation of the Mixedwood Growth Model (MGM) for use in forest management decision making. Forests **4**(1): 1-27. doi: 10.3390/f4010001.

Bontemps, J.-D., and Bouriaud, O. 2014. Predictive approaches to forest site productivity: recent trends, challenges and future perspectives. Forestry **87**(1): 109-128. doi: 10.1093/forestry/cpt034.

Burger, J.A. 2009. Management effects on growth, production and sustainability of managed forest ecosystems: Past trends and future directions. For. Ecol. Manag. **258**(10): 2335-2346. doi: 10.1016/j.foreco.2009.03.015.

Chen, H.Y.H., and Popadiouk, R.V. 2002. Dynamics of North American boreal mixedwoods. Environmental Reviews **10**(3): 137-166. doi: 10.1139/a02-007.

Holmgren, P. 1994. Topographic and geochemical influence on the forest site quality, with respect to *Pinus sylvestrys* and *Picea abies* in Sweden. Scand. J. For. Res. **9**(1): 75-82. doi: 10.1080/02827589409382815.

Husch, B., Beers, T.W., and Kershaw Jr., J.A. 2003. Forest mensuration. 4th ed. John Wiley & Sons, Inc., Hoboken, New Jersey.

Iverson, L.R., Dale, M.E., Scott, C.T., and Prasad, A. 1997. A GIS-derived integrated moisture index to predict forest composition and productivity of Ohio forests (USA). Landsc. Ecol. **12**(5): 331-348. doi: 10.1023/a:1007989813501.

Jenny, H. 1941. Factors of soil formation: a system of quantitative pedology. McGraw-Hill, New York, NY. pp. 11-12.

Klinka, K., and Carter, R.E. 1990. Relationships between site index and synoptic environmental-factors in immature coastal Douglas-fir stands. For. Sci. **36**(3): 815-830.

Kopecky, M., and Cizkova, S. 2010. Using topographic wetness index in vegetation ecology: does the algorithm matter? Appl. Veg. Sci. **13**(4): 450-459. doi: 10.1111/j.1654-109X.2010.01083.x.

Lanner, R.M. 1985. On the insensitivity of height growth to spacing. For. Ecol. Manag. **13**(3-4): 143-148. doi: 10.1016/0378-1127(85)90030-1.

Moore, I.D., Gessler, P.E., Nielsen, G.A., and Peterson, G.A. 1993. Soil attribute prediction using terrain analysis. Soil Sci. Soc. Am. J. **57**(2): 443-452. doi: 10.2136/sssaj1993.03615995005700020026x.

Murphy, P.N.C., Ogilvie, J., and Arp, P. 2009. Topographic modelling of soil moisture conditions: a comparison and verification of two models. Eur. J. Soil Sci. **60**(1): 94-109. doi: 10.1111/j.1365-2389.2008.01094.x.

Murphy, P.N.C., Ogilvie, J., Connor, K., and Arpl, P.A. 2007. Mapping wetlands: A comparison of two different approaches for New Brunswick, Canada. Wetlands **27**(4): 846-854. doi: 10.1672/0277-5212(2007)27[846:mwacot]2.0.co;2.

Osika, D.E., Stadt, K.J., Comeau, P.G., and MacIsaac, D.A. 2013. Sixty-year effects of deciduous removal on white spruce height growth and site index in the Western Boreal. Can. J. For. Res. **43**(2): 139-148. doi: 10.1139/cjfr-2012-0169.

Skovsgaard, J.P., and Vanclay, J.K. 2008. Forest site productivity: a review of the evolution of dendrometric concepts for even-aged stands. Forestry **81**(1): 13-31. doi:

10.1093/forestry/cpm041.

Sorensen, R., Zinko, U., and Seibert, J. 2006. On the calculation of the topographic wetness index: evaluation of different methods based on field observations. Hydrol. Earth Syst. Sci. **10**(1): 101-112.

Ung, C.H., Bernier, P.Y., Raulier, F., Fournier, R.A., Lambert, M.C., and Regniere, J. 2001. Biophysical site indices for shade tolerant and intolerant boreal species. For. Sci. **47**(1): 83-95.

Wang, G.G., and Klinka, K. 1996. Use of synoptic variables in predicting white spruce site index. For. Ecol. Manag. **80**(1-3): 95-105. doi: 10.1016/0378-1127(95)03630-x.

Chapter 2

Linking the depth-to-water topographic indices to soil properties on boreal forest sites in Alberta

Abstract

The depth-to-water (DTW) index is defined as the cumulative slope along the least-cost pathway from any cell in the landscape to the nearest flow channel. The flow channel network is determined by the flow initiation area selected, allowing the representation of various geological and topographical attributes of the landscape. We used data from 125 plots across five locations in the boreal forest of Alberta, Canada, to evaluate (1) the relationships between soil attributes and DTW, (2) the optimal flow initiation area, and (3) models to map the spatial variation of soil properties. Soil moisture regime (SMR), drainage class and depth-to-mottles were strongly related with DTW, whereas soil nutrient regime, organic matter thickness, soil texture and coarse fragments content exhibited weak and inconsistent relationships with DTW. A flow initiation area of 2 ha yielded the best representation for SMR, drainage class and depth-to-mottles. DTW, flow accumulation (FA) and local slope were combined in a linear model to estimate and map SMR, whereas only DTW and FA were used to model drainage and depth-to-mottles. These results suggest that the DTW index can capture soil properties closely influenced by the water table but cannot characterize site and soil factors which are also determined by parent material, climate and vegetation.

1. Introduction

Site and soil properties interact with climate to define forest site productivity, a key input for sustainable forest management and conservation applications. Numerous studies have sought to establish relationships between various soil properties and site productivity in order to overcome challenges associated with using tree height (e.g., site index) to characterize productivity (Bontemps and Bouriaud 2014). Several studies have indicated that soil moisture and nutrient regime are associated with site index of Douglas-fir (Klinka and Carter 1990), western redcedar (Kayahara et al. 1997), trembling aspen (Chen et al. 2002), or white spruce (Wang and Klinka 1996). Other studies have also tested, with limited success, soil aeration (Gale et al. 1991), mineral soil pH and C:N ratio (Kayahara et al. 1995), or a water holding capacity index that integrates coarse fragments content, depth of the B and C soil horizons and textural classes (Ung et al. 2001). The potential applicability of these models would be greatly enhanced if such soil properties could be predicted from remotely-sensed data.

Accurate digital elevation models (DEM) which provide valuable information about the morphology of the terrain are becoming increasingly available for large forested areas. Since topography controls soil formation processes at a relatively fine scale (e.g., hillslope, sub-watershed), DEMs can provide information at appropriate resolutions for mapping mesoscale variation in major soil properties (Major 1951; Moore et al. 1991). The topographic wetness index (TWI) proposed by Beven and Kirkby (1979) and defined as the ratio of the contributing area to the local slope has been widely used to estimate soil wetness from DEM data. The TWI has also been named the topographic convergence index, soil wetness index or compound topographic index. Simpler indices such as landscape position, potential solar radiation and exposure have also been employed in studies of vegetation gradients (Allen et al. 1991), while

flow accumulation, local shape of the terrain and water-holding capacity were combined by Iverson et al. (1997) to derive an integrated moisture index used to map the composition and productivity of oak forests.

The TWI has been tested in a large number of applications across a variety of landscapes. Moore et al. (1993) found that TWI and other terrain attributes (e.g., slope, profile curvature) explained up to 64% of the variation in A horizon depth, organic matter, extractable phosphorus, and sand and silt proportion. Hillslope hollows can raise water table levels by increasing subsurface lateral flow, thus adding a measure of local plane convexity to TWI was found to improve prediction of soil saturation (Burt and Butcher 1985). The relationship becomes poor if soil moisture is measured at a finer scale with electromagnetic sensors due to the micro-scale variation that cannot be captured by a topographic index (Iverson et al. 2004). In contrast to previous studies that were conducted within homogenous watersheds with strong topography, Seibert et al. (2007) reported significant associations between a series of physical and chemical soil properties and TWI in the flat landscape of the Swedish boreal forest. Their results showed the strongest correlations with variables measured in the organic horizon, suggesting that terrain morphology has a greater influence on soil surface processes while attributes of deeper horizons are more closely controlled by parent material. Moreover, different algorithms for calculating TWI are better suited for particular landscapes and applications. TWI calculated using a more distributed flow routing algorithm (e.g., FD8) worked better for locating forested wetlands (Lang et al. 2013) and other broad features (Kopecky and Cizkova 2010; Petroselli et al. 2013), whereas the determination of linear features (e.g., flow channels) is more consistent under algorithms with greater flow convergence (e.g., D8, D∞) (Sorensen et al. 2006; Tarboton 1997).

The depth-to-water (DTW) index, proposed by Murphy et al. (2007), considers the effect

of both the horizontal and vertical distance from any cell in the landscape to the nearest flow channel. The DTW and accessory (i.e., flow accumulation, flow channel network) data have been adopted by the Government of Alberta and are being used to guide forest operations for an area of approximately 30 million hectares. Studies indicated the superiority of DTW over TWI for mapping wet areas in the boreal forest (Murphy et al. 2009) and also in the riparian forests of the tropical zone (Maillard and Alencar-Silva 2013). Since DEM resolution and landscape variations have a larger influence on TWI values, soil moisture regime was more accurately predicted by DTW than TWI in a study from the boreal forest of Sweden (Ågren et al. 2014). Relationships between a suite of soil variables and DTW were also reported by Murphy et al. (2011), who noted that TWI can complement, at least in certain areas, the information provided by DTW. The DTW algorithm requires the delineation of flow channel networks, the extent of which can be controlled by adjusting the flow initiation area in order to simulate general changes in soil moisture (e.g. wet or dry year, early or late season conditions). The general consensus is that a flow initiation area of 4 ha would be suitable to represent wetness conditions late in the season and stream channels with permanent or intermittent flow (White et al. 2012). Therefore, most studies have focused on this threshold (Murphy et al. 2009; Murphy et al. 2011). However, Ågren et al. (2014) reported that flow initiation area must be adjusted based on the hydraulic conductivity of the terrain. These results support further testing of different threshold values to evaluate the capabilities and limitations of the DTW index.

The availability of depth-to-water rasters and the necessity to estimate key site and soil properties that influence productivity, silviculture, and harvesting in the boreal forest require a clear understanding of the limitations of DTW to predict these soil attributes. Furthermore, the effect of different flow initiation areas on the relationship between DTW and soil properties is

not clearly understood and optimal thresholds have not been proposed. The objectives of the study presented in this paper were (1) to explore relationships between soil properties and depth-to-water, (2) to find an optimal flow initiation area, and (3) to develop and demonstrate application of empirical models capable of mapping the spatial variation of soil attributes using only remotely-sensed data. We hypothesize that depth-to-water will show stronger associations with water-related soil properties than with other physical attributes (e.g., coarse fragments content, texture), and that a smaller flow initiation area will better capture the effects of topography on soil moisture.

2. Materials and methods

2.1. Study sites

Soil and site data were collected at five areas located in the Central Mixedwood natural subregion of the boreal forest of northern Alberta (Fig. 2.1, Table 2.1). Four of these sites are part of a long-term study established between 1991 and 1992 by the Western Boreal Growth and Yield Association (WESBOGY) to study the development of aspen and spruce mixtures (Bokalo et al. 2007), while the Judy Creek (JC) research site was established in 2003 to evaluate selected strategies for establishment of intimate mixtures (Pitt et al. 2010). Glacial erosion has shaped the fine textured glacial till deposits to define the geomorphology of the region. The parent material at JC is similar but presents a layer of rounded cobble at about 25 – 40 cm, indicating the effect of postglacial fluvial activity. The terrain of the studied areas has gentle slopes (0 – 10%) and elevational differences between the plots at one location ranging from 3 m at SRD (area of 16 ha) to 14 m at JC (area of 18 ha). This lack of strong topographic gradients reduces the control of relief on soil formation processes, thus decreasing the performance of topographic indices to

Table 2.1. Summary of the geographic position and climate for the five study locations: Judy Creek (JC), Weyerhaeuser Grande Prairie (WGP), Alberta Sustainable Resource Development (SRD), Daishowa-Marubeni International (DMI), Hines Creek (HC), Peace River (PR). MAT – mean annual temperature, MST – mean summer temperature, MAP – mean annual precipitation, MSP – mean summer precipitation (summer is defined as May – August).

Study area	Plots	Latitude (°)	Longitude (°)	Elevation (m)	MAT* (°C)	MST* (°C)	MAP* (mm/yr)	MSP* (mm /summer)	Weather Canada station
JC	37	54.3826	−115.6398	1002.09	2.88	13.58	544.42	334.56	Whitecourt A
WGP	30	54.8864	−118.9393	701.11	2.35	13.40	478.23	243.60	Grovedale RS
SRD	20	55.2982	−114.0982	622.39	2.05	13.59	480.63	288.54	Slave Lake A
DMI_HC	18	56.3992	−118.6029	795.69	0.04	12.58	436.24	251.43	Eureka River
DMI_PR	20	56.4071	−117.7777	731.43	1.55	13.88	386.34	215.37	Peace River A

*data extracted from "1981 - 2010 Canadian Climate Normals" available at http://climate.weather.gc.ca accessed on July 10, 2014.

predict soil attributes.

The climate of this area is characterized by long cold winters and warm summers with mean annual temperature of 1.5 °C and total precipitation of 389 mm, while summer (i.e., May – August) has mean temperature of 13.7 °C and receives 60% of the total precipitation (Beckingham and Archibald 1996). The site at JC is the warmest (2.9 °C) but receives the most precipitation (544 mm) whereas DMI_PR is the driest (386 mm) and DMI_HC has the lowest mean annual temperature (0 °C). The majority of the soils developed in these five areas fall in the Great Group of gray luvisols, diagnosed by a clay accumulation horizon (i.e., Bt) with fine texture, while some soils are better developed, with a higher pH, classified as eutric brunisols. The woody vegetation of the Central Mixedwood subregion consists mainly of mixtures of white spruce (*Picea glauca* (Moench) Voss) and trembling aspen (*Populus tremuloides* Michx.), but lodgepole pine (*Pinus contorta* Douglas) and black spruce (*Picea mariana* Mill.) can be found on drier raised sites and wetter depressions, respectively.

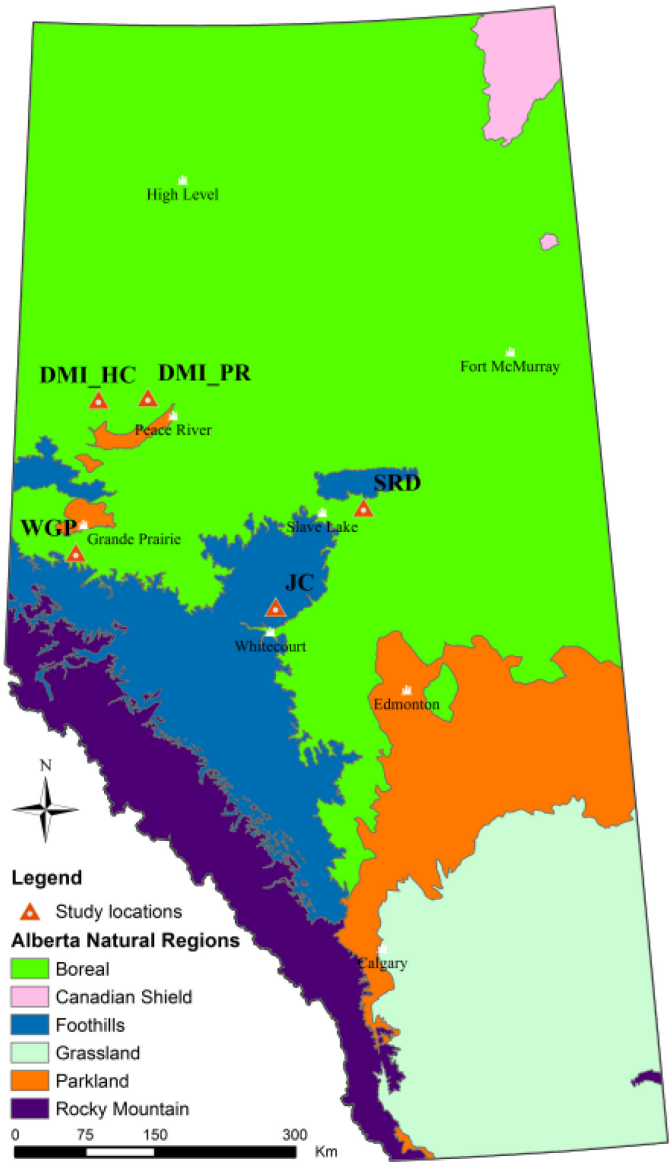

Figure 2.1. Location of the five study areas in the Boreal natural region of Alberta (AESRD 2005).

2.2. Field assessments

During the summer of 2013, 125 plots were sampled across the five study sites as shown in Table 2.1. The size of the plots assessed at the WESBOGY sites is 20 m by 20 m with a 5 m buffer on each side, while 12 plots at JC are 35 x 35 m and the other 25 plots are 45 x 45 m. The geographic location of the plots was recorded with a Trimble GeoExplorer 6000 series GeoXT handheld device (Trimble, Los Altos, California) with GNSS capabilities (the Global Navigation

Satellite System combines the GPS, GLONASS and Galileo systems) that, under clear sky conditions, assured sub-meter accuracy. Site reconnaissance, assessment of understory species composition and the excavation of a soil pit were conducted according to the methodology described in Beckingham and Archibald (1996). Slope and aspect were measured using a clinometer and a compass, respectively, while the field guide was used to determine plant species composition. A soil pit limited by the C horizon (i.e., 55 to 90 cm) was dug in the center of each plot and thickness of the organic matter, humus form, effective texture (i.e., texture of the finest textured horizon at least 10 cm thick located 20 – 60 cm below the mineral soil surface), depth-to-mottles (DtMot), coarse fragments content and drainage class (imperfect, moderately well, well) were determined. Drainage regime was determined based on features of the organic matter horizon and mottling layer together with texture of the mineral soil horizon.

Site-level information (i.e., topographic position, aspect, slope and primary water source) was used together with information on effective texture, drainage class, and organic matter thickness to determine soil moisture regime (SMR) and soil nutrient regime (SNR) as described by Beckingham and Archibald (1996). Thus, these measures of SMR and SNR integrate the spatial and temporal effect of all environmental variables that control moisture conditions and nutrient richness of the plots. The gradient of moisture regimes covered by our plots was limited to subhygric – mesic – submesic, sites most suitable for spruce-aspen mixedwoods. *Subhygric* sites were found on lower slight slopes that are receiving water from precipitation and through seepage and which are imperfectly to moderately well drained favoring the accumulation of organic material. Sites on midslopes where precipitation is the main source of water and soils have better drainage with a thinner organic layer were considered *mesic*. Sites located on upper slopes were defined as *submesic* and showed rapid to well drainage and organic matter thickness

was shallower.

Additionally, four microclimate stations were installed in selected plots at each of the four WESBOGY sites to measure volumetric water content (VWC) and soil temperature (Tsoil) across the entire range of soil moisture present at each site. A total of 16 S-SMD-M005 10HS moisture sensors and E348-S-TMB-M006 temperature sensors were placed at 15 cm depth in the soil and were connected to a HOBO U30 datalogger (Onset Computer Corporation, Bourne, MA, USA). The length of the soil moisture sensor (i.e., 10 cm) permitted the sampling of a soil volume of about 1000 cm^3 while the temperature sensor only measured around 125 cm^3 of soil. However, some of the stations were damaged by wildlife (e.g., bear, deer) and we could only use the data collected from between 9 and 11 stations during June, July and August of 2013.

2.3. The model for the depth-to-water index

The depth-to-water (DTW) index, measured in meters, is the sum of slopes along the least-cost path from any cell in the landscape to the nearest flow channel, expressed as

$$DTW = \left[\sum \frac{dz_i}{dx_i} a \right] x_c(m),$$

where dz_i and dx_i are the vertical and horizontal distance between two cells, respectively, a is a constant equal to 1 if the path that connects two cells is parallel to the cell boundaries and $\sqrt{2}$ if it connects the cells diagonally, and x_c is the size of the raster cell. Thus, a cell farther or at higher elevation from a flow channel will have a larger DTW value and is considered to be less hydrologically connected (i.e., drier) with the flow channel (Murphy et al. 2009).

The airborne LiDAR (Light Detection and Ranging) point cloud used to generate the digital elevation model (DEM) for the study sites had between 0.5 and 3 returns per square

meter with vertical accuracy of 30 cm at 95% confidence interval. The 1 m resolution DEM was hydrologically conditioned to remove false depressions that obstruct water flow in order to determine flow direction based on the slope to the eight neighboring cells and flow accumulation (FA). The D8 single direction algorithm, which directs flow from each cell to one adjacent cell with the steepest downslope gradient (O'Callaghan and Mark 1984), was used since a dispersive flow direction algorithm (e.g., D∞) provides little improvement over D8 (Murphy et al. 2009). The FA value for a particular raster cell represents the number of 1 m^2 cells that divert flow to that cell, hence defining the area from which water is collected in any cell of the raster. Flow channels start in the cell for which FA meets the chosen threshold for the flow initiation area. We used threshold values of 0.5, 1, 2, 4, 8, 12 and 16 ha to define the flow channels based on which the iterative function can calculate the DTW raster. To further illustrate the variation of the DTW index across the landscape, a diagram of the DMI_PR area shows the terrain and the DTW (belowground thick line) calculated at 2 ha flow initiation area in Fig. 2.2. Note that DTW is 0 m in the flow channels and it integrates both horizontal and vertical distance from any cell to the flow channel; a cell located 1 m higher and 150 m away from a channel receives a DTW value of 3.06 m, whereas with the same horizontal distance but a 6 m difference in elevation the DTW value doubles to 6.33 m.

2.4. Statistical analysis

Linear mixed-effects models were used to explore relationships between the response and the predictor variables, except for DtMot where we used a nonlinear mixed model of the form $f(x) = ax^b$. Site and soil properties (i.e., SMR, drainage, DtMot, SNR, organic matter thickness, coarse fragments content, and effective texture) were treated as continuous dependent variables sampled from normally distributed populations. In the analysis of DtMot we only used the plots

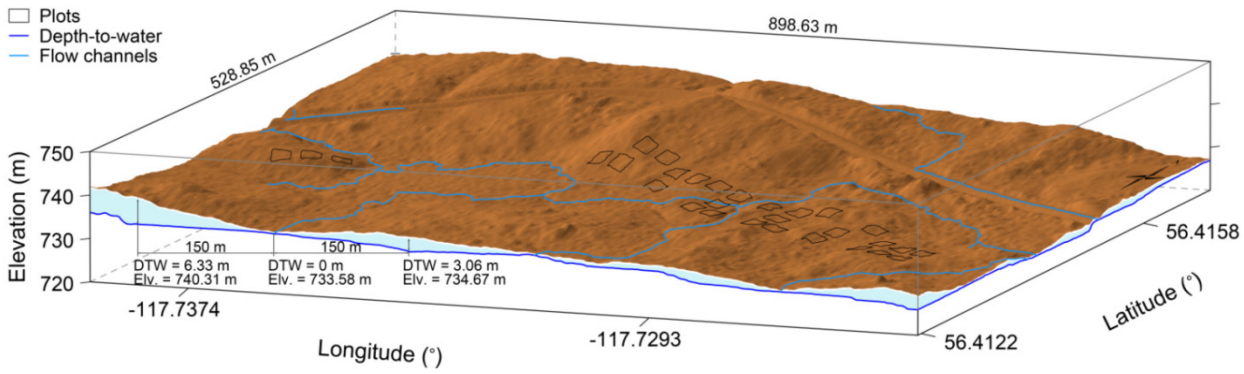

Figure 2.2. Perspective view and cross-section of the DMI_PR study site with the flow channels and DTW index calculated at 2 ha flow initiation area. The area of 47.5 ha has a minimum elevation of 725 m in the NE corner and a maximum of 741 m in the SW corner. See text (2.3.) for interpretation of the DTW values shown on the diagram.

where the mottling layer was found and the actual depth-to-mottles could be measured (n = 72). The average DTW, FA and slope were calculated and extracted for each of the 125 plots with ArcGIS 10.1 (ESRI, Redlands, California) and used as independent variables to explain variation in the site and soil attributes. We used buffer areas of 1 m radius around the microclimate stations to calculate DTW and FA averages because preliminary analyses with radii of 1, 2, 3, 4, 5 and 10 m did not suggest a scale effect and the reported accuracy based on the geographic data collected is <1 m for 84% of the positions. Logarithm in base 10 was applied to FA and the transformed values were used in the analysis to ensure linear relationships.

The random factor in the mixed-effects model was considered to be the site location since the SRD site was generally drier and the WGP was classified as the wettest while the three other sites had both dry and wet plots. Likelihood ratio tests were used to select the optimal structure for the random effects. In the case of SMR, the intercept and slope were allowed to vary from site to site within a multiple of identity variance-covariance matrix (Pinheiro and Bates 2000) that constrains the random effects to be independent and have the same variance. A random effect was used for parameter *a* when modeling DtMot, while all the other soil properties were

modeled with a random intercept only. The structure of the random effects can be simplified when significant covariates enter the model (Pinheiro and Bates 1995), thus the final models will either have different random effects structure described in section 3.3 or no random effects. Visual examination of the diagnostic plots for the final models revealed that the variance of the errors differed between location, therefore a variance function that calculates different weights for each study site was used. The variance parameter for one site was fixed at 1 for identifiability (Pinheiro and Bates 2000). The structure of the variance function differed between models and it is presented in section 3.3.

The fixed effects parameters, variance components and functions were estimated using the restricted maximum likelihood method for the linear models while the computational complexity of the nonlinear equation used for DtMot restricted us to the method of maximum likelihood. Thus, the traditional coefficient of determination (i.e., R^2) could not be used to assess the strength of the relationships and compare among models. Instead, we used a generalized R^2 defined as

$$R^2_{LR} = 1 - \left[\frac{L(0)}{L(\hat{\beta})}\right]^{\frac{2}{n}} = 1 - \exp\left\{-\frac{2}{n}\left[l(\hat{\beta}) - l(0)\right]\right\},$$

where n is the sample size, and $l(0) = \log L(0)$ and $l(\hat{\beta}) = \log L(\hat{\beta})$ represent the log-likelihoods of the null and the fitted model, respectively (Cox and Snell 1989; Maddala 1983; Magee 1990). This measure of fit (i.e., R^2_{LR}) is consistent with classical R^2 defined in the context of simple linear regression but it fails to achieve the maximum of 1 for models where the likelihood is calculated as a product of probabilities. Nagelkerke (1991) calculates this maximum for R^2_{LR} and proposes the following definition

$$\overline{R}^2_{LR} = \frac{R^2_{LR}}{\max\left(R^2_{LR}\right)},$$

$$\text{where } \max\left(R^2_{LR}\right) = 1 - L(0)^{\frac{2}{n}} = 1 - \exp\left\{\frac{2}{n} l(0)\right\}.$$

To compare the predictive power of the DTW index calculated at the seven flow initiation areas, the $\overline{R}^2_{LR}$ values in Table 2.2 were calculated against a null model that included the same random effect structure to ensure that it reflects only the additional model improvement given by the fixed effect. The $\overline{R}^2_{LR}$ values reported for the final models in section 3.3 and Table 2.3 were calculated using a simple mean model with no random effects.

The covariates included in the final models were selected based on conditional or Wald-type t-tests and model parsimony was ensured using Akaike weights. Multicollinearity was avoided because there was not a clear pattern between DTW and FA or slope and the correlation coefficients were relatively low (DTW vs. $\log_{10}$(FA): r = −0.39; DTW vs. slope: r = 0.40; $\log_{10}$(FA) vs. slope: r = −0.18). The validity of the normality assumption on the errors was confirmed by visual examination of Q-Q plots and formal hypothesis testing with the Shapiro-Wilk test. All mixed-effects models were fit using version 3.1-117 of the nlme library (Pinheiro and Bates 2000; Pinheiro et al. 2015) implemented in the R environment, version 3.1.0 (R Core Team 2015). A significance level of $\alpha = 0.05$ was used for all statistical tests.

3. Results

3.1. Site and soil properties in relation to terrain attributes

Soil moisture regime, drainage class and depth-to-mottles were the site and soil attributes most strongly ($\overline{R}^2_{LR} > 0.16$) and significantly ($P < 0.0001$) associated with plot averages of DTW,

FA and slope, whereas SNR, the thickness of the organic layer, the percentage of coarse fragments and effective texture did not show strong relationships ($\overline{R}^2_{LR} < 0.11$) with any of the topographic characteristics (Table 2.2). Soil wetness, as described by SMR, drainage and DtMot, was negatively related to DTW (Fig. 2.3) and terrain slope while FA showed the opposite trend (i.e., plots with large FA were wetter). Model estimates indicated that DTW (calculated at 2 ha) values of 1.10, 2.29 and 4.45 m corresponded to subhygric, mesic and submesic conditions, respectively. Plots characterized with poor SNR were found at lower DTW while medium and rich plots were associated with higher DTW values. No clear pattern was found between organic matter thickness, coarse fragments content or effective texture and any of the terrain attributes.

Monthly averages for June, July and August of volumetric water content and soil temperature were significantly related to DTW (not shown)—explaining 30 to 50% of the variation in the data—but did not show any trend with FA (not shown). Volumetric water content was negatively related with DTW, soils with low water content were found on plots with high DTW, and low DTW values were associated with cold soils. However, the small sample sizes (i.e., 9 – 11 observations) reduce the reliability of goodness of fit statistics, and limit the strength of our inferences.

3.2. Optimal flow initiation area

Depth-to-water calculated at a flow initiation area of 2 ha was the strongest predictor of soil moisture regime, drainage class and depth-to-mottles. However, threshold areas of 1, 2, 4 or 12 ha showed limited degree of association with the other soil properties (Table 2.2 – boldfaced values). When flow initiation area was lowered or increased from 2 ha, the relationships between DTW and SMR, drainage and DtMot became weaker. The spatial effect of changing flow

Table 2.2. Generalized coefficient of determination and statistical significance of the models that describe the relationships between soil properties and depth-to-water calculated at different flow initiation areas, flow accumulation and local slope. The boldfaced values show the strongest relationships across the seven variants of DTW. Depth to mottles was modeled using a power function of the form $f(x) = ax^b$ and the associated *P*-values for the two parameters are reported.

		Flow initiation area used to calculate depth-to-water							$\log_{10}$(FA)	Slope
		0.5 ha	1ha	2 ha	4 ha	8 ha	12 ha	16 ha		
Soil moisture regime	$\overline{R}^2_{LR}$	0.09	0.14	**0.16**	0.12	0.09	0.05	0.05	0.13	0.06
	P-val	0.0001	<.0001	**<.0001**	<.0001	0.0010	0.0275	0.0275	<.0001	0.0069
Drainage class	$\overline{R}^2_{LR}$	0.15	0.19	**0.30**	0.18	0.17	0.02	0.02	0.19	0.05
	P-val	<.0001	<.0001	**<.0001**	<.0001	<.0001	0.1311	0.1314	<.0001	0.0231
Depth-to-mottles	$\overline{R}^2_{LR}$	0.28	0.17	**0.42**	0.26	0.21	0.13	0.13	0.28	0.04
	P-val (a)	<.0001	<.0001	**<.0001**	<.0001	<.0001	<.0001	<.0001	<.0001	<.0001
	P-val (b)	<.0001	0.0006	**<.0001**	0.0001	0.0001	0.0018	0.0018	<.0001	0.0009
Soil nutrient regime	$\overline{R}^2_{LR}$	0.06	**0.06**	0.01	0.02	0.02	0.02	0.02	0.09	0.02
	P-val	0.0218	**0.0170**	0.3511	0.2242	0.1912	0.1528	0.1543	0.0035	0.2273
Organic matter thickness	$\overline{R}^2_{LR}$	0.00	0.00	**0.01**	0.00	0.00	0.00	0.00	0.01	0.01
	P-val	0.4627	0.6286	**0.2480**	0.9081	0.5453	0.4153	0.4144	0.4141	0.3489
Coarse fragments content	$\overline{R}^2_{LR}$	0.00	0.00	0.00	0.02	0.04	**0.08**	0.08	0.00	0.02
	P-val	0.9952	0.8821	0.4598	0.0978	0.0144	**0.0004**	0.0004	0.5311	0.1684
Effective texture	$\overline{R}^2_{LR}$	0.00	0.00	0.01	**0.11**	0.10	0.07	0.07	0.02	0.01
	P-val	0.9685	0.8016	0.4185	**0.0002**	0.0005	0.0025	0.0025	0.2169	0.2593

initiation area is shown in Fig. 2.4 where one can note that at 0.5 ha a dense channel network is constructed ($L_{channels}$ = 6445.7 m) and consequently a larger area has low DTW values ($A_{DTW<1}$ = 29.3 ha of the 47.5 ha), whereas at 16 ha only 1857.4 m of flow channels are delineated with only 12.49 ha below 1 m. An intermediate area of 2 ha identifies a channel network of 3458.4 m with 19.7 ha under 1m DTW. Threshold areas of 12 and 16 ha yielded similar results both spatially (Fig. 2.4) and statistically (Table 2.2).

Although statistically significant, the relationships between DTW at different flow

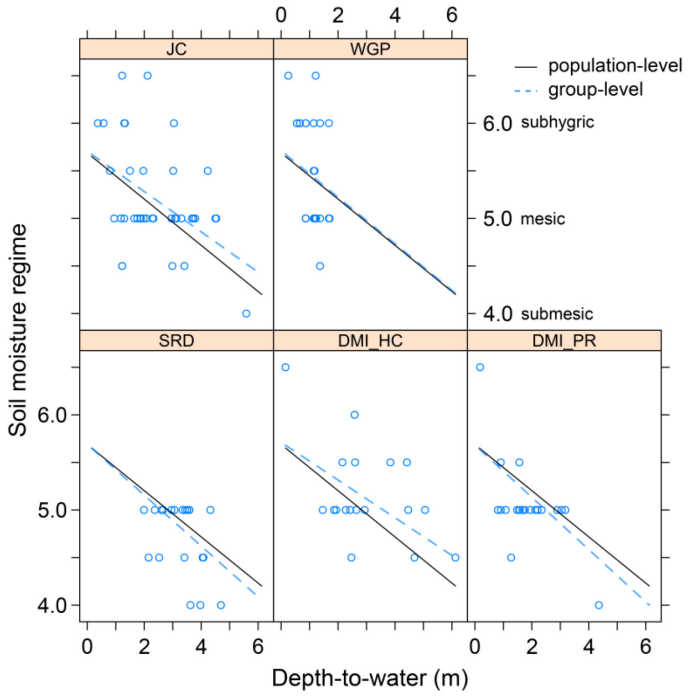

Figure 2.3. Soil moisture regime in relation to depth-to-water calculated using a flow initiation area of 2 ha shown by location. The solid line represents the population-average model while the dashed line shows how the random effect for the intercept and slope affects the linear model parameters at each location.

initiation areas and the other soil characteristics were not strong ($\overline{R}^2_{LR} < 0.11$) and the pattern of gradual decrease in $\overline{R}^2_{LR}$ with larger or smaller flow initiation areas cannot be observed. Moreover, visual assessments of scatterplots revealed that the linear relationships between these soil properties and DTW are either driven by a few points or even change slope direction at different flow initiation thresholds.

3.3. Modeling significant site and soil properties

Soil moisture regime was initially modeled linearly with DTW, calculated at a flow initiation area of 2 ha, as fixed effect and random intercept and slope by location. Once $\log_{10}$(FA) and slope were introduced, the random effects did not contribute significantly to the model and were consequently dropped from the model. Because the variances of SRD and DMI_PR as well as those of JC and WGP were similar, these sites were aggregated into two groups, while the

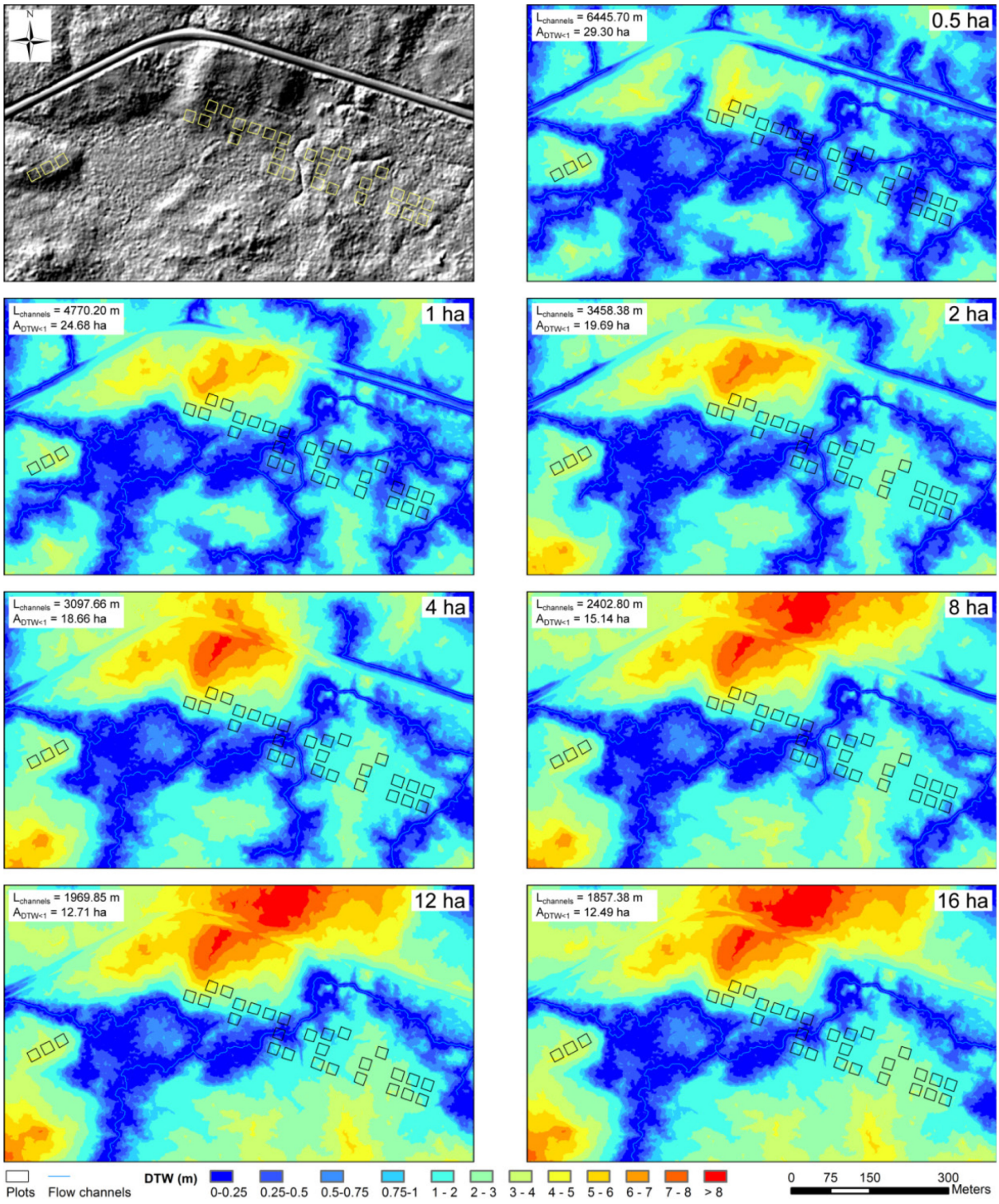

Figure 2.4. The depth-to-water raster and flow channels calculated at flow initiation areas of 0.5, 1, 2, 4, 8, 12, and 16 ha illustrated for the DMI_PR study site. The top-left image represents a hillshade view of the DEM raster to facilitate identification of landscape features (e.g., raised and low-lying areas, the road). The 20 x 20 m rectangles are the 30 plots established at this WESBOGY site. $L_{channels}$ – length of the flow channels identified in the area; $A_{DTW<1}$ – area of terrain with DTW < 1 m.

variance parameter of DMI_HC was set to 1. The final equation was of the form

$$SMR_{ij} = \beta_0 + \beta_1 DTW_{ij} + \beta_2 \log_{10}(FA_{ij}) + \beta_3 Slope_{ij} + \varepsilon_{j(i)} \quad \text{(Eq. 2.1)}$$

where SMR_{ij} was the observation in the jth plot nested in location i, β_0, β_1, β_2 and β_3 represented the intercept and coefficients of DTW, FA and slope, respectively. The errors were assumed to be independent and identically distributed (i.i.d.) as $\varepsilon_{j(i)} \sim N(0, \sigma^2 \delta_i^2)$ where σ^2 was the error variance and δ_i the variance parameter. This model provided a $\overline{R}^2_{LR}$ of 0.43 against a simple mean model and was exemplified for the DMI_PR location to produce the map in Fig. 2.5.

Drainage regime was at first modeled as a function of DTW at 2 ha with a location-level random effect for the intercept. Adding $\log_{10}$(FA) to the model significantly increased the value of the likelihood function but did not affect the significance of the random effect, while slope did not improve the fit of the model significantly (P = 0.1627) and hence was not included. The variance parameter of SRD was set to 1 while DMI_HC was grouped with DMI_PR and JC with WGP. This model was described by the following equation

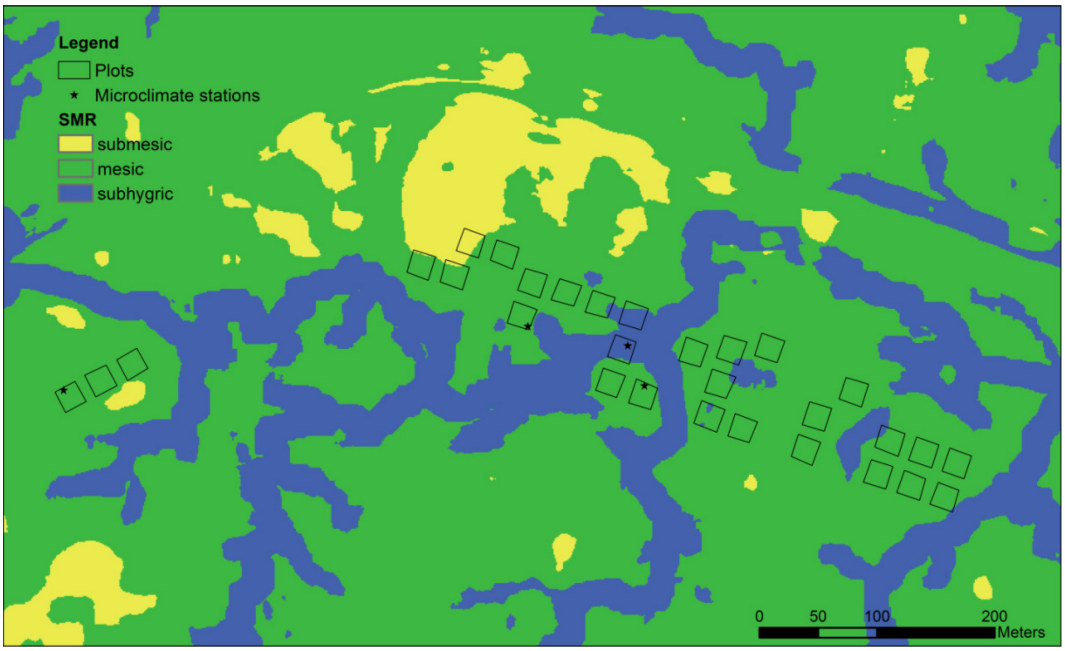

Figure 2.5. Map of the DMI_PR area showing soil moisture regime calculated using Eq. 2.1.

$$Drainage_{ij} = (\beta_0 + b_i) + \beta_1 DTW_{ij} + \beta_2 \log_{10}(FA_{ij}) + \varepsilon_{j(i)} \quad \text{(Eq. 2.2)}$$

where $Drainage_{ij}$ was the jth observation at location i, β_0, β_1 and β_2 indicated the intercept and coefficients of DTW and FA, respectively. The random effects b_i were assumed to be normally distributed as $b_i \sim N(0, \sigma_b^2)$, where σ_b^2 was the variance component, and the residuals to be i.i.d. as $\varepsilon_{j(i)} \sim N(0, \sigma^2 \delta_i^2)$, where σ^2 was the error variance and δ_i the variance parameter. A $\overline{R}_{LR}^2$ of 0.62 was obtained for this model which is illustrated in Fig. 2.6.

To model depth to mottles we used a power function of the form $f(x) = ax^b$, where x was DTW at 2 ha and a random effect was allowed on parameter a. Subsequently, the estimated best linear unbiased predictors (i.e., estimated location-level random effects) were linearly related with $\log_{10}$(FA) and the random effect dropped. Slope did not explain variation in DtMot. A variance function was not required. The resulting equation was

$$DtMot_{ij} = [\beta_{a0} + \beta_{a1} \log_{10}(FA_{ij})] * DTW^{[\beta_{b0} + \beta_{b1} \log_{10}(FA_{ij})]} + \varepsilon_{j(i)} \quad \text{(Eq. 2.3)}$$

where $DtMot_{ij}$ was the jth measurement at study site i, β_{a0}, β_{a1} were the intercept and slope used to derive parameter a while β_{b0}, β_{b1} were the intercept and slope needed to calculate parameter b

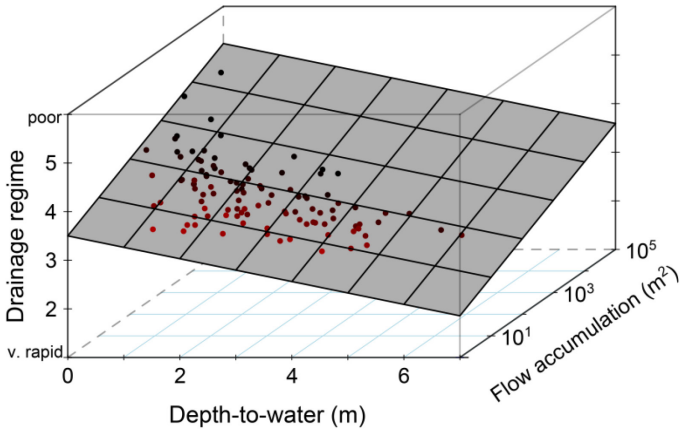

Figure 2.6. The geometric plane that illustrates the relationship between drainage regime, depth-to-water calculated at 2 ha flow initiation area and flow accumulation as defined by Eq. 2.2. Note that the points on the plot are the fitted values and not the raw observations.

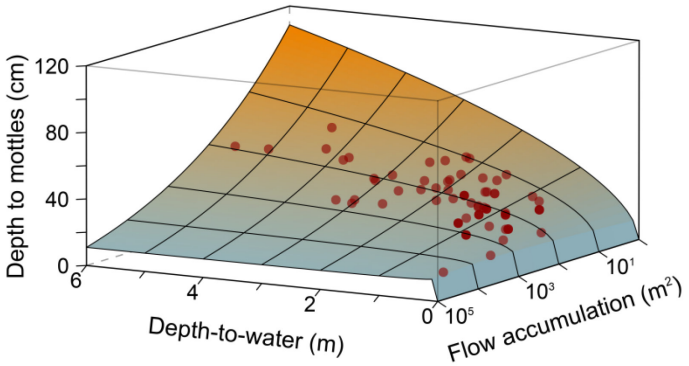

Figure 2.7. The shaded surface indicates the relationship between depth to mottles, depth-to-water calculated at flow initiation are of 2 ha and flow accumulation as determined by Eq. 2.3. Note that the points on the graph are the fitted values.

of the power function. The error terms were assumed to be i.i.d and $\varepsilon_{j(i)} \sim N(0, \sigma^2)$, where σ^2 was the variance of the residuals. The $\overline{R}^2_{LR}$ yielded from this model was 0.63 with Fig. 2.7 showing the surface generated by it. The residual plot and observed versus fitted values plot indicates that this model yielded the best fit among the three models (Fig. 2.8). The parameter estimates for these three equations are provided in Table 2.3.

4. Discussion

4.1. Site and soil properties in relation to terrain attributes

The general assumption behind the concept of topographic indices is that terrain morphology influences soil formation processes through its control on the accumulation and distribution of organic and mineral matter (i.e., slope) and exposure to the effects of weather phenomena (i.e., aspect). However, topography has strong effects on the gravitational movement of water on and in the soil, which will influence pedogenesis and soil properties (Jenny 1941; Major 1951). Our first objective was to explore the relationships between depth-to-water and a set of general site and soil characteristics based on the hypothesis that water-related soil

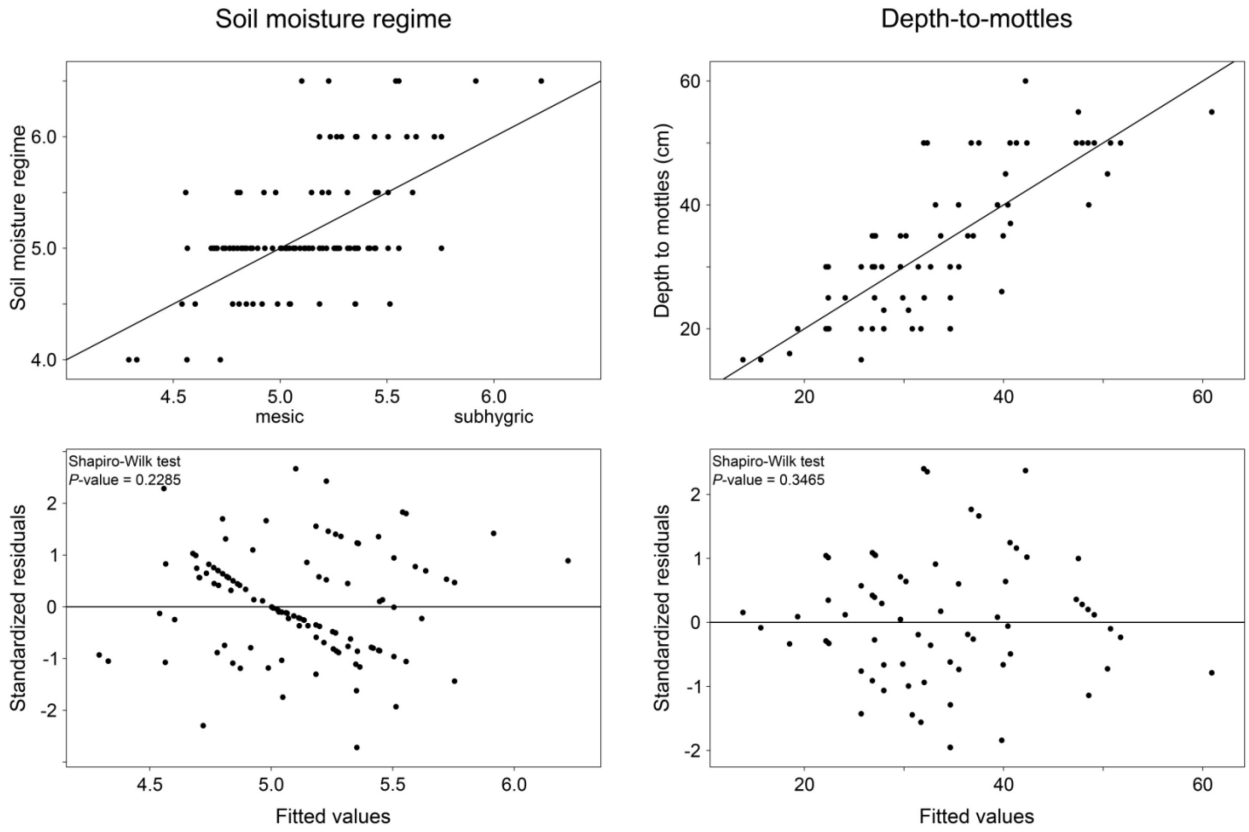

Figure 2.8. Observed vs. fitted values of soil moisture regime (SMR, top-left panel) and depth-to-mottles (DtMot, top-right panel), where the solid line shows the 1:1 relation, and standardized residuals against fitted values of SMR (bottom-left panel) and DtMot (bottom-right panel).

attributes will show stronger association with the remotely-sensed depth-to-water index.

Expected relationships were found between DTW, soil moisture regime, drainage class and depth to mottles (Table 2.2), which supports our hypothesis and agrees with previous findings. Depth-to-water has been linked directly to soil wetness (Ågren et al. 2014) and explained 64% of variation in soil drainage (Murphy et al. 2011), and indirectly through a vegetation index (Hiltz et al. 2012), which integrates soil properties, with an R^2 of 0.68. However, these studies used data collected from sites with more pronounced topography than ours, providing a wider range of soil characteristics and environmental conditions in terms of climate parameters and vegetation. For example, Murphy et al. (2011) were able to sample the

Table 2.3. Estimates of the fixed-effects, variance components (as standard deviations, SD), variance parameters and residual variances (as SDs) with the associated 95% confidence intervals (CI) for equations 2.1, 2.2 and 2.3. Results from conditional significance tests of the fixed-effects and the generalized coefficient of determination ($\overline{R}^2_{LR}$) are shown for each model.

Fixed effect	Estimated coefficient (95% CI)	*P*-value	Variance function / Random effect	Estimated parameter (95% CI)
Soil moisture regime ($\overline{R}^2_{LR} = 0.43$)				
β_0 (intercept)	5.277 (4.896 – 5.658)	<.0001	δ_1 (DMI_HC)	1 (set value)
β_1 (DTW)	−0.141 (−0.209 – −0.074)	0.0001	δ_2 (DMI_PR, SRD)	0.760 (0.499 – 1.157)
β_2 ($\log_{10}$(FA))	0.295 (0.168 – 0.422)	<.0001	δ_3 (JC, WGP)	1.272 (0.867 – 1.868)
β_3 (Slope)	−0.078 (−0.131 – −0.024)	0.0052	Residual SD (σ)	0.412 (0.293 – 0.581)
Drainage class ($\overline{R}^2_{LR} = 0.62$)				
β_0 (intercept)	3.501 (3.099 – 3.902)	<.0001	δ_1 (SRD)	1 (set value)
β_1 (DTW)	−0.235 (−0.308 – −0.162)	<.0001	δ_2 (DMI_HC, DMI_PR)	1.686 (1.132 – 2.513)
β_2 ($\log_{10}$(FA))	0.347 (0.209 – 0.485)	<.0001	δ_3 (JC, WGP)	3.154 (2.192 – 4.539)
			Random effect SD (σ_b)	0.200 (0.084 – 0.476)
			Residual SD (σ)	0.214 (0.156 – 0.296)
Depth to mottles ($\overline{R}^2_{LR} = 0.63$)				
β_{a0} (*a* intercept)	40.037 (32.939 – 47.134)	<.0001		
β_{a1} (*a* $\log_{10}$(FA))	−5.661 (−8.673 – −2.648)	0.0004		
β_{b0} (*b* intercept)	0.557 (0.309 – 0.805)	<.0001		
β_{b1} (*b* $\log_{10}$(FA))	−0.120 (−0.235 – −0.005)	0.0418	Residual SD (σ)	7.502 (6.426 – 9.015)

entire range of moisture (i.e., hydric – subxeric) and drainage (i.e., very poor – rapid) conditions. Our study was conducted in the Central Mixedwood natural subregion of the boreal forest, on sites without large landscape features (e.g., valley, hill) that would accentuate the control of topography on soil properties and create stronger environmental gradients. Further, slopes at our

sites ranged from 2.6 to 9.6% with a median of 4.5%, thus the gravitational movement of water in and on the surface of the ground is not strongly influenced by terrain. Our results suggest that DTW values (calculated at 2 ha) between 1 and 5 m can provide valuable information to describe subhygric to submesic site and soil conditions, thus wetter (i.e., hygric to hydric) or drier (i.e., xeric) sites must be captured by DTW values <1 and >5 m, respectively.

Since topography alone does not control soil nutrient regime, organic matter thickness, coarse fragments content and texture, DTW did not relate strongly and predictably with these soil attributes. Moreover, the low relief of this landscape together with the strong influence of other pedogenetic factors (i.e., parent material, climate and biota) make these soil attributes less predictable from terrain information only. Similarly, Ziadat (2005) reported weak or no associations between texture or water holding capacity of soils and terrain attributes on a large and flat (i.e., 1 – 4%) area in Jordan with similar topography to the boreal landscape. However, dividing the large areas into homogeneous landscape facets made soil-topography relationships more obvious and easier to prove statistically (Ziadat 2005). Although decomposition rates are closely related to water table levels, we did not find a strong association of DTW with organic matter thickness, in contrast to Murphy et al. (2011) who were able to establish a relationship between forest floor depth and DTW. This could be partly explained by the influence of other factors (e.g., vegetation, climate) on decomposition of organic matter and the wide range (i.e., 1 – 65 cm) of forest floor depths sampled by Murphy et al. (2011) compared to our data that spanned a range of only 3 to 15 cm. The weak to nonexistent associations between texture or coarse fragments content of the soil and DTW may be explained by the strong influence of the parent material and the weathering processes controlled by climate on these physical soil attributes. Further, the lack of steep slopes which can control the distribution of coarse fragments

and the thickness of certain soil horizons (e.g., through erosion rates) (Daniel et al. 1979) reduces the connection between topography and these soil characteristics.

The significant relationships found between volumetric water content or soil temperature measured with sensors placed at 15 cm depth in the soil and DTW further support our initial hypothesis and serve as evidence of the relation between DTW and water-related soil properties. Iverson et al. (2004) were not able to find a relationship between TWI based on a 4 m resolution DEM and VWC, concluding that micro-scale phenomena around the soil moisture sensors could not be accounted for by TWI. The 1 m resolution DEM based on LiDAR point clouds represents a clear advantage of our dataset and could explain the relationships we found between DTW and VWC or Tsoil. A high resolution DEM also enabled Murphy et al. (2011) to link DTW to total Mn, Fe, Zn, K, Ca, and Mg concentrations indicating the high sensitivity of the DTW index to micro-scale changes in soil properties. Further, high resolution DEMs were recommended for TWI by Maclean et al. (2012) who found a relationship with soil moisture using a 1 m DEM on the Lizard Peninsula of Britain.

4.2. Optimal flow initiation area

The algorithm that calculates the depth-to-water values for a cell in the landscape requires the identification of flow channels. The delineation of these terrain features starts at a certain threshold value (i.e., the flow initiation area) of the FA raster and follows the cells into which most of the neighboring cells drain the runoff and infiltrated water. As flow initiation thresholds decrease, flow channels extend further into the headwaters of the watershed and thus DTW values become smaller because the horizontal and vertical distance from any cell in the landscape to the nearest flow channel is shorter. On the other hand, large flow initiation thresholds will only identify the major channels of the basin (i.e., these collect water drained

from larger areas), thus generating larger DTW values, especially in the upper zone of the watershed. The modeling of the spatial and temporal variation of the channel network and adjacent wet areas can be improved by changing the flow initiation area, with lower threshold values being used for wetter years while larger thresholds can represent soil conditions during drier seasons (Ågren et al. 2014). A threshold area of 4 ha, for example, represents conditions frequently occurring late in the season in Alberta (White et al. 2012) and generates a network of channels corresponding to field-mapped ephemeral draws (Murphy et al. 2011).

We found that a flow initiation area of 2 ha provides the strongest relationships with soil moisture regime, drainage class and depth-to-mottles (Table 2.2). This is consistent with the findings of Ågren et al. (2014) who reported that a threshold value of 1 – 2 ha yields best results when mapping soil wetness in a landscape whose geology consists of glacial till, characterized by low permeability. The same authors found that larger flow initiation areas (i.e., 10 – 16 ha) performed better in an area with high hydraulic conductivity given by the different geology (i.e., ice-river alluvium). A smaller catchment area was also recommended for predicting drainage and vegetation class (Murphy et al. 2011), but in this study the smallest threshold area used was limited to 4 ha (they also tested 5 and 6 ha) which does not exclude the possibility that smaller areas would have offered better results. A similar result was found when DTW calculated at 1 ha outperformed a threshold value of 4 ha in predicting the location of ruts in the boreal forest (Campbell et al. 2013). The results found for SNR, organic matter, coarse fragments content and texture are weak and do not follow expected trends, thus no conclusion can be made about the optimal threshold area for these parameters.

The site descriptors we used (i.e., SMR and drainage class) integrate site and soil factors at different scales (e.g., topographic position, slope gradient, diagnostic species, effective texture,

organic material thickness) representing average long-term conditions found at the plots. However, this does not eliminate the flexibility of adapting the DTW index to particular weather conditions (e.g., very dry or wet) by changing the flow initiation area, especially for operational applications (e.g., harvesting) when the extent of wet areas with soft ground that need to be avoided must be carefully delineated (White et al. 2012). Moreover, different threshold values can be used to adapt the DTW index to potential applications requested by various stakeholders (e.g., identification of protected wet areas, prediction of areas prone to flooding).

4.3. Modeling significant site and soil properties

Our third objective was to integrate remotely-sensed topographic variables into empirical models that could be used to map the spatial variation of water-related soil attributes in the boreal forest. The final equation proposed for the soil moisture regime model includes DTW, FA and slope (Eq. 2.1, Table 2.3). In this model, DTW and slope are negatively influencing the SMR value whereas higher FA values will increase the wetness of the site. For each raster cell, DTW provides information about hydrological connectivity with flow channels while FA indicates water supply from the upslope area, which is then corrected by the terrain slope. The use of a variance function to account for the heterogeneity of the error variance across the five locations indicates that sites with more uniform topographic conditions (e.g., DMI_HC, WGP) naturally create a narrower range of SMR whereas a diverse landscape allows for a wider spectrum of soil conditions to develop. The scatterplot (Fig. 2.8) of observed versus fitted values shows some departures from the 1:1 relationship on both sides of the SMR spectrum indicating that the model tends to pull wetter and drier plots closer to mesic conditions. This could be an artifact of the large influence exerted by the greater number of observations for mesic SMR which are spread across a relatively wide range of DTW overlapping with submesic and sughygric DTW values.

Similar to our model, Gessler et al. (2000) used TWI, FA and slope to model the thickness of the A horizon and concluded that short-term processes are not captured by landform indices since these processes are more random and variable. This argument cannot be used to explain the poor fit of our SMR model because SMR integrates site and soil factors to provide long-term average soil conditions at the plots. However, Murphy et al. (2011) showed that DTW and soil depth can account for 68% of variation in a more specific measure of soil moisture (i.e., water-filled pore space) indicating that DTW cannot capture the totality of phenomena integrated by SMR. Based on our field observations we can confirm the deficiency of Eq. 2.1 noted in the 1:1 scatterplot (Fig. 2.8) because the actual spatial extent of subhygric and submesic areas is larger than that portrayed in Fig. 2.5, where we applied the SMR model to the DMI_PR location. This lack of fit also suggests that Eq. 2.1 may not follow a linear function and that it might be useful to incorporate additional variables (e.g., soil texture) other than terrain attributes to improve the predictive power of the model.

The final equation to model drainage (Fig. 2.6, Eq. 2.2, Table 2.3) consists of a positive relation with DTW and a negative coefficient for FA, indicating that areas with low DTW and high FA values drain more poorly while actively drained sites will be found in zones farther away from flow channels. Local slope is not included in the model since it does not have a large influence on the drainage of the soils at our study areas, since their fine texture exerts a stronger control on water movement, especially under saturated conditions (Kimmins 2004). This claim is supported by the necessity to use random effects to account for variation in drainage across the five study sites, as a result of differences in soil texture. The negative conditional modes of the random effects for DMI_PR, SRD and JC indicate that these sites were more actively drained, which is consistent with the lighter texture of these soils. On the other hand, the fine texture of

soils at DMI_HC and WGP was incorporated in the model with positive conditional modes. Since our objective was to use remotely-sensed indices to predict site and soil properties, we did not include field-assessed texture in the model. This limitation is also visible in the scatterplot of observed versus fitted values which shows a slight tendency of Eq. 2.2 to overestimate drainage of imperfectly drained soils (graph not shown).

We used a power function to model the functional relationship between depth-to-mottles and DTW because we do not expect DtMot to be bound by an asymptote. If data from soil pits where mottles were not found was grouped in a class labeled '>50 cm' than a sigmoidal curve would have been favored, but this functional form is not acceptable because the DtMot is not limited to an arbitrary depth of 50 cm. The final form of the model (Eq. 2.3, Table 2.3) uses DTW as the driving variable, while parameters *a* and *b* were negatively dependent on FA indicating that cells collecting water from a larger area are more likely to undergo mottling (Fig. 2.7). The process of soil mottling is directly dependent on fluctuations in the level of the water table, thus the good agreement between observed and fitted values was to be expected (Fig. 2.8). The strong connection between mottling and depth to the water table was also reflected in Eq. 2.3 which yielded the highest $\overline{R}^2_{LR}$ of 0.63 relative to Eq. 2.2 ($\overline{R}^2_{LR}$ = 0.62) and Eq. 2.1 ($\overline{R}^2_{LR}$ = 0.43). From this perspective, we can note that DTW combined with FA can predict processes closely related to water movement in the soil, but when more complex factors (i.e., SMR) that integrate additional variables (e.g., soil texture, dynamics of the organic layer, aspect, primary water source) are modeled, terrain attributes are not sufficient and predictive power decreases.

5. Conclusions

This study focused on evaluating relationships between site and soil properties relevant to

forest management (e.g., SMR, SNR, drainage regime) and remotely-sensed topographic indices (i.e., DTW, FA, slope) emphasizing the effect of flow initiation area on DTW calculation. The DTW index has the potential to be incorporated in site productivity models since it can predict water-related soil attributes. However, it cannot be the only predictor of site productivity because it lacks the ability to characterize other relevant soil properties (e.g., SNR, texture). Furthermore, we explored the limitations of DTW by showing that simple soil attributes (i.e., depth to mottles) are better predicted by DTW than complex site properties (i.e., SMR), which integrate overall site and soil conditions (e.g., topographic position, texture). The DTW index is currently available for approximately 80% of the forested area of Alberta as well as for areas in the province of New Brunswick and Sweden, thus our results can directly inform management of forest resources and stimulate research activities.

Literature cited

AESRD. 2005. Natural regions and subregions of Alberta. Alberta Sustainable Resource Development http://www.albertaparks.ca/albertaparksca/library/downloadable-data-sets.aspx, Edmonton, AB.

Ågren, A.M., Lidberg, W., Strömgren, M., Ogilvie, J., and Arp, P.A. 2014. Evaluating digital terrain indices for soil wetness mapping – a Swedish case study. Hydrol. Earth Syst. Sci. **18**(9): 3623-3634. doi: 10.5194/hess-18-3623-2014.

Allen, R.B., Peet, R.K., and Baker, W.L. 1991. Gradient analysis of latitudinal variation in Southern Rocky Mountain forests. J. Biogeogr. **18**(2): 123-139. doi: 10.2307/2845287.

Beckingham, J.D., and Archibald, J.H. 1996. Field guide to ecosites of northern Alberta. North. For. Cent., Edmonton, AB.

Beven, K.J., and Kirkby, M.J. 1979. A physically based, variable contributing area model of

basin hydrology. Hydrol. Sci. Bul. **24**(1): 43-69. doi: 10.1080/02626667909491834.

Bokalo, M., Comeau, P.G., and Titus, S.J. 2007. Early development of tended mixtures of aspen and spruce in western Canadian boreal forests. For. Ecol. Manag. **242**(2-3): 175-184. doi: 10.1016/j.foreco.2007.01.038.

Bontemps, J.-D., and Bouriaud, O. 2014. Predictive approaches to forest site productivity: recent trends, challenges and future perspectives. Forestry **87**(1): 109-128. doi: 10.1093/forestry/cpt034.

Burt, T.P., and Butcher, D.P. 1985. Topographic controls of soil moisture distributions. J. Soil Sci. **36**(3): 469-486.

Campbell, D.M.H., White, B., and Arp, P.A. 2013. Modeling and mapping soil resistance to penetration and rutting using LiDAR-derived digital elevation data. J. Soil Water Conserv. **68**(6): 460-473. doi: 10.2489/jswc.68.6.460.

Chen, H.Y.H., Krestov, P.V., and Klinka, K. 2002. Trembling aspen site index in relation to environmental measures of site quality at two spatial scales. Can. J. For. Res. **32**(1): 112-119. doi: 10.1139/x01-179.

Cox, D.R., and Snell, E.J. 1989. The analysis of binary data. 2nd ed. Chapman and Hall, London. pp. 208-209.

Daniel, T.W., Helms, J.A., and Baker, F.S. 1979. Principles of Silviculture. 2nd ed. ed. McGraw-Hill, New York, N.Y. pp. 186-187.

Gale, M.R., Grigal, D.F., and Harding, R.B. 1991. Soil productivity index: predictions of site quality for white spruce plantations. Soil Sci. Soc. Am. J. **55**(6): 1701-1708. doi: 10.2136/sssaj1991.03615995005500060033x.

Gessler, P.E., Chadwick, O.A., Chamran, F., Althouse, L., and Holmes, K. 2000. Modeling soil-landscape and ecosystem properties using terrain attributes. Soil Sci. Soc. Am. J. **64**(6): 2046-2056.

Hiltz, D., Gould, J., White, B., Ogilvie, J., and Arp, P. 2012. Modeling and mapping vegetation

type by soil moisture regime across boreal landscapes. *In* Restoration and reclamation of boreal ecosystems: Attaining sustainable development. Cambridge Univ. Press, New York, NY. pp. 56-75.

Iverson, L.R., Dale, M.E., Scott, C.T., and Prasad, A. 1997. A GIS-derived integrated moisture index to predict forest composition and productivity of Ohio forests (USA). Landsc. Ecol. **12**(5): 331-348. doi: 10.1023/a:1007989813501.

Iverson, L.R., Prasad, A., and Rebbeck, J. 2004. A comparison of the integrated moisture index and the topographic wetness index as related to two years of soil moisture monitoring in Zalenski State Forest, Ohio. *In* 14th Central Hardwoods Forest Conference, Wooster, OH. pp. 515 - 517.

Jenny, H. 1941. Factors of soil formation: a system of quantitative pedology. McGraw-Hill, New York, NY. pp. 11-12.

Kayahara, G.J., Carter, R.E., and Klinka, K. 1995. Site index of western hemlock (*Tsuga heterophylla*) in relation to soil nutrient and foliar chemical measures. For. Ecol. Manag. **74**(1-3): 161-169. doi: 10.1016/0378-1127(94)03493-g.

Kayahara, G.J., Klinka, K., and Schroff, A.C. 1997. The relationship of site index to synoptic estimates of soil moisture and nutrients for western redcedar (*Thuja plicata*) in southern coastal British Columbia. Northwest Sci. **71**(3): 167-173.

Kimmins, J.P. 2004. Forest ecology: a foundation for sustainable forest management and environmental ethics in forestry. 3rd ed. Prentice Hall, Upper Saddle River, NJ. pp. 291-292.

Klinka, K., and Carter, R.E. 1990. Relationships between site index and synoptic environmental-factors in immature coastal Douglas-fir stands. For. Sci. **36**(3): 815-830.

Kopecky, M., and Cizkova, S. 2010. Using topographic wetness index in vegetation ecology: does the algorithm matter? Appl. Veg. Sci. **13**(4): 450-459. doi: 10.1111/j.1654-109X.2010.01083.x.

Lang, M., McCarty, G., Oesterling, R., and Yeo, I.Y. 2013. Topographic metrics for improved mapping of forested wetlands. Wetlands **33**(1): 141-155. doi: 10.1007/s13157-012-0359-8.

Maclean, I.M.D., Bennie, J.J., Scott, A.J., and Wilson, R.J. 2012. A high-resolution model of soil and surface water conditions. Ecol. Model. **237–238**(0): 109-119. doi: 10.1016/j.ecolmodel.2012.03.029.

Maddala, G.S. 1983. Limited-dependent and qualitative variables in econometrics. Cambridge Univ. Press, Cambridge, UK.

Magee, L. 1990. R^2 measures based on wald and likelihood ratio joint significance tests. Am. Stat. **44**(3): 250-253. doi: 10.2307/2685352.

Maillard, P., and Alencar-Silva, T. 2013. A method for delineating riparian forests using region-based image classification and depth-to-water analysis. Int. J. Remote Sens. **34**(22): 7991-8010. doi: 10.1080/01431161.2013.827847.

Major, J. 1951. A functional, factorial approach to plant ecology. Ecology **32**(3): 392-412. doi: 10.2307/1931718.

Moore, I.D., Gessler, P.E., Nielsen, G.A., and Peterson, G.A. 1993. Soil attribute prediction using terrain analysis. Soil Sci. Soc. Am. J. **57**(2): 443-452. doi: 10.2136/sssaj1993.03615995005700020026x.

Moore, I.D., Grayson, R.B., and Ladson, A.R. 1991. Digital terrain modelling: a review of hydrological, geomorphological, and biological applications. Hydrol. Process. **5**(1): 3-30. doi: 10.1002/hyp.3360050103.

Murphy, P.N.C., Ogilvie, J., and Arp, P. 2009. Topographic modelling of soil moisture conditions: a comparison and verification of two models. Eur. J. Soil Sci. **60**(1): 94-109. doi: 10.1111/j.1365-2389.2008.01094.x.

Murphy, P.N.C., Ogilvie, J., Connor, K., and Arpl, P.A. 2007. Mapping wetlands: A comparison of two different approaches for New Brunswick, Canada. Wetlands **27**(4): 846-854. doi: 10.1672/0277-5212(2007)27[846:mwacot]2.0.co;2.

Murphy, P.N.C., Ogilvie, J., Meng, F.R., White, B., Bhatti, J.S., and Arp, P.A. 2011. Modelling and mapping topographic variations in forest soils at high resolution: A case study. Ecol. Model.

222(14): 2314-2332. doi: 10.1016/j.ecolmodel.2011.01.003.

Nagelkerke, N.J.D. 1991. A note on a general definition of the coefficient of determination. Biometrika **78**(3): 691-692. doi: 10.1093/biomet/78.3.691.

O'Callaghan, J.F., and Mark, D.M. 1984. The extraction of drainage networks from digital elevation data. Comput. Vision Graph. **28**(3): 323-344. doi: 10.1016/s0734-189x(84)80011-0.

Petroselli, A., Vessella, F., Cavagnuolo, L., Piovesan, G., and Schirone, B. 2013. Ecological behavior of *Quercus suber* and *Quercus ilex* inferred by topographic wetness index (TWI). Trees-Struct. Funct. **27**(5): 1201-1215. doi: 10.1007/s00468-013-0869-x.

Pinheiro, J.C., and Bates, D.M. 1995. Model building for nonlinear mixed-effects models. University of Wisconsin–Madison. 91.

Pinheiro, J.C., and Bates, D.M. 2000. Mixed-effects models in S and S-PLUS. Springer-Verlag, New York, NY. pp. 57-96; 201-225; 305-336.

Pinheiro, J.C., Bates, D.M., DebRoy, S., Sarkar, D., and Team, R.C. 2015. nlme: Linear and nonlinear mixed effects models. *In* http://CRAN.R-project.org/package=nlme.

Pitt, D.G., Comeau, P.G., Parker, W.C., MacIsaac, D., McPherson, S., Hoepting, M.K., Stinson, A., and Mihajlovich, M. 2010. Early vegetation control for the regeneration of a single-cohort, intimate mixture of white spruce and trembling aspen on upland boreal sites. Can. J. For. Res. **40**(3): 549-564. doi: 10.1139/x10-012.

R Core Team. 2015. *R: A language and environment for statistical computing*. R Foundation for Statistical Computing, Vienna, Austria.

Seibert, J., Stendahl, J., and Sorensen, R. 2007. Topographical influences on soil properties in boreal forests. Geoderma **141**(1-2): 139-148. doi: 10.1016/j.geoderma.2007.05.013.

Sorensen, R., Zinko, U., and Seibert, J. 2006. On the calculation of the topographic wetness index: evaluation of different methods based on field observations. Hydrol. Earth Syst. Sci. **10**(1): 101-112.

Tarboton, D.G. 1997. A new method for the determination of flow directions and upslope areas in grid digital elevation models. Water Resour. Res. **33**(2): 309-319. doi: 10.1029/96wr03137.

Ung, C.H., Bernier, P.Y., Raulier, F., Fournier, R.A., Lambert, M.C., and Regniere, J. 2001. Biophysical site indices for shade tolerant and intolerant boreal species. For. Sci. **47**(1): 83-95.

Wang, G.G., and Klinka, K. 1996. Use of synoptic variables in predicting white spruce site index. For. Ecol. Manag. **80**(1-3): 95-105. doi: 10.1016/0378-1127(95)03630-x.

White, B., Ogilvie, J., Campbell, D.M.H., Hiltz, D., Gauthier, B., Chisholm, H.K., Wen, H.K., Murphy, P.N.C., and Arp, P.A. 2012. Using the cartographic depth-to-water index to locate small streams and associated wet areas across landscapes. Can. Water Resour. J. **37**(4): 333-347. doi: 10.4296/cwrj2011-909.

Ziadat, F.M. 2005. Analyzing digital terrain attributes to predict soil attributes for a relatively large area. Soil Sci. Soc. Am. J. **69**(5): 1590-1599. doi: 10.2136/sssaj2003.0264.

Chapter 3

Carbon isotope discrimination in *Picea glauca* and *Populus tremuloides* is related to the topographic depth-to-water index

Abstract

The topographic depth-to-water (DTW) index measures the hydrological connectivity between any cell in the landscape and the nearest flow channel by integrating the horizontal and vertical distance between them. Carbon isotope ratios ($\delta^{13}C$) have been used as indicator of water stress, since plants discriminate less against ^{13}C when under stress. We selected three time periods, which differed in the amount of annual precipitation (MAP), from tree cores collected from 42 trembling aspen and 43 white spruce trees growing along DTW gradients at two locations in central Alberta, Canada. Increasing MAP lead to lower $\delta^{13}C$, indicating less drought stress as water availability increases, while $\delta^{13}C$ increased with DTW up to a threshold value, after which the relationship levelled off suggesting that large DTW values represent stress inducing soil conditions. The small scale topographic index, DTW, and the large scale climate variable, MAP, were then combined into models (aspen $R^2 = 0.72$, spruce $R^2 = 0.44$) that could be used to delineate drought prone areas during periods of low MAP. Tree height and diameter were also related with DTW suggesting a functional relationship between an index capturing soil properties and tree size. Our results demonstrate the potential to use the DTW index as an indicator of site conditions and to predict stand level characteristics.

1. Introduction

Terrain morphology has strong effects on the gravitational movement of water, determining site and soil properties that are integrated over space and time by woody plants (Major 1951). The remotely-sensed depth-to-water (DTW) index captures the hydrological connectivity between any cell in the landscape and the nearest flow channel, representing soil moisture conditions in the rooting zone (Murphy et al. 2009). Carbon isotope discrimination during photosynthesis changes under different environmental conditions, thus it has been employed to assess the status of plants, particularly in relation to soil water availability (Meinzer et al. 1992). Consequently, analysis of the isotopic signal of tree tissues provides a potentially useful way to evaluate the performance of the DTW index for characterizing soil conditions.

The increasing availability of remotely-sensed accurate digital elevation models (DEM) allows the collection of valuable up-to-date information about the topography of large forested areas with relatively low costs (Moore et al. 1991). Simple topographic indices such as slope, aspect or profile curvature have been used to predict soil pH and texture (Moore et al. 1993), which are also related to landscape position (Brubaker et al. 1993), whereas Allen et al. (1991) combined topographic position, potential solar radiation and aspect into a topographic moisture index to predict species composition. The most widely used complex terrain index is the topographic wetness index (TWI), defined as the logarithm of the ratio of upslope area to local slope (Beven and Kirkby 1979). TWI has been used to map the extent of water-saturated areas (Burt and Butcher 1985; Guntner et al. 2004) or predict detailed soil properties (e.g., thickness, pH and C:N ratio of the organic horizon) in the Swedish boreal forest (Seibert et al. 2007). These and other authors have highlighted that different algorithms must be used in different landscapes and application. A flow routing algorithm with greater flow convergence (e.g., D8, D∞) was

recommended to delineate flow channels (Sorensen et al. 2006; Tarboton 1997), whereas more distributed flow algorithms (e.g., MD∞, FD8) are better suited for mapping of broad features such as species composition (Kopecky and Cizkova 2010).

The depth-to-water index integrates the horizontal and vertical distance from any cell in the landscape to the nearest flow channel, which is defined by a selected flow initiation area (Murphy et al. 2007). The DTW index was found to be superior to TWI in mapping of wet areas in the boreal forest since TWI is strongly dependent on the upslope area, while local downslope topography is a major determinant of soil moisture conditions (Murphy et al. 2009). Further, more detailed soil properties (e.g., textural composition, pH, total C, N, P, K) were also more strongly correlated with DTW than TWI (Murphy et al. 2011), but the authors note that TWI could complement DTW in delineating water flow direction and accumulation. Changing the flow initiation area affects the extent of the flow channel network, adapting the DTW index to various landscape configurations and geologies, and temporal changes in soil moisture (e.g., wet or dry years). DTW calculated at a large flow initiation area (i.e., >8 ha) performed better on terrain with strong topography and high hydraulic conductivity while a smaller threshold area (i.e., 1 ha) was suggested for an area with low topography and poor drainage (Ågren et al. 2014). Field observations in the boreal forest of Alberta indicated that flow channels delineated at a flow initiation area of 4 ha correspond to streams with permanent or intermittent flow representing soil conditions late in the season (White et al. 2012). Further testing of the DTW index is needed to evaluate its capabilities and limitations in areas with contrasting topography.

Discrimination against the heavier stable isotope of carbon (i.e., ^{13}C) can occur during the diffusion of atmospheric CO_2 through stomata and at the site of carbon fixation by RuBisCO (Berry 1988). The strength of discrimination is measured by the $^{13}C/^{12}C$ ratio of tree tissues

relative to the isotopic composition of the Pee Dee Belemnite material and is denoted $\delta^{13}_{sample}C$ (Farquhar et al. 1982). A more informative definition of $\delta^{13}\mathrm{C}$ is

$$\delta^{13}\mathrm{C} = \delta^{13}_{\mathrm{air}} - a - (b - a)\, c_i/c_a,$$

where $\delta^{13}_{\mathrm{air}}$ represents the carbon isotope ratio of the air surrounding the leaf, c_a and c_i are the CO_2 concentrations of the atmosphere and leaf intercellular spaces (Francey and Farquhar 1982). Constant a is the diffusivity of CO_2 in air with a value of 4.4‰, and b is the isotope fractionation of RuBisCO considered to be approximately 30‰. With $\delta^{13}_{\mathrm{air}}$ equal to about −8‰, the value of $\delta^{13}\mathrm{C}$ is controlled by the c_i/c_a ratio representing photosynthesis rate and stomatal conductance. Therefore, $\delta^{13}\mathrm{C}$ reflects the effects of environmental factors on the c_i/c_a ratio (Francey and Farquhar 1982). Environmental conditions limiting assimilation rates (e.g., low light intensities) will increase c_i/c_a and reduce $\delta^{13}\mathrm{C}$, whereas factors reducing stomatal conductance (e.g., water stress, strong vapour pressure deficits) will lower c_i/c_a and increase $\delta^{13}\mathrm{C}$ (Farquhar et al. 1989). Obviously, photosynthetic rates and stomatal conductance are intimately connected and factors influencing one will impact the other without having a net effect on c_i/c_a. As predicted by theory, increasing annual precipitation from 216 to 1800 mm resulted in lower leaf $\delta^{13}\mathrm{C}$ for 50 tree species from northern Australia, with most of the $\delta^{13}\mathrm{C}$ change occurring up to 450 mm after which it stabilized (Schulze et al. 1998). Consistently, topography that creates xeric conditions (e.g., ridges, steep slopes) was associated with high $\delta^{13}\mathrm{C}$ in leaves of temperate deciduous trees (Garten and Taylor 1992), however small topographic features (e.g., gullies) did not influence wood $\delta^{13}\mathrm{C}$ in *Sequoia sempervirens* (D. Don) (Roden et al. 2011). In contrast to leaves, wood $\delta^{13}\mathrm{C}$ has the advantage to integrate the large variation of leaf $\delta^{13}\mathrm{C}$ within a crown due to crown exposure (Waring and Silvester 1994) or vertical canopy gradients (Leavitt and Long 1986), as

well as capturing environmental conditions over multiple seasons.

Depth-to-water rasters are available for extensive areas in Alberta and New Brunswick where it was shown to perform better than TWI (Murphy et al. 2009; Murphy et al. 2011), thus a deeper understanding of the ecological significance of DTW values, as well as its potential and limitations, is necessary. The objectives of the present study were (1) to evaluate the relationship between DTW and $\delta^{13}C$, (2) to explore a gradient of flow initiation areas in contrasting terrains, and (3) to assess the association between DTW and tree size (i.e., height and diameter). We expect that DTW will be related with $\delta^{13}C$ and tree size but will present a threshold after which its influence diminishes, and that optimal flow initiation area will depend on terrain morphology.

2. Materials and methods

2.1. Study sites

We selected a trembling aspen (*Populus tremuloides* Michx.) stand located 30 km south of Grande Prairie in the Boreal Mixedwoods ecoregion of Alberta, and a white spruce (*Picea glauca* (Moench) Voss) stand situated 16 km west of Whitecourt on the eastern side of the Foothills ecoregion (Fig. 3.1). The aspen site has developed on fine-textured deposits of glacial origin forming a typical flat terrain (i.e., slope of 2.5%), whereas coarser material washed from the Canadian Rockies and deposited in the Foothills area (MacCormack et al. 2015) formed steeper slopes (i.e., 10.9%) at the spruce site. Consequently, these two sites provided suitable conditions to evaluate the DTW index in terrains with contrasting geology and topography. The climate at these two locations is dominated by long cold winters and warm summers, with Grande Prairie having a lower mean annual temperature (i.e., 2.2 °C) and receiving less annual precipitation (i.e., 445.1 mm) than the site near Whitecourt (i.e., 2.9 °C and 544.4 mm; Table

3.1). These differences in topography and climate between the two areas can change water availability in the soil, thus affecting the carbon isotope ratio of trees growing on these sites. Both stands were 23 years old at the time of sampling; the aspen stand had regenerated from root suckers after harvest in the winter of 1990 – 91, but it was sampled early in the spring of 2014 before bud break, whereas the spruce stand had been planted in May 1993 with 1 year old stock and was sampled in late-summer of 2014.

2.2. Sample collection and preparation

We used existing DEM and DTW rasters for the two sites to select locations that cover a wide range of topographic conditions and DTW values (Fig. 3.1). We navigated to each point and then selected a dominant tree, for which we measured the diameter at breast height (dbh), total height, height to live crown, crown radii on the northern and western directions, and made

Table 3.1. Geographic location, topography and climate at the two study sites where trembling aspen and white spruce trees were sampled for carbon isotope analyses. MAT – mean annual temperature, MAP – mean annual precipitation.

	Grande Prairie	**Whitecourt**
Species	trembling aspen	white spruce
Number of trees	42	43
Height (m)	11.5	8.2
Diameter (cm)	9.5	13.7
Latitude (° N)	54.9099	54.1198
Longitude (° W)	118.9251	115.9269
Elevation (m)	711.8	839.7
Slope (%)	2.5	10.9
MAT* (°C)	2.2	2.9
MAP* (mm/yr)	445.1	544.4
Weather Canada station	Grande Prairie A	Whitecourt A

* extracted from "1981–2010 Canadian Climate Normals" available online at http://climate.weather.gc.ca accessed on August 27, 2014.

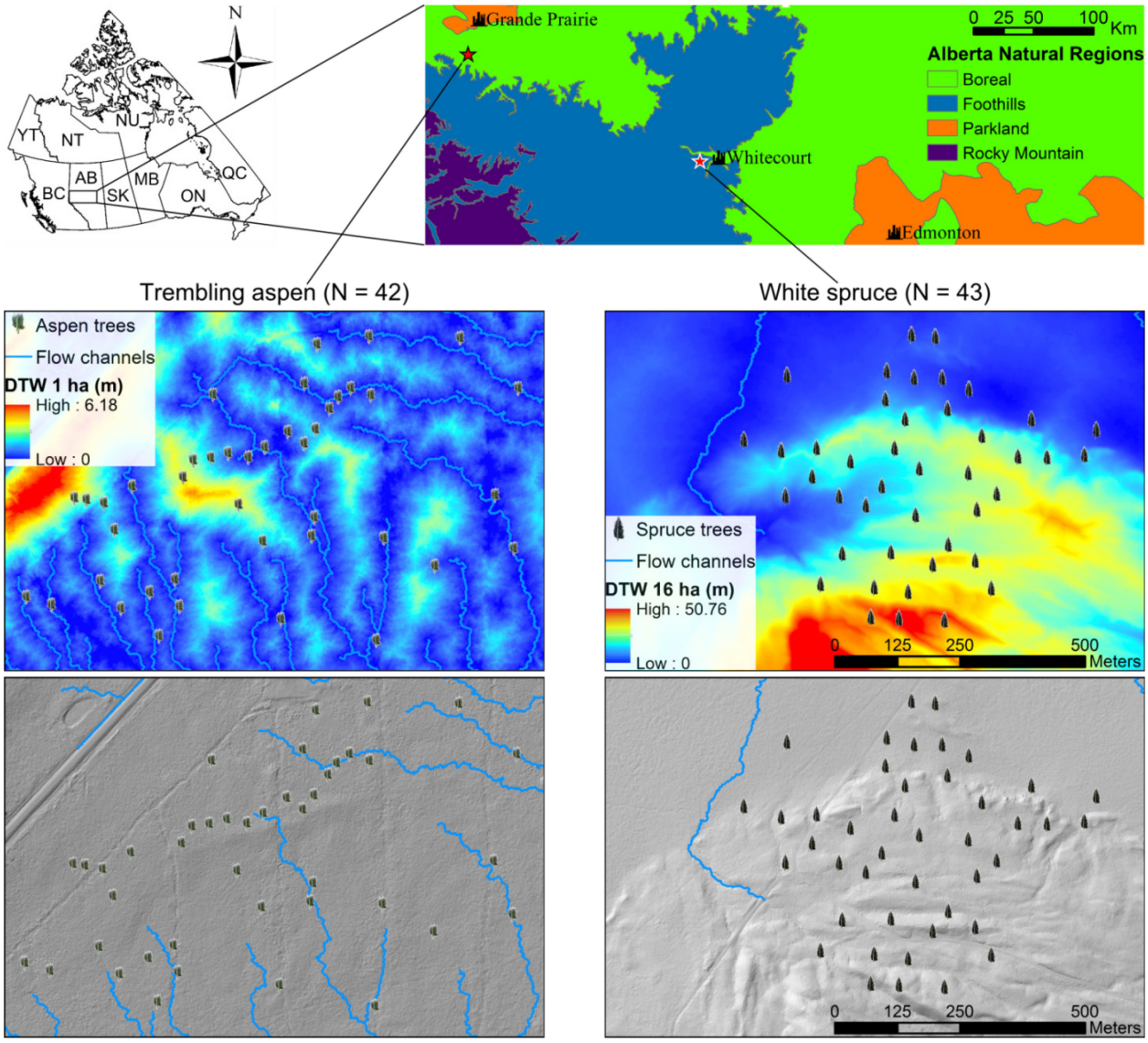

Figure 3.1. Location of the two study sites in the Boreal Mixedwoods and Foothills ecoregions of Alberta, Canada, from where trembling aspen and white spruce trees were selected (points). The hillshade images (bottom panels) show the contrasting topography between the two sites, which controls the flow channel delineation and depth-to-water (DTW) raster calculation (top panels). Note that DTW was calculated at a flow initiation area of 2 ha for the aspen site and 16 ha for the spruce site.

notes about the conditions in which the trees were growing (e.g., edge tree, open grown). A total of 42 trembling aspen and 43 white spruce trees were selected and their locations recorded with a Trimble GeoExplorer 6000 series GeoXT handheld device (Trimble, Los Altos, California) with GNSS capabilities ensuring sub-meter accuracy for 78% of the aspen and 87% of the spruce tree positions. The crown measurements were used to calculate the volume, projected and surface

area of the crowns, which were assumed to be paraboloids for the aspen and conical for the spruce trees.

From each tree we collected two cores from the north and south facing side of the stem as recommended by Leavitt and Long (1984). The cores were cleaned and carefully divided into three periods selected based on the annual precipitation relative to the 30-year (1981 – 2010) normals. For the aspen site we selected the 1999 – 2003 and 2008 – 2010 as dry and 2004 – 2007 as wet periods, while the periods 2002 – 2003 and 2008 – 2009 were dry and 2011 – 2012 was relatively wet at the spruce site (Fig. 3.2). For each period and species, the sections from the north and south core were both placed in a vial and dried in an oven at 70 °C for 48 hours. The dried wood samples were finely ground with a Retsch MM 200 ball grinder (Retsch, Dusseldorf, Germany) to ensure sample homogeneity, and then analyzed for their isotopic composition using a mass spectrometer at the Natural Resources Analytical Laboratory. We did not separate lignin and holocellulose since Walia et al. (2010) found that the $\delta^{13}C$ of whole wood remains constant even if the ratio of the two wood components changes.

2.3. The depth-to-water index

The depth-to-water index is defined as the cumulative slope along the least cost path from any cell in the landscape to the nearest flow channel (Murphy et al. 2007). The measurement unit for DTW is meters and is calculated as

$$DTW = \left[\sum \frac{dz_i}{dx_i} a\right] x_c \ (m),$$

where dz_i and dx_i are the vertical and horizontal distance between two cells, a is a constant equal to 1 if the path is parallel to the cell edge or $\sqrt{2}$ if the cells are connected across the diagonal, and x_c is the size of the raster cell (i.e., 1 m). Thus, a cell farther from the channel or at a higher

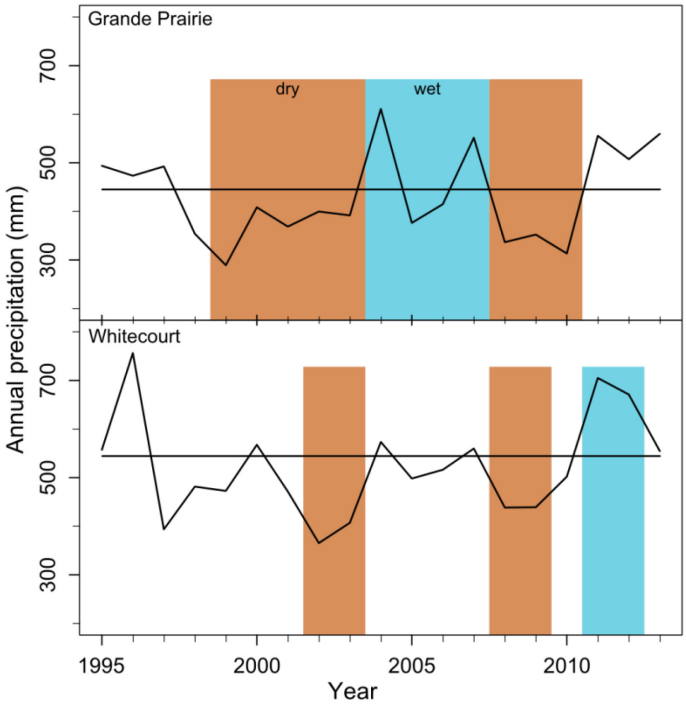

Figure 3.2. Annual precipitation and 30-year (1981-2010) normals (flat line) at the Grande Prairie (aspen) and Whitecourt (spruce) study sites from 1995 to 2013. The selected periods for carbon isotope analysis are shaded in the darker brown color if precipitation was less than normal (i.e., dry) and lighter blue if it exceeded normal values (i.e., wet).

elevation will receive a large DTW value indicating the weak hydrological connection between that cell and its source of water (Murphy et al. 2009). DTW was calculated using a digital elevation model derived from an airborne LiDAR (Light Detection and Ranging) point cloud with 0.5 to 3 points per square meter and vertical accuracy of 30 cm. False depressions and other artifacts that artificially obstruct water flow were removed from the 1 m resolution DEM, and flow direction based on the slope to the neighbouring cells was determined for each cell. Flow accumulation (FA) area, defined as the upslope area draining to each cell, was calculated using the highly convergent D8 flow routing algorithm which directs flow to the adjacent cell with the steepest slope (O'Callaghan and Mark 1984). The flow direction and FA rasters were used to determine the cells delineating the flow channels, which receive a DTW value of 0 m. Flow initiation areas of 0.5, 1, 2, 4, 8, 12 and 16 ha were used as starting points for the flow channels,

with a new DTW raster being calculated for each threshold.

2.4. Statistical analysis

To address the first two objectives we used $\delta^{13}C$ as the dependent variable and modeled it as a function of DTW, FA and slope averaged over a circular plot centered on the tree and with a radius of 3 m. Preliminary analyses did not show differences between radii of 1, 3, 5, 7.5 and 10 m, thus the selected radius was consistent with the accuracy of the tree locations and it also captured the bulk of the root system in these young dense stands. Since the conditions in which tree crowns develop has strong effects on carbon isotope discrimination (Leavitt 1993), we first tested the $\delta^{13}C$ difference between trees growing in a closed canopy and those that were in open conditions or at stand edge. Values of $\delta^{13}C$ in trees exposed to more radiation and stronger vapour pressure deficits were significantly higher for both aspen ($-26.08 > -26.36$, $P = 0.0468$) and spruce ($-25.47 > -26.15$, $P < 0.0001$), thus the open-grown and stand edge trees were removed prior to any analyses of $\delta^{13}C$ data. This reduced our sample sizes to 30 aspen and 26 spruce trees.

We began our analysis with a linear mixed-effects model between $\delta^{13}C$ and mean annual precipitation (MAP) for each time period with random effects for the intercept, which induces a compound symmetry correlation structure for the $\delta^{13}C$ measurements made on the same tree. Likelihood ratio tests, recommended to select the optimal structure for the random effects (Pinheiro and Bates 2000), indicated that a random effect for the slope was not needed. Since each tree was allowed to have a different intercept, the conditional modes of the random effects represented the variation of $\delta^{13}C$ between tree locations. Therefore, the null hypothesis of no relationship between $\delta^{13}C$ and the topographic indices (i.e., DTW, FA slope) was tested using

the conditional modes. Moreover, this approach allowed us to combine the three $\delta^{13}C$ values per tree into a single number. The relation between $\delta^{13}C$ and DTW, calculated at the seven flow initiation areas, was modeled with an asymptotic function of the form

$$y(x) = a + (b - a)\exp[-\exp(c)\,x], \quad \text{(Eq. 3.1)}$$

where a is the asymptote as $x \to \infty$ and b is the value of y at $x = 0$. The expression $\exp(c)$ is the rate parameter and is used in this form to ensure that the model approaches an asymptote. This curve becomes a flat line when $\exp(c) = 0$, indicating no relationship between the two variables. A significance test for the estimate of c cannot be devised since $\exp(0) = 1$ and $\exp(c) \to 0$ as c becomes more negative ($\exp(-2) = 0.14$). Instead, we used the coefficient of determination (i.e., R^2) to compare among the different flow initiation areas while providing the estimate of c for the relevant models to judge significance. We selected this asymptotic function based on an expected functional relationship between $\delta^{13}C$ and DTW (i.e., $\delta^{13}C$ is not influenced by large DTW values), which was supported by empirical evidence. Simple linear regression was used to test the association between the conditional modes of the random effects and FA and slope.

Once the strongest predictor was selected, we introduced it as a covariate in the initial mixed model which included only MAP. In this updated model formulation, the random effect for the intercept was removed since that variability was now explained by the topographic index (Pinheiro and Bates 1995). However, the autocorrelation between the three $\delta^{13}C$ measurements made on the same tree was accounted for with a general correlation structure found most suitable using likelihood ratio tests (Pinheiro and Bates 2000). This correlation model is more parameter expensive but our short time series (i.e., 3 periods) introduced only two extra parameters over a first order autoregressive model suggested by Monserud and Marshall (2001) while allowing for greater flexibility. Furthermore, their study focused on a time-series analysis of $\delta^{13}C$ much

longer than ours (i.e., 90 years) which made an autoregressive model necessary. Residual plots and the Shapiro-Wilk normality test were used to assess model fit and the validity of the assumptions imposed on the models. Equation 3.1 was also used to model the relationship between tree size and the topographic indices but a correlation structure or random effects were not necessary since the data did not present a hierarchical structure with multiple measurements on the same individual. We applied the same modeling approach to both aspen and spruce. The parameters of the mixed-effects models were estimated using the method of maximum likelihood implemented in the nlme library v. 3.1-120 (Pinheiro et al. 2015) within the R environment for statistical modeling v. 3.2.0 (R Core Team 2015).

3. Results

3.1. Annual precipitation and $\delta^{13}C$

Carbon isotope ratio was negatively related with mean annual precipitation for both aspen and spruce (Fig. 3.3). The linear mixed-effects model fit for each species had the form

$$\delta^{13}\mathrm{C}_{\mathrm{i,t}} = (\beta_0 + b_i) + \beta_1 \mathrm{MAP} + \varepsilon_{i,t}, \qquad \text{(Eq. 3.2)}$$

where $\delta^{13}\mathrm{C}$ was the carbon isotope ratio for tree *i* at period *t*, β_0 and β_1 were the intercept and slope, respectively. The slope was fixed but b_i represented the deviations of the intercept among trees, considered to be independent and identically distributed (i.i.d.) as $b_i \sim N(0, \sigma_b^2)$. The errors were also considered i.i.d. as $\varepsilon_{i,t} \sim N(0, \sigma^2)$. The variation between trees (σ_b^2) was larger than the unexplained variability (σ^2) in the case of both species (Fig. 3.3). Aspen had $\sigma_b = 0.48$ and $\sigma = 0.37$ while spruce had $\sigma_b = 0.58$ and $\sigma = 0.52$. The mean $\delta^{13}\mathrm{C}$ value for aspen (−26.36) was lower than that of spruce (−26.15), but this difference diminished as annual precipitation decreased due to the more negative slope for aspen ($\beta_1 = -0.0047$, $P < 0.0001$) than for spruce ($\beta_1 = -0.0016$,

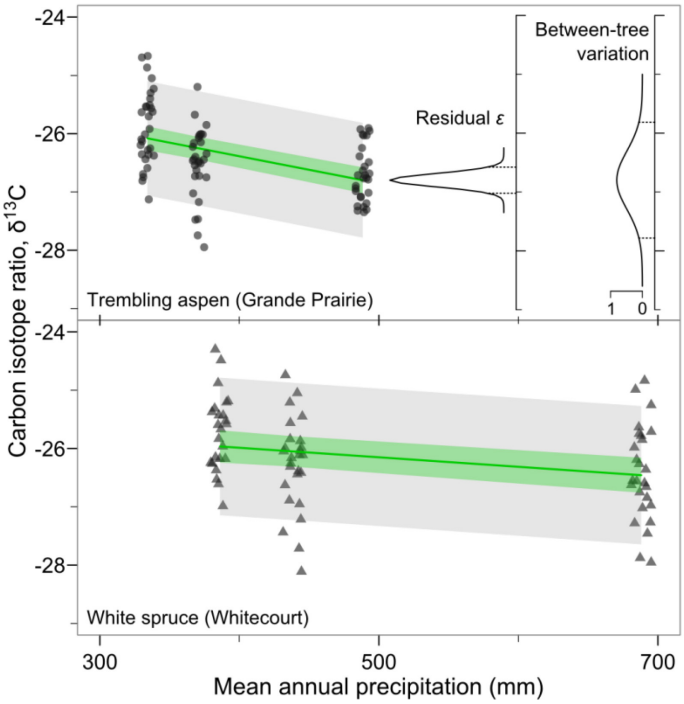

Figure 3.3. Carbon isotope ratio in woody tissue of trembling aspen and white spruce decreased with mean annual precipitation. The darker green shading shows the 95% confidence band for the linear mixed-effects model in Eq. 3.2 while the lighter gray shows the 95% confidence envelope including the intercept variance (σ_b^2). Note the greater variation between trees compared to the residual error.

$P = 0.0008$). According to parameter estimates for Eq. 3.2, aspen has a less negative $\delta^{13}C$ ($\beta_0 = -24.53$) than spruce ($\beta_0 = -25.34$) at nil annual precipitation. The intercept varied about 2‰ between trees, from −27.14 to −25.18 for aspen and from −26.85 to −24.95 for spruce.

3.2. The depth-to-water index and $\delta^{13}C$

The conditional modes (b_i) of the random effects for the intercept in Eq. 3.2 were most strongly related to DTW (Fig. 3.4) based on a flow initiation area of 1 ha for aspen ($R^2 = 0.419$) and 16 ha for spruce ($R^2 = 0.160$). The corresponding estimates of the rate parameter in Eq. 3.1 were $\exp(2.297) = 9.944$ for aspen and $\exp(-2.193) = 0.112$ in the case of spruce. Increasing or decreasing flow initiation area at the aspen site resulted in a gradual decline in the strength of the relationship, with threshold areas of 8, 12 and 16 ha providing similar results ($R^2 = 0.107$,

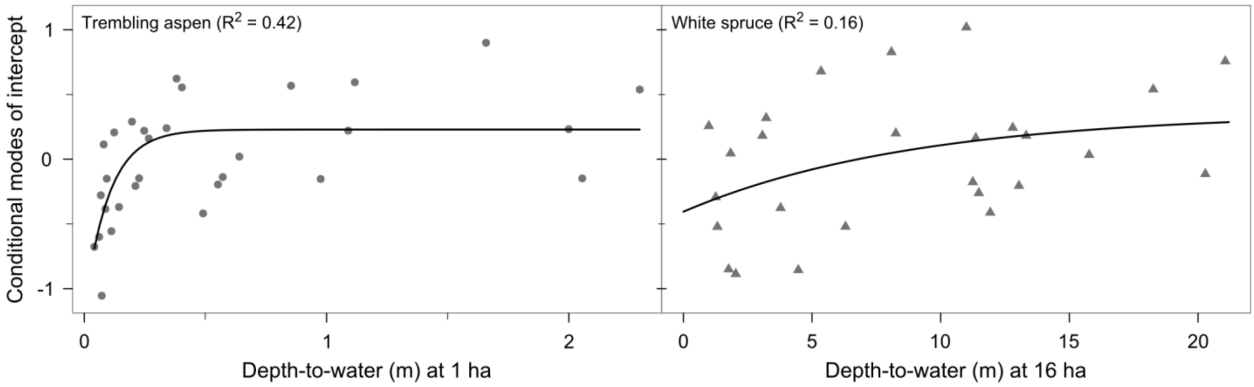

Figure 3.4. Fitted asymptotic (Eq. 3.1) regression between the conditional modes (b_i) of the random effects in Eq. 3.2, representing the inter-tree variation in carbon isotope ratio, and depth-to-water calculated at a flow initiation area of 1 ha for trembling aspen and 16 ha for white spruce.

Table 3.2). In the case of spruce, the coefficients of determination remained below those for aspen while following the same pattern of gradual increase with larger flow initiation areas, reaching a plateau at catchment areas of 12 and 16 ha (Table 3.2). Flow accumulation and local slope were not significantly linearly related with the conditional modes (b_i) of the random effects ($P > 0.2500$), yielding weak relationships ($R^2 < 0.047$) for both species.

Table 3.2. Coefficients of determination (R^2) shown for the regression models between the topographic indices and the conditional modes (b_i) of the random effects in Eq. 3.2, height, and diameter of the trembling aspen and white spruce trees. The asymptotic function in Eq. 3.1 was used for the models with the depth-to-water index as predictor, and simple linear regression for flow accumulation (FA) and slope.

R^2	Flow initiation area used to calculate the depth-to-water index							$\log_{10}$(FA)	Slope
	0.5 ha	1 ha	2 ha	4 ha	8 ha	12 ha	16 ha		
Trembling aspen									
b_i ($\delta^{13}C$)	0.176	**0.419**	0.296	0.143	0.107	0.107	0.107	0.008	0.047
height	0.148	**0.272**	0.235	0.187	0.059	0.060	0.060	0.001	0.000
diameter	0.088	0.119	**0.158**	0.002	0.016	0.017	0.017	0.000	0.019
White spruce									
b_i ($\delta^{13}C$)	0.002	0.028	0.108	0.063	0.139	0.158	**0.160**	0.035	0.003
height	0.129	0.277	0.393	0.278	0.362	0.546	**0.563**	0.018	0.126
diameter	0.088	0.226	0.161	0.139	0.208	0.410	**0.414**	0.002	0.046

The strongest predictor from Table 3.2 (boldfaced values) was incorporated into Eq. 3.2 to obtain a model that combines climate and topography to explain variation in $\delta^{13}C$, for each species (Fig. 3.5). The two models thus obtained can be expressed as

$$\delta^{13}C_{i,t} = \beta_1 + (\beta_2 - \beta_1)\exp(-\exp(\beta_3)DTW) + \beta_4 MAP + \varepsilon_{i,t}, \quad \text{(Eq. 3.3)}$$

where $\delta^{13}C$ was the carbon isotope ratio for tree i at period t., β_1 was the asymptote, β_2 the value of $\delta^{13}C$ at DTW of 0 m, $\exp(\beta_3)$ the rate parameter, and β_4 the slope parameter for mean annual precipitation. The errors were considered to be i.i.d. as $\varepsilon_{i,t} \sim N(0, \sigma^2)$, with a general correlation structure for the within-tree residuals. The parameter estimates indicate that aspen experienced greater $\delta^{13}C$ values than spruce at very large or 0 m DTW and no annual precipitation (β_1 and β_2 in Table 3.3). However, aspen $\delta^{13}C$ were lower than those of spruce at average and high levels of

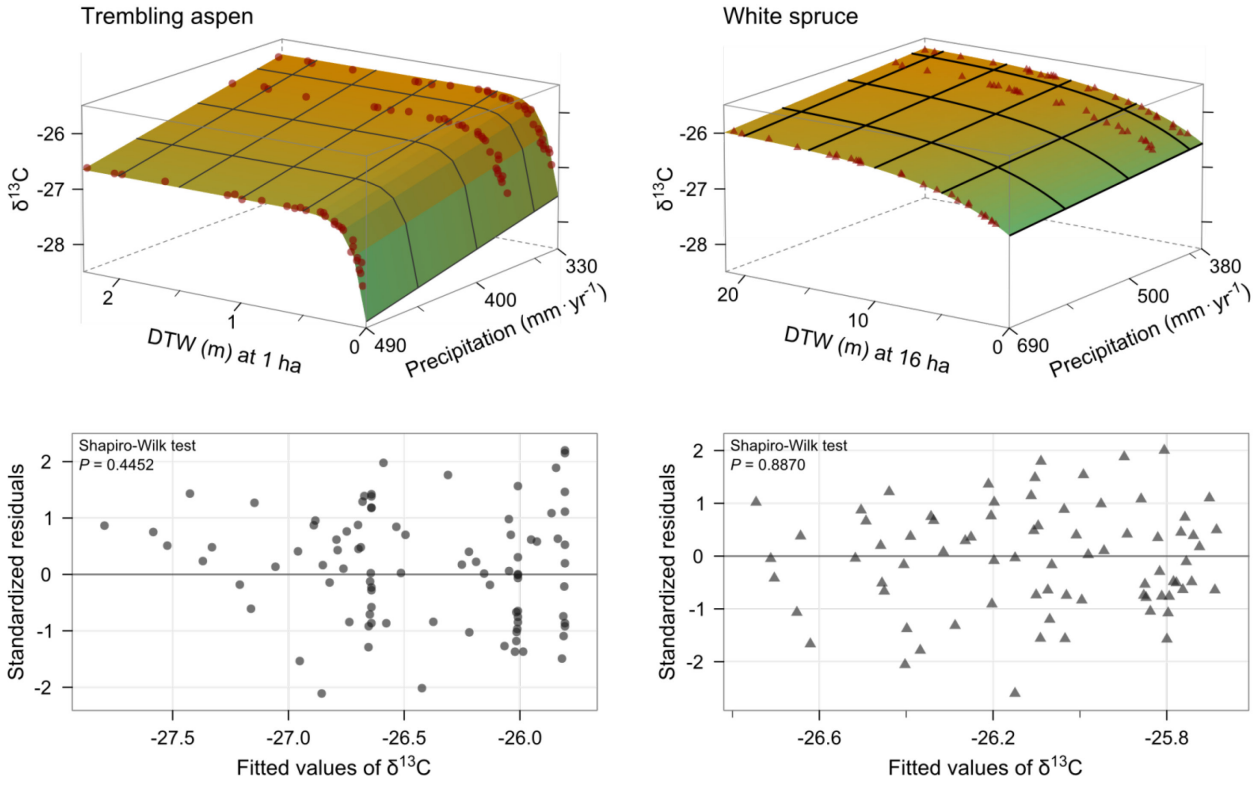

Figure 3.5. Carbon isotope ratio ($\delta^{13}C$) in wood tissue of trembling aspen and white spruce modeled as a function of depth-to-water (DTW) and mean annual precipitation (Eq. 3.3). DTW was calculated at a flow initiation area of 1 ha for aspen and 16 ha for spruce. The residual plots (bottom) and the Shapiro-Wilk test confirm the good fit of the model. Note that the points on the model surface are the fitted values.

Table 3.3. Parameter estimates and 95% confidence intervals (CI) for the models (Eq. 3.3) of carbon isotope ratio ($\delta^{13}C$) in wood tissue of trembling aspen and white spruce as a function of depth-to-water (DTW) and mean annual precipitation (MAP). DTW was calculated at a flow initiation area of 1 ha for aspen and 16 ha for spruce. The generalized coefficient of determination ($\overline{R}^2_{LR}$) is shown for both models.

	Parameters in Eq. 3.3				Residual SD (σ)
	β_1 (asymptote)	β_2 (= y(0,0))	β_3 (DTW)	β_4 (MAP)	
Trembling aspen ($\overline{\mathrm{R}}^2_{\mathrm{LR}} = 0.72$)					
Estimated parameter	−23.997	−25.740	2.305	−0.0054	0.505
(95% CI)	(−24.349 – −23.645)	(−27.160 – −24.321)	(1.261 – 3.350)	(−0.0061 – −0.0047)	(0.424 – 0.603)
White spruce ($\overline{\mathrm{R}}^2_{\mathrm{LR}} = 0.44$)					
Estimated parameter	−25.265	−26.187	−1.795	−0.0010	0.733
(95% CI)	(−26.236 – −24.295)	(−27.267 – −25.106)	(−5.105 – 1.515)	(−0.0018 – −0.0002)	(0.604 – 0.890)

precipitation since the slope of MAP was more negative for aspen than spruce (β_4 in Table 3.3). The relationship between δ^{13}C and DTW was steeper for aspen, while a gradual change in δ^{13}C with DTW was observed in the case of spruce (β_3 in Table 3.3). The plateau was reached at DTW around 0.4 m for aspen and 7 – 8 m for spruce, but these values cannot be directly compared since different flow initiation areas were used to calculate DTW for each species (Fig. 3.5). Since these two models were fit using the method of maximum likelihood, we calculated a generalized coefficient of determination ($\overline{\mathrm{R}}^2_{\mathrm{LR}}$) using the likelihood ratio of the candidate model with the null model (Cox and Snell 1989; Nagelkerke 1991). The δ^{13}C model for aspen yielded a $\overline{\mathrm{R}}^2_{\mathrm{LR}}$ value of 0.72, whereas the model for spruce had a lower $\overline{\mathrm{R}}^2_{\mathrm{LR}}$ of 0.44. The residual plots showed a generally good fit, while the Shapiro-Wilk test indicated that the normality assumption was met for both models (Fig. 3.5).

3.3. The depth-to-water index and tree size

Height of aspen and spruce trees was more strongly related with DTW than diameter at breast height (Eq. 3.1, Table 3.2). Both height and diameter of spruce (i.e., R^2 of 0.56 and 0.41,

respectively) showed stronger relationships with DTW than in the case of aspen (i.e., R^2 of 0.27 and 0.16, respectively). Similarly to $\delta^{13}C$, flow initiation areas of 1 ha for aspen and 16 ha for spruce provided the strongest relationship for height and diameter of both species (Fig. 3.6). Although diameter of aspen was more strongly related with DTW calculated at 2 ha (Table 3.2), the difference is not very large, thus we focus our presentation and discussion on the model with DTW calculated at 1 ha. The aspen trees were taller than the spruce, with a narrower range of heights from low DTW (b = 10.4 m) to high DTW conditions (a = 12.4 m), whereas the spruce trees varied from 4.3 m at low DTW to 8.9 m at large DTW (Table 3.4). Tree height became independent of DTW after DTW values of 0.9 m for aspen and 11 m for spruce (Fig. 3.6). Diameter of aspen trees was smaller than that of the spruce trees, and quickly increased with DTW from 8.1 cm to 9.9 cm at DTW > 0.4 m. In the case of spruce, diameter increased more

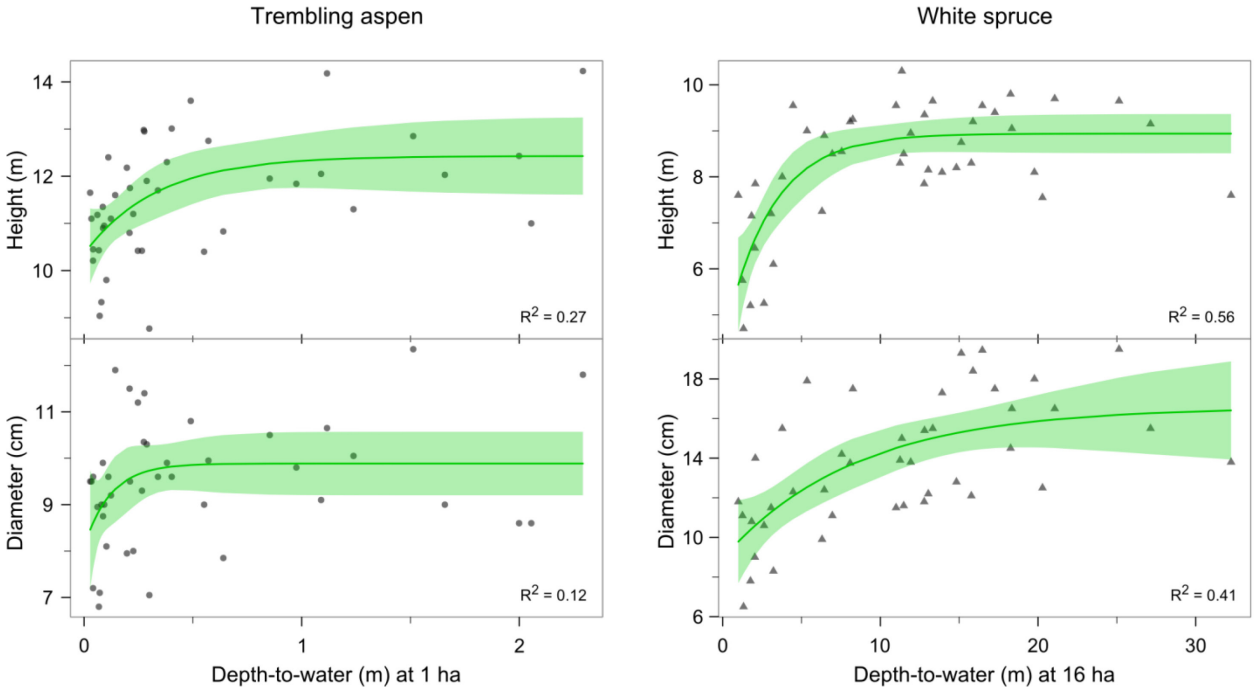

Figure 3.6. Fitted nonlinear regression (Eq. 3.1) and 95% confidence envelope for tree height and diameter at breast height of trembling aspen and white spruce modeled as a function of depth-to-water, calculated at a flow initiation area of 1 ha for aspen and 16 ha for spruce. Note that the scale of the *y*-axis is not the same across panels.

Table 3.4. Parameter estimates and associated standard errors (SE) for the nonlinear models (Eq. 3.1) of height and diameter at breast height of trembling aspen and white spruce with depth-to-water. These models are illustrated in Fig. 3.6.

		Parameters in Eq. 3.1			Residual SE (σ)	R^2
		a (asymptote)	*b* (= *y*(0))	*c* (DTW)		
Trembling aspen (DTW calculated at 1 ha)						
Height	Estimate (± SE)	12.429 (± 0.412)	10.354 (± 0.501)	1.099 (± 0.696)	1.093	0.272
Diameter	Estimate (± SE)	9.886 (± 0.338)	8.090 (± 1.111)	2.107 (± 1.085)	1.288	0.119
White spruce (DTW calculated at 16 ha)						
Height	Estimate (± SE)	8.939 (± 0.211)	4.341 (± 1.142)	−1.081 (± 0.379)	0.914	0.563
Diameter	Estimate (± SE)	16.573 (± 1.603)	8.935 (± 1.465)	−2.127 (± 0.645)	2.554	0.414

gradually with DTW from 8.9 cm at low DTW to 16.6 cm at DTW > 25 m. Tree height was estimated more tightly with standard error of about 1 m, whereas diameter estimates had a standard error of up to 2.5 cm in the case of spruce (Table 3.4). Flow accumulation was not associated with height or diameter of either species, whereas slope was positively related only with height of the spruce trees with a slope of 0.05 ($P = 0.0196$).

4. Discussion

4.1. Topography and precipitation

The model described by Eq. 3.3 incorporates both a topographic index and a climate variable to explain variation in carbon isotope ratio of trembling aspen and white spruce. As expected, the largest values of $\delta^{13}C$ indicating water stress in trees are found in areas with high DTW and periods with low annual precipitation (Fig. 3.5). Leavitt and Long (1986) suggest that a high resolution topographic index that reflects site conditions could account for about 2 and 3‰ of the variation in $\delta^{13}C$ between trees. The relationship between $\delta^{13}C$ and DTW is positive until a certain threshold after which it levels off (Fig. 3.4). Areas that are farther away from

water (i.e., flow channel) are expected to be drier and have larger DTW values (Murphy et al. 2009), consistent with trends in $\delta^{13}C$. Murphy et al. (2011) reported that soil moisture availability decreased sharply with DTW, indicating that water availability is captured within a narrow range of small DTW values. An effect of topography on $\delta^{13}C$ was also found by Garten and Taylor (1992), who reported that foliar $\delta^{13}C$ was higher for deciduous trees growing on drier areas (i.e., ridges and slopes) than for those from wetter conditions (i.e., riparian). Similarly, more positive $\delta^{13}C$ values were reported for leaves of broadleaved species growing on ridges than for those found in the valley (Hanba et al. 2000).

The relationship between $\delta^{13}C$ and DTW was not very strong (i.e., R^2 of 0.42 for aspen and 0.16 for spruce) since $\delta^{13}C$ enrichment can result from a range of environmental factors or genotypic variation between trees. Weak relationships with DTW may also occur because the DTW index does not completely or accurately integrate all site conditions influencing stomatal conductance and carbon fixation. Photosynthesis is directly controlled by the amount of radiation intercepted by the leaf, thus increasing light availability can lead to higher carbon demand which can also result in larger $\delta^{13}C$ (Sohn et al. 2013; Warren et al. 2001). Greater $\delta^{13}C$ were also reported for mature aspen trees that had been left standing after variable retention harvesting as a result of sudden exposure to full sunlight, which led to higher evaporative demand and water stress (Bladon et al. 2007). An effect of shading was found in our dataset, but we removed trees receiving more radiation (i.e., edge and open grown trees) since they had higher $\delta^{13}C$ values than the trees growing in closed canopy stands. Furthermore, mineral nutrition of trees controls carbon assimilation and $\delta^{13}C$ (Francey and Farquhar 1982), as it was shown to affect $\delta^{13}C$ in wood of *Tsuga heterophylla* (Raf.) Sarg. (Walia et al. 2010). In a companion study we found that DTW cannot predict soil nutrient regime (see Chapter 2), which may also contribute to the weak

relationships. A proportion of the unexplained variation in $\delta^{13}C$ might also be the result of inherited differences between trees, since foliar $\delta^{13}C$ in seedlings of white spruce could vary by as much as 2‰ among genotypes (Sun et al. 1996). This is further supported by a study that found high heritability of $\delta^{13}C$ (i.e., 0.54 compared to 0.39 for height) in *Picea mariana* (Mill.) BSP (Johnsen et al. 1999).

Although topography influences water movement in and on the soil, several other studies have reported that topography was not related with $\delta^{13}C$. Topographic position did not have an effect on $\delta^{13}C$ in tree rings of *Sequoia sempervirens* D. Don growing in an area with homogeneous terrain morphology (Roden et al. 2011), while the effect of topography on $\delta^{13}C$ was masked by the ability of *Pinus ponderosa* Dougl. ex Laws. trees to access deep water sources and reduce water stress (Adams et al. 2014). Thus, topographic effects on $\delta^{13}C$ might be inhibited by redistribution of water taken up from deep soil layers or adjacent wet areas trough tree roots and root grafts (Burgess et al. 1998). The clonal nature of aspen can contribute and increase the magnitude of water redistribution among trees. Moreover, site conditions can directly impact stand structure altering light interception and anatomy of leaves, which might lead to changes in the isotopic signature of tree tissues. For example, light acclimation and interception by needles of *Pinus sylvestris* L. was reduced on nutrient limited sites (Niinemets et al. 2002), and foliar $\delta^{13}C$ values of *Metrosideros polymorpha* Gaudich. were higher for trees growing on bog sites with poor drainage and frequently hypoxic conditions (Meinzer et al. 1992), since physiological availability of water to plants also depends on soil texture and proportion of coarse fragments.

The negative relationship between $\delta^{13}C$ and mean annual precipitation suggests that trees experienced less stress during periods of higher precipitation (Fig. 3.3). A strong influence of

precipitation as well as air temperature on the seasonal pattern of $\delta^{13}C$ was found in semi-arid ecosystems with an aspen component in Utah (Buchmann et al. 1997). A similar effect of water availability was found for 50 tree species growing along a rainfall gradient in northern Australia (Schulze et al. 1998). However, $\delta^{13}C$ did not change when MAP levels exceeded 450 mm since substitution of species with different physiological requirements maintained a constant $\delta^{13}C$ even if precipitation increased. We found that the relationship (Eq. 3.2) was less negative at the site with generally higher MAP (i.e., Whitecourt) than at the site receiving less precipitation (i.e., Grande Prairie). Although our study did not include several species to replace each other along the precipitation gradient, we might argue that the trees growing at the wetter site experienced lower water stress overall and periods with more precipitation did not change their isotopic composition. The different response of $\delta^{13}C$ to precipitation might also be attributed to differences in drought tolerance of each species, since white spruce is better adapted to water deficits (Silim et al. 2001) and would be able to endure drier conditions without a strong and immediate effect on carbon discrimination. Further, $\delta^{13}C$ values from the earlier periods might also be increased by the more open stand conditions characteristic of young forests (i.e., about 10 years), particularly in the planted spruce stand.

4.2. Optimal flow initiation area

Flow initiation area controls the extent of the flow channel network used to calculate the DTW raster. Smaller catchment areas extend flow channels farther into the headwaters of the watershed creating an extensive network of flow channels, which results in generally lower DTW values. On the other hand, only major channels which collect water from larger catchment areas are identified with larger flow initiation areas generating greater DTW values. Our results show that optimal flow initiation area depends on the topography of the terrain. The relatively

flat (i.e., slope of 2.5%) topography of the Grande Prairie site was better captured with a smaller flow initiation area (i.e., 1 ha), whereas the Whitecourt site with a more pronounced topography (i.e., 10.9%) was more strongly represented by larger flow initiation areas (i.e., 12 or 16 ha). These findings are consistent with a study from Sweden that also emphasized the importance of substrate permeability, since it controls drainage rate of water (Ågren et al. 2014).

At the Whitecourt site, DTW calculated at a larger flow initiation area provided better differentiation between raster cells on the ridge and those at the bottom of the slope. For example, with a flow initiation area of 16 ha only 7.75 ha of the 77.52 ha (Fig. 3.1) were classified with DTW < 1 m, whereas at 0.5 ha catchment area 37.44 ha had DTW < 1 m. In contrast, the effects of the minor topographic variation at the Grande Prairie site is only reflected with a small flow initiation area as lateral water movement is slow and the soil becomes saturated quickly. The 0.5 ha flow initiation area produced a DTW raster with 66.02 ha below 1 m, while around 21.36 ha had DTW < 1 m with a 16 ha catchment area. As expected, a larger proportion of the area has low DTW values in the flat landscape while the difference between small and large flow initiation areas is less visible than at the steeper site.

4.3. Differences between the species

The mean $\delta^{13}C$ of aspen was slightly lower than that of spruce, pattern consistent but less distinct than a study which found that $\delta^{13}C$ of *Acer saccharinum* L. was lower by over 2‰ than $\delta^{13}C$ of *Pinus strobus* L. (Leavitt 1993). However, the order of aspen relative to spruce in our study changed under different climatic and topographic conditions. Aspen $\delta^{13}C$ showed a steep increase with increasing DTW after which it levelled off, while the relationship was more gradual for spruce (Fig. 3.4). This suggests that even very subtle changes in topography, captured thanks to the high resolution of the DEM, might create site conditions different enough to result

in variation in stomatal regulation in aspen. The relationship between aspen $\delta^{13}C$ and DTW is similar to the response of stomatal conductance and photosynthesis measured in aspen seedlings to drought treatments (Lu et al. 2010); stomatal conductance drops sharply starting at 0.5 fraction of extractable soil water, followed by a sudden decline in photosynthetic rates. Thus, the relation between aspen $\delta^{13}C$ and DTW does not imply that all microsite conditions are the same at DTW > 0.4 m, but it indicates the sensitivity and swift response of aspen to water stress. In contrast, the gradual increase of spruce $\delta^{13}C$ with DTW might be attributed to the higher drought tolerance of spruce but also to the higher MAP at the Whitecourt site. Aspen stomata are fully closed and leaves start to die at xylem pressure potential of −2 MPa (Lu et al. 2010) while spruce can still show high stomatal conductance and carbon fixation rates, but with large variability between individuals (Bigras 2005). Further, the higher amounts of precipitation, as well as possibly more favourable soil conditions, at the Whitecourt site might diminish the importance of topography in creating water stress in spruce trees. At very high DTW values (i.e., larger than 7 – 8 m), site conditions might lower the capacity of soils to hold water due to steeper slopes with shallow soils that have coarse texture (Murphy et al. 2011), effectively overriding the effects of abundant precipitation.

4.4. Tree size and topography

The different origin of the two stands and subsequent silvicultural operations have had a strong influence on the height and diameter growth rates of the trees; the aspen stand regenerated naturally from very dense root suckers whereas the spruce trees were planted at a lower density and deciduous competition was controlled with herbicides. Tree height varied more widely at the spruce site since the northern part of that area (i.e., dark blue in Fig. 3.1) was covered by a bog where trees were shorter. Tree height was more strongly related to DTW than diameter since

secondary growth is affected by stand structure to a greater extent than elongation of the terminal shoot (Oliver and Larson 1996). The stronger relationship between height and DTW in the case of spruce might be explained by the stronger topographic gradients at the Whitecourt site, exerting a tighter control on soil attributes.

The relationship between tree size and DTW followed a similar pattern to that found for $\delta^{13}C$, suggesting that tree size does not increase with DTW after a certain DTW value. Most of the range in aspen tree height occurred at DTW < 0.9 m, but the over 3 m variation in height at larger DTW values (Fig. 3.6) indicates that some site conditions responsible for this variation are not captured by DTW. The same happened in the case of spruce, where the DTW threshold shifted to 11 m. As indicated previously, DTW was not able to represent soil nutrient regime (see Chapter 2), which may contribute to this variation in tree heights at larger DTW values. Other authors reported weak to no relationships between tree size and other topographic indices. The coarse resolution (i.e., 30 – 35 m) DEM used to calculate TWI might not reveal enough terrain details to accurately represent site conditions and predict tree height of *Chamaecyparis obtusa* (Siebold & Zucc.) Endl. (Ehara et al. 2009) or radial growth in *Pinus densiflora* Siebold & Zucc. (Byun et al. 2013).

The positive relationship between $\delta^{13}C$ and tree size implied by Fig. 3.4 and Fig. 3.6 would suggest that water stressed trees reach larger sizes. However, this relationship between biomass production and $\delta^{13}C$ has been attributed to higher carbon demand and water use efficiency by larger trees (Johnsen et al. 1999; Livingston et al. 1999; Sun et al. 1996). This perspective might imply that the relationship between $\delta^{13}C$ and DTW is not direct and was only found because of the effect of DTW on tree size. But tree size is controlled by water and nutrient availability, soil properties that are partly captured by DTW (see Chapter 2). Moreover, $\delta^{13}C$ was

not related with crown surface area per unit basal area for either of the two species, which indicates that higher water demand from trees with larger crowns per unit basal area does not alter isotopic composition. Another alternative explanation is that bigger trees might actually grow better on well drained sites (i.e., larger DTW values), with fast rates of carbon assimilation leading to less discrimination against ^{13}C.

5. Conclusions

This study presents a model that uses information at two scales, small-scale through a topographic index and large-scale through a climate variable, to explain variation in carbon isotope discrimination as a measure of tree physiological activity. The DTW topographic index could potentially be used to delineate the most and least drought prone areas during years with low amounts of precipitation, and help explain the spatial variability in drought related mortality in the boreal forest (Hogg et al. 2008). More importantly, our results validate the DTW index as a tool that can provide information about the status of individual trees, particularly the effects of water availability in the soil on tree functioning. Results also highlight the importance of choosing flow initiation areas that are appropriate to local site characteristics to permit accurate representation of site properties through the DTW index. Tree height can be measured from LiDAR point clouds or estimated using empirical models, but the model presented here implies a functional relationship of tree height with a terrain attribute that captures site conditions controlling tree growth. This opens the way for future studies that can evaluate the potential to use the DTW index as predictor of stand-levels properties, especially site productivity.

Literature cited

Adams, H.R., Barnard, H.R., and Loomis, A.K. 2014. Topography alters tree growth-climate relationships in a semi-arid forested catchment. Ecosphere **5**(11). doi: 10.1890/es14-00296.1.

Ågren, A.M., Lidberg, W., Strömgren, M., Ogilvie, J., and Arp, P.A. 2014. Evaluating digital terrain indices for soil wetness mapping – a Swedish case study. Hydrol. Earth Syst. Sci. **18**(9): 3623-3634. doi: 10.5194/hess-18-3623-2014.

Allen, R.B., Peet, R.K., and Baker, W.L. 1991. Gradient analysis of latitudinal variation in Southern Rocky Mountain forests. J. Biogeogr. **18**(2): 123-139. doi: 10.2307/2845287.

Berry, J.A. 1988. Studies of mechanisms affecting the fractionation of carbon isotopes in photosynthesis. *In* Stable isotopes in ecological research. *Edited by* P.W. Rundel, J. R. Ehleringer and K. A. Nagy. pp. 82-94.

Beven, K.J., and Kirkby, M.J. 1979. A physically based, variable contributing area model of basin hydrology. Hydrol. Sci. Bul. **24**(1): 43-69. doi: 10.1080/02626667909491834.

Bigras, F.J. 2005. Photosynthetic response of white spruce families to drought stress. New For. **29**(2): 135-148. doi: 10.1007/s11056-005-0245-9.

Bladon, K.D., Silins, U., Landhausser, S.M., Messier, C., and Lieffers, V.J. 2007. Carbon isotope discrimination and water stress in trembling aspen following variable retention harvesting. Tree Physiol. **27**(7): 1065-1071.

Brubaker, S.C., Jones, A.J., Lewis, D.T., and Frank, K. 1993. Soil properties associated with landscape position. Soil Sci. Soc. Am. J. **57**(1): 235-239.

Buchmann, N., Kao, W.Y., and Ehleringer, J. 1997. Influence of stand structure on carbon-13 of vegetation, soils, and canopy air within deciduous and evergreen forests in Utah, United States. Oecologia **110**(1): 109-119. doi: 10.1007/s004420050139.

Burgess, S.S.O., Adams, M.A., Turner, N.C., and Ong, C.K. 1998. The redistribution of soil water by tree root systems. Oecologia **115**(3): 306-311. doi: 10.1007/s004420050521.

Burt, T.P., and Butcher, D.P. 1985. Topographic controls of soil moisture distributions. J. Soil Sci. **36**(3): 469-486.

Byun, J.G., Lee, W.K., Kim, M., Kwak, D.A., Kwak, H., Park, T., Byun, W.H., Son, Y., Choi, J.K., Lee, Y.J., Saborowski, J., Chung, D.J., and Jung, J.H. 2013. Radial growth response of Pinus densiflora and Quercus spp. to topographic and climatic factors in South Korea. Journal of Plant Ecology **6**(5): 380-392. doi: 10.1093/jpe/rtt001.

Cox, D.R., and Snell, E.J. 1989. The analysis of binary data. 2nd ed. Chapman and Hall, London. pp. 208-209.

Ehara, H., Matsue, K., Shuin, Y., Aizawa, M., and Ohkubo, T. 2009. Validity of height estimation of Hinoki cypress using soil moisture indices based on the digital terrain model in Utsunomiya University Forests at Funyu. Bul. Utsunomiya Univ. For.(45): 9-16.

Farquhar, G.D., Ehleringer, J.R., and Hubick, K.T. 1989. Carbon isotope discrimination and photosyntehsis. Annu. Rev. Plant Physiol. Plant Molec. Biol. **40**: 503-537. doi: 10.1146/annurev.arplant.40.1.503.

Farquhar, G.D., Oleary, M.H., and Berry, J.A. 1982. On the relationship between carbon isotope discrimination and the inter-cellular carbon dioxide concentration in leaves. Aust. J. Plant Physiol. **9**(2): 121-137.

Francey, R.J., and Farquhar, G.D. 1982. An explanation of 13C/12C variations in tree rings. Nature **297**(5861): 28-31.

Garten, C.T., and Taylor, G.E. 1992. Foliar delta C-13 within a temperate deciduous forest - spatial, temporal, and species sources of variation. Oecologia **90**(1): 1-7. doi: 10.1007/bf00317801.

Guntner, A., Seibert, J., and Uhlenbrook, S. 2004. Modeling spatial patterns of saturated areas: An evaluation of different terrain indices. Water Resour. Res. **40**(5). doi: 10.1029/2003wr002864.

Hanba, Y.T., Noma, N., and Umeki, K. 2000. Relationship between leaf characteristics, tree

sizes and species distribution along a slope in a warm temperate forest. Ecological Research **15**(4): 393-403. doi: 10.1046/j.1440-1703.2000.00360.x.

Hogg, E.H., Brandt, J.P., and Michaellian, M. 2008. Impacts of a regional drought on the productivity, dieback, and biomass of western Canadian aspen forests. Can. J. For. Res. **38**(6): 1373-1384. doi: 10.1139/x08-001.

Johnsen, K.H., Flanagan, L.B., Huber, D.A., and Major, J.E. 1999. Genetic variation in growth, carbon isotope discrimination, and foliar N concentration in *Picea mariana*: analyses from a half-diallel mating design using field-grown trees. Can. J. For. Res. **29**(11): 1727-1735. doi: 10.1139/cjfr-29-11-1727.

Kopecky, M., and Cizkova, S. 2010. Using topographic wetness index in vegetation ecology: does the algorithm matter? Appl. Veg. Sci. **13**(4): 450-459. doi: 10.1111/j.1654-109X.2010.01083.x.

Leavitt, S.W. 1993. Seasonal C-13/C-12 changes in tree rings - species and site coherence, and a possible drought influence. Can. J. For. Res. **23**(2): 210-218. doi: 10.1139/x93-028.

Leavitt, S.W., and Long, A. 1984. Sampling strategy for stable carbon isotope analysis of tree rings in pine. Nature **311**(5982): 145-147. doi: 10.1038/311145a0.

Leavitt, S.W., and Long, A. 1986. Stable carbon isotope variability in tree foliage and wood. Ecology **67**(4): 1002-1010. doi: 10.2307/1939823.

Livingston, N.J., Guy, R.D., Sun, Z.J., and Ethier, G.J. 1999. The effects of nitrogen stress on the stable carbon isotope composition, productivity and water use efficiency of white spruce (Picea glauca (Moench) Voss) seedlings. Plant Cell and Environment **22**(3): 281-289. doi: 10.1046/j.1365-3040.1999.00400.x.

Lu, Y., Equiza, M.A., Deng, X., and Tyree, M.T. 2010. Recovery of *Populus tremuloides* seedlings following severe drought causing total leaf mortality and extreme stem embolism. Physiologia Plantarum **140**(3): 246-257. doi: 10.1111/j.1399-3054.2010.01397.x.

MacCormack, K.E., Atkinson, N., and Lyster, S. 2015. Bedrock topography of Alberta, Canada.

Alberta Geological Survey, Edmonton, AB.

Major, J. 1951. A functional, factorial approach to plant ecology. Ecology **32**(3): 392-412. doi: 10.2307/1931718.

Meinzer, F.C., Rundel, P.W., Goldstein, G., and Sharifi, M.R. 1992. Carbon isotope composition in relation to leaf gas-exchange and environmental conditions in Hawaiian *Metrosideros polymorpha* populations. Oecologia **91**(3): 305-311. doi: 10.1007/bf00317617.

Monserud, R.A., and Marshall, J.D. 2001. Time-series analysis of delta C-13 from tree rings. I. Time trends and autocorrelation. Tree Physiol. **21**(15): 1087-1102.

Moore, I.D., Gessler, P.E., Nielsen, G.A., and Peterson, G.A. 1993. Soil attribute prediction using terrain analysis. Soil Sci. Soc. Am. J. **57**(2): 443-452. doi: 10.2136/sssaj1993.03615995005700020026x.

Moore, I.D., Grayson, R.B., and Ladson, A.R. 1991. Digital terrain modelling: a review of hydrological, geomorphological, and biological applications. Hydrol. Process. **5**(1): 3-30. doi: 10.1002/hyp.3360050103.

Murphy, P.N.C., Ogilvie, J., and Arp, P. 2009. Topographic modelling of soil moisture conditions: a comparison and verification of two models. Eur. J. Soil Sci. **60**(1): 94-109. doi: 10.1111/j.1365-2389.2008.01094.x.

Murphy, P.N.C., Ogilvie, J., Connor, K., and Arpl, P.A. 2007. Mapping wetlands: A comparison of two different approaches for New Brunswick, Canada. Wetlands **27**(4): 846-854. doi: 10.1672/0277-5212(2007)27[846:mwacot]2.0.co;2.

Murphy, P.N.C., Ogilvie, J., Meng, F.R., White, B., Bhatti, J.S., and Arp, P.A. 2011. Modelling and mapping topographic variations in forest soils at high resolution: A case study. Ecol. Model. **222**(14): 2314-2332. doi: 10.1016/j.ecolmodel.2011.01.003.

Nagelkerke, N.J.D. 1991. A note on a general definition of the coefficient of determination. Biometrika **78**(3): 691-692. doi: 10.1093/biomet/78.3.691.

Niinemets, U., Cescatti, A., Lukjanova, A., Tobias, M., and Truus, L. 2002. Modification of light-acclimation of Pinus sylvestris shoot architecture by site fertility. Agric. For. Meteorol. **111**(2): 121-140. doi: 10.1016/s0168-1923(02)00011-4.

O'Callaghan, J.F., and Mark, D.M. 1984. The extraction of drainage networks from digital elevation data. Comput. Vision Graph. **28**(3): 323-344. doi: 10.1016/s0734-189x(84)80011-0.

Oliver, C.D., and Larson, B.C. 1996. Forest stand dynamics. Update edition ed. John Wiley & Sons, Inc., New York.

Pinheiro, J.C., and Bates, D.M. 1995. Model building for nonlinear mixed-effects models. University of Wisconsin–Madison. 91.

Pinheiro, J.C., and Bates, D.M. 2000. Mixed-effects models in S and S-PLUS. Springer-Verlag, New York, NY. pp. 57-96; 201-225; 305-336.

Pinheiro, J.C., Bates, D.M., DebRoy, S., Sarkar, D., and Team, R.C. 2015. nlme: Linear and nonlinear mixed effects models. *In* http://CRAN.R-project.org/package=nlme.

R Core Team. 2015. *R: A language and environment for statistical computing*. R Foundation for Statistical Computing, Vienna, Austria.

Roden, J.S., Johnstone, J.A., and Dawson, T.E. 2011. Regional and watershed-scale coherence in the stable-oxygen and cabon isotope ratio time series in tree rings of coast redwood (*Sequoia sempervirens*). Tree-Ring Research **67**(2): 71-86.

Schulze, E.D., Williams, R.J., Farquhar, G.D., Schulze, W., Langridge, J., Miller, J.M., and Walker, B.H. 1998. Carbon and nitrogen isotope discrimination and nitrogen nutrition of trees along a rainfall gradient in northern Australia. Aust. J. Plant Physiol. **25**(4): 413-425.

Seibert, J., Stendahl, J., and Sorensen, R. 2007. Topographical influences on soil properties in boreal forests. Geoderma **141**(1-2): 139-148. doi: 10.1016/j.geoderma.2007.05.013.

Silim, S.N., Guy, R.D., Patterson, T.B., and Livingston, N.J. 2001. Plasticity in water-use efficiency of *Picea sitchensis*, *Picea glauca* and their natural hybrids. Oecologia **128**(3): 317-

325.

Sohn, J.A., Gebhardt, T., Ammer, C., Bauhus, J., Haeberle, K.-H., Matyssek, R., and Grams, T.E.E. 2013. Mitigation of drought by thinning: Short-term and long-term effects on growth and physiological performance of Norway spruce (Picea abies). For. Ecol. Manag. **308**: 188-197. doi: 10.1016/j.foreco.2013.07.048.

Sorensen, R., Zinko, U., and Seibert, J. 2006. On the calculation of the topographic wetness index: evaluation of different methods based on field observations. Hydrol. Earth Syst. Sci. **10**(1): 101-112.

Sun, Z.J., Livingston, N.J., Guy, R.D., and Ethier, G.J. 1996. Stable carbon isotopes as indicators of increased water use efficiency and productivity in white spruce (*Picea glauca* (Moench) Voss) seedlings. Plant Cell and Environment **19**(7): 887-894. doi: 10.1111/j.1365-3040.1996.tb00425.x.

Tarboton, D.G. 1997. A new method for the determination of flow directions and upslope areas in grid digital elevation models. Water Resour. Res. **33**(2): 309-319. doi: 10.1029/96wr03137.

Walia, A., Guy, R.D., and White, B. 2010. Carbon isotope discrimination in western hemlock and its relationship to mineral nutrition and growth. Tree Physiol. **30**(6): 728-740. doi: 10.1093/treephys/tpq020.

Waring, R.H., and Silvester, W.B. 1994. Variation in foliar delta C-13 values within the crowns of *Pinus radiata* trees. Tree Physiol. **14**(11): 1203-1213.

Warren, C.R., McGrath, J.F., and Adams, M.A. 2001. Water availability and carbon isotope discrimination in conifers. Oecologia **127**(4): 476-486. doi: 10.1007/s004420000609.

White, B., Ogilvie, J., Campbell, D.M.H., Hiltz, D., Gauthier, B., Chisholm, H.K., Wen, H.K., Murphy, P.N.C., and Arp, P.A. 2012. Using the cartographic depth-to-water index to locate small streams and associated wet areas across landscapes. Can. Water Resour. J. **37**(4): 333-347. doi: 10.4296/cwrj2011-909.

Chapter 4

Using the topographic depth-to-water index to estimate trembling aspen site index in the boreal forest

Abstract

Accurate estimates of site index in the boreal forest are needed to support growth and yield projections, and management decisions. Topographic indices have been linked to site and soil properties which control potential forest productivity and consequently can serve as estimators of site index. The depth-to-water (DTW) index quantifies the hydrological connectivity between any cell in the landscape and flow channels, as sources of water. We obtained DTW averages and trembling aspen site index (SI) estimates for 150 stands, and completed field assessments of soil attributes in 115 of these stands across five locations in the mixedwood natural subregion of the boreal forest of Alberta, Canada. Our objectives were (1) to show the relation between soil attributes and aspen SI, (2) find the optimal flow initiation area to calculate DTW, and (3) evaluate the utility of DTW in estimating aspen SI. We found that slightly rich mesic sites with larger depth to the mottling layer produce maximum aspen SI. Rich sites would be expected to improve growing conditions but they are also wetter which reduces site quality for aspen. Although not statistically significant well drained soils yield highest SI, while texture, coarse fragments content and organic matter thickness were not related with aspen productivity. DTW calculated at 4 ha (or 2 ha) flow initiation area produced best results, but this model was only half as strong as the soil-SI model due to its inability to capture nutrient regime.

1. Introduction

Accurate estimation of forest site productivity is critical to growth and yield models, making effective silvicultural decisions and predicting the response of forest productivity under altered climate regimes. Site index has been used to generate yield tables (Barnes et al. 1998) and is the key driver of the growth functions developed for the Mixedwood Growth Model used in the western Canadian boreal forest (Bokalo et al. 2013). Furthermore, in order to achieve forest management goals, the nature, timing and intensity of silvicultural operations is adapted to site quality defined by site index classes (Daniel et al. 1979).

Site index (SI) is widely used as a measure of site productivity because of its direct relationship with volume growth and ease of measurement (Skovsgaard and Vanclay 2008). Despite its extensive application and wide acceptability, SI of a species cannot be estimated if there are no suitable trees present on site or their age cannot be accurately determined. This occurs frequently in older stands of the boreal mixedwood forests when the overstory dominated by trembling aspen (*Populus tremuloides* Minchx.) breaks up due to stem decay (Chen and Popadiouk 2002). Furthermore, stem analysis will not reveal the true SI if early height growth is suppressed by an overstory, as commonly happens with white spruce (*Picea glauca* (Moench) Voss) growing under an aspen canopy in these stands (Osika et al. 2013). It is generally accepted that top height is not influenced by thinning regimes and Lanner (1985) provides a source-sink physiology argument to support this, although empirical observations suggests that very low or very high stand densities can impact height and volume growth (Assmann 1970; Smith et al. 1997). Given the great importance of SI as a measure of site productivity and the noted limitations, numerous studies have sought to establish functional relationships between SI and environmental factors defining site quality (Bontemps and Bouriaud 2014).

Soil moisture and nutrient levels along with climate variables that control their availability have been widely found to explain variation in SI across species and areas. Wang and Klinka (1996) found that soil moisture regime (SMR) accounted for 81% of variation in SI of white spruce in the Sub-Boreal Spruce zone in British Columbia, which increased to 90% if aeration and nutrient regime (SNR) were added to the regression model. A slightly lower R^2 value of 85% was reported for coastal Douglas-fir (*Pseudotsuga menziesii* (Mirb.) Franco) using field estimates of SMR and SNR (Klinka and Carter 1990). They also showed that characterizing SMR and SNR with a calculated water deficit index and mineralizable nitrogen yielded a poorer model (i.e., R^2 = 63%). Ung et al. (2001) combined water holding capacity, degree-days and aridity index into a biophysical SI model for four species in the boreal forest, of which aspen SI was best described with an R^2 of 69%. More detailed soil properties including C:N ratio, electrical conductivity and proportion of very fine sand were also significantly correlated with aspen SI (Pinno et al. 2009). Larger scale studies allow the integration of climate into SI prediction models as showed by Chen et al. (2002) who used elevation, latitude and longitude together with SMR and SNR to model aspen SI in British Columbia. A regional study focused on climatic factors found that degree-days below 0 °C, growing season precipitation and temperature amplitude explain 68% of the variation in SI in the western United States (Weiskittel et al. 2011). While these examples highlight the potential utility of soil moisture and nutrients as predictors of SI, the use of such models is restricted by the effort and cost associated with acquiring these site and soil data (Bontemps and Bouriaud 2014).

Topography directs the gravitational movement of water on and in the soil and thus controls fine scale (e.g., hillslope, sub-watershed) spatial variation in soil properties. This, coupled with the wide availability of high accuracy digital elevation models (DEM) derived from

LiDAR point clouds (Hodgson et al. 2003) enables predictive mapping of site and soil properties using topographic indices. The topographic wetness index (TWI), defined as the ratio of the contributing area to the local slope (Beven and Kirkby 1979), has been widely used for this purpose. In one study, up to 64% of the variation in A horizon depth, organic matter, extractable phosphorus, pH, and sand and silt proportion was explained by TWI and other terrain attributes (Moore et al. 1993), while 53% of soil moisture variability was accounted for by TWI in the boreal landscape of Sweden (Sorensen et al. 2006). In the same area, Holmgren (1994) found that a combination of remotely sensed topographic indices and field-assessed soil properties were more strongly related with SI of Scots pine (*Pinus sylvestris* L.) than Norway spruce (*Picea abies* (L.) H.Karst). Earlier, Tom and Miller (1980) employed Landsat imagery to map SI in a north-western Colorado forest, emphasizing the need for high quality remotely sensed data.

In this study we evaluate use of the depth-to-water index (DTW), developed by Murphy et al. (2007) to map wet areas. Studies indicate that DTW performed better than TWI when used to map wet areas in the boreal forest (Murphy et al. 2009) and in the riparian forests of the tropical zone (Maillard and Alencar-Silva 2013). Further, SMR was more accurately mapped using DTW than with TWI in the boreal forest (Ågren et al. 2014). The extent of the flow channel network necessary to initiate the DTW algorithm is defined by the flow initiation area (i.e., catchment area). Adjusting flow initiation area was shown to enhance DTW performance in areas with different topography and geology (Ågren et al. 2014). The objectives of our study were: (1) to explore the relationship between trembling aspen SI and site and soil properties, (2) to determine the optimal flow initiation area for estimating SI, and (3) to evaluate remotely-sensed topographic indices in site index prediction models. We hypothesize that SMR and SNR will be the strongest predictors of aspen SI, while DTW calculated at a smaller flow initiation

area will better represent the spatial variation of aspen SI in the boreal landscape.

2. Materials and methods

2.1. Study sites

Five sites dominated by aspen from the Central Mixedwood natural subregion of the boreal forest in northern Alberta were used to collect the SI and soil data (Table 4.1). Four of these sites were harvested between 1991 and 1992 and subsequently became part of a long term study (Bokalo et al. 2007), involving thinning of aspen to a range of densities from 200 stems per ha to unthinned. The fifth, Judy Creek (JC), research site (Pitt et al. 2010) was harvested in 2003 without applying a general thinning regime. The four older study sites (i.e., DMI_HC, DMI_PR WGP, SRD,) had soils defined by fine textured glacial till deposits, while at JC a layer of rounded cobble at a depth of 25–40 cm was formed by postglacial fluvial activity. Slopes range from 2 to 11% creating elevational differences of 3 m at SRD (16 ha) up to 14 m at JC (18 ha).

The Boreal Mixedwood ecological area has a mean annual temperature of 1.5 °C and receives around 389 mm of precipitation, of which 60% falls in the summer when the mean temperature is around 13.7 °C (Beckingham and Archibald 1996). Climatic variation across the

Table 4.1. Summary of the geographic location, range of aspen site index, soil moisture regime (SMR) and climate at the five study sites. MAT – mean annual temperature, MAP – mean annual precipitation.

Study site	Plots	Latitude (° N)	Longitude (° W)	Elevation (m)	Site index (m)	SMR	MAT* (°C)	MAP* (mm/yr)	Weather Canada station
JC	34	54.3826	115.6398	1002.1	17.3–21.0	5.2	2.9	544.4	Whitecourt A
WGP	38	54.8864	118.9393	701.1	15.8–23.4	5.4	2.4	478.2	Grovedale RS
SRD	26	55.2982	114.0982	622.4	19.6–23.7	4.7	2.1	480.6	Slave Lake A
DMI_HC	26	56.3992	118.6029	795.7	19.5–24.8	5.2	0.0	436.2	Eureka River
DMI_PR	26	56.4071	117.7777	731.4	18.1–23.1	5.1	1.6	386.3	Peace River A

* extracted from "1981–2010 Canadian Climate Normals" available online at http://climate.weather.gc.ca accessed on July 10, 2014.

five locations can induce systematic differences which need to be considered in the analysis. Most of the soils formed at these five sites fall in the Great Group of gray luvisols—with a characteristic clay accumulation horizon—while some are eutric brunisols. Trembling aspen dominates the forest cover with some white spruce in the understory and lodgepole pine (*Pinus contorta* Douglas) on drier raised sites or black spruce (*Picea mariana* Mill.) in wet depressions.

2.2. Site index estimation and soil data collection

The geographical location of the plots was mapped using a Trimble GeoExplorer 6000 series GeoXT handheld device (Trimble, Los Altos, California) with GNSS capabilities which ensured sub-meter accuracy for 89% of the positions. We used the top height model for aspen published by Huang et al. (2009) to estimate SI at age 50 for all plots (N = 150) based on top height and total age, where top height trees are defined as the 100 largest diameter trees per ha. Total age of trees for site index estimation was 10 yrs for JC and 17 at the other sites. Top height trees in the unthinned plots (n = 8) at WGP were measured at age 21. Tree density ($P = 0.10$) or total age ($P = 0.06$) did not have a strong effect on the estimated SI values.

During the summer of 2013 a soil pit was excavated in 115 plots and the methodology in Beckingham and Archibald (1996) was followed to determine organic matter thickness, humus form, effective texture (i.e., texture of the finest textured horizon at least 10 cm thick located within the first 60 cm), depth-to-mottles (DtMot), coarse fragments content and drainage class (imperfect, moderately well, well). General site characteristics (i.e., slope, aspect) and plant species composition were used together with soil properties to determine SMR and SNR, thus these two measures integrate the spatial and temporal variability of moisture and nutrient conditions of the plots and can be considered site properties. Imperfectly to moderately well drained sites on slight slopes that receive water from precipitation and through seepage were

considered *subhygric*. Sites in midslope positions where precipitation is the main source of water were defined as *mesic* if they are more actively drained with a thinner organic matter layer. *Submesic* sites were located on upper slopes which were rapidly to well drained with a shallow organic layer.

2.3. The depth-to-water index

The DEM used was derived from an airborne Light Detection and Ranging point cloud with 0.5 to 3 returns per square meter at a vertical accuracy of 30 cm. The 1 m resolution DEM was hydrologically conditioned to remove false depressions that artificially obstruct water flow and then used to determine flow direction based on the slope to the eight neighbouring cells. Flow accumulation (FA) area was calculated using the D8 flow routing algorithm, which directs flow to one adjacent cell with the steepest downslope gradient, recommended to define flow channels (Tarboton 1997). We used threshold values of 0.5, 1, 2, 4, 8, 12 and 16 ha to define the flow initiation area which indicates the starting point of the flow channels (Fig. 4.1). Once the flow channels are found, the DTW index can be computed as the cumulative slope along the least-cost path from any cell in the landscape to the nearest flow channel, expressed as

$$DTW = \left[\sum \frac{dz_i}{dx_i} a\right] x_c \ (m),$$

where dz_i and dx_i are the vertical and horizontal distance between two cells, a is a constant equal to 1 if the path is parallel to the cell edge or $\sqrt{2}$ if the connection is made across the diagonal, and x_c is the size of the raster cell (i.e., 1 m). The cells which delineate the flow channels are assigned a DTW value of 0. Thus, both horizontal and vertical distance are integrated and a cell at a higher elevation or farther from the channel will receive a larger DTW value indicating that the cell and the flow channel are less hydrologically connected (Murphy et al. 2009).

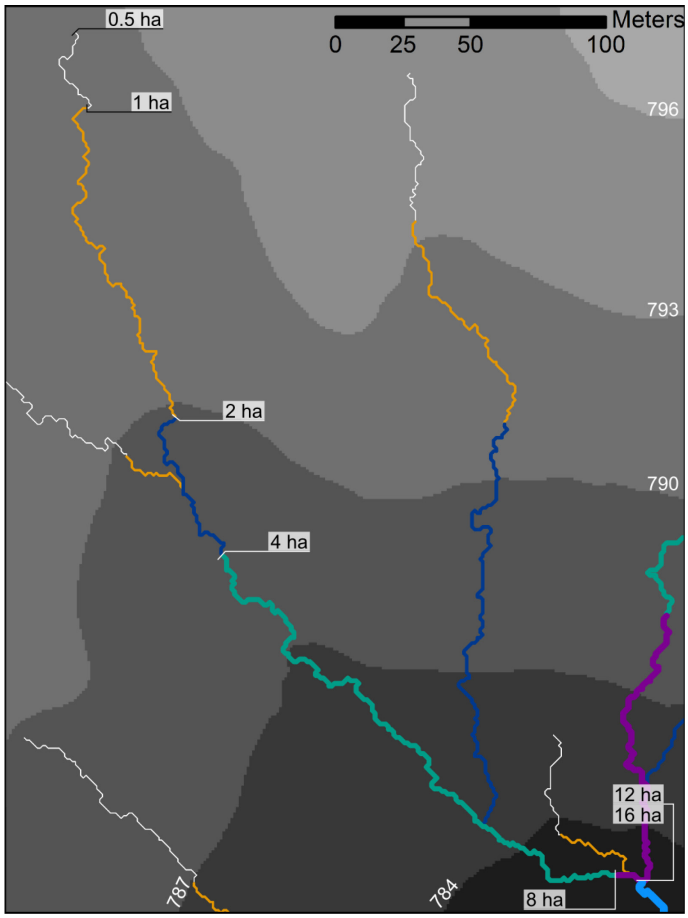

Figure 4.1. Flow channels defined at 0.5, 1, 2, 4, 8, 12 and 16 ha flow initiation area overlaid on the digital elevation model. The numbers on the margins indicate the elevation in meters. Note that the 12 and 16 ha points overlap.

2.4. Statistical analysis

Trembling aspen SI was the dependent variable and was treated as a continuous variable sampled from a normally distributed population. Site and soil properties were considered continuous variables; drainage regime was assigned values of 3, 4, and 5 corresponding to well, moderately well and imperfect drainage, respectively; SNR took values of 3 and 4 for medium and rich sites; and SMR classes of submesic, mesic and subhygric were coded with values 4, 5, and 6, respectively. Treating these as continuous variables agrees with their continuous nature and permitted us to accurately code intermediate sites. Elevation, slope, DTW and FA were averaged for each plot and extracted using ArcGIS 10.1 (ESRI, Redlands, California); FA can

take very large values, therefore it was log-transformed. Total sample size was 150 plots of which only 115 plots were assessed for soil attributes; only 64 plots could be used in the analysis of DtMot (i.e., the plots where the mottling layer was present).

Linear and nonlinear mixed-effects models were used in order to account for the variation among the five locations—the WGP and JC sites had lower average SI values (19.2 and 19.3 m), while DMI_HC had the highest (22.2 m). The normal function was used to model the nonlinear relationship suggested by Shelford's law of tolerance where it was supported by ecological reasoning. The advantage of this function is given by the biologic interpretation of its parameters (Fig. 4.2) and its superiority over a second order polynomial. The extremum value is controlled by parameter *a*, while parameter *c* gives the location of the extremum. If parameter $b = 1$ then the function becomes a straight horizontal line indicating no association between the two variables. When $b > 1$ the curve is concave and has a minimum, while $b < 1$ gives a convex curve with a maximum. In our analyses only values of *b* less than 1 support the pattern described by the law of tolerance, therefore the null hypothesis of no relationship between SI and the environmental factors (i.e., $b \geq 1$) was tested using one-tailed t-tests conditional on the random effects.

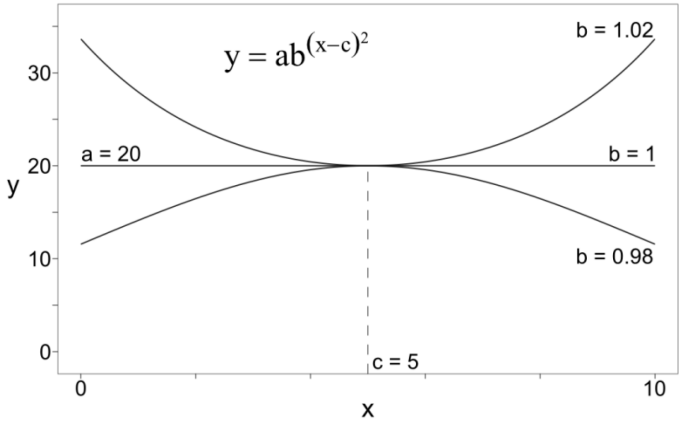

Figure 4.2. Diagram showing the interpretation of the parameters involved in the normal function used in the analysis. See text in section 2.4 for details.

The parameters corresponding to the fixed effects and the conditional modes of the random effects were found with the method of maximum likelihood as implemented by Pinheiro and Bates (2000) in the S language. The value of the maximized log-likelihood (l) was used to assess the explanatory power of the different independent variables tested. The model used was

$$\boldsymbol{y}_i = f(\boldsymbol{A}_i\boldsymbol{\beta} + \boldsymbol{B}_i b_i) + \boldsymbol{\varepsilon}_i, \qquad i = 1, \ldots, 5, \tag{Eq. 4.1}$$

$$b_i \sim N(0, \sigma_b^2), \qquad \boldsymbol{\varepsilon}_i \sim N(\mathbf{0}, \sigma^2 \boldsymbol{\Lambda}_i),$$

where $\boldsymbol{y}_i$ is a vector of SI at each location, f is the normal function or a linear model, $\boldsymbol{\beta}$ is a vector of the fixed effects, $\boldsymbol{A}_i$ and $\boldsymbol{B}_i$ are regressor matrices of the fixed and random effects. The random effects, b_i, were applied to the intercept of the linear models and to parameter a of the normal function, for all models shown in Table 4.1 in order to ensure comparability of the fixed-effects. The errors were assumed to be independent and identically distributed (i.i.d.) as normal with mean 0 and variance that was weighted by location, in order to reduce the standard error of the estimates which could otherwise inflate the probability of Type II error. Location WGP had the widest range of SI values and JC the narrowest, whereas DMI_HC, DMI_PR and SRD had similar variances and were pooled to reduce the number of estimated parameters and set to 1 in order to solve for the variance parameters, δ_i. For models 2 and 3 we used the strategy outlined by Pinheiro and Bates (1995) to determine the necessary random effects and select covariates to explain parameter variability between location. All mixed-models were fit using the nlme library v. 3.1-120 (Pinheiro et al. 2015) within the R environment v. 3.2.0 (R Core Team 2015).

3. Results

3.1. Site index in relation to site and soil properties

Soil nutrient and moisture regime exhibited the expected pattern and were the strongest

predictors of aspen SI (Table 4.2). The shape parameter of the normal function used to model these relations was less than 1 for both SMR ($b = 0.97$, $P = 0.0079$) and SNR ($b = 0.93$, $P = 0.0008$). Drainage regime showed the predicted nonlinear trend but $b = 0.98$ was not significantly less than 1 ($P = 0.1298$) at $\alpha = 0.05$. Depth-to-mottles produced a positive linear trend with SI (Fig. 4.3) with a slope of $b = 0.03$ that was significantly different from 0 ($P = 0.0284$). Effective texture, coarse fragment content and organic matter thickness were not related with aspen SI (Table 4.2).

The two most important site and soil factors—SMR and SNR—were then combined into a normal model with two independent variables, which provided a superior fit to that of SMR or SNR used individually ($l = -187.87 > -190.34 > -191.08$, Table 4.3). Both predictors contributed significantly (SMR: $P = 0.0180$; SNR: $P = 0.0114$) and indicated that maximum SI of 21.1 m was achieved on slightly rich mesic sites (Fig. 4.4). This model can be expressed as

$$SI_{ij} = (\beta_1 + b_i)\beta_2^{(SMR_{ij}-\beta_3)^2}\beta_4^{(SNR_{ij}-\beta_5)^2} + \varepsilon_{j(i)}, \quad \text{(Eq. 4.2)}$$

where SI_{ij} was the jth observation at study site i, and $\beta_1 ... \beta_5$ represented the parameters of the normal function. The random effects b_i were assumed to be i.i.d. as $b_i \sim N(0, \sigma_b^2)$, where σ_b^2 was the variance component, and the errors nested within the location to be i.i.d. as $\varepsilon_{j(i)} \sim N(0, \sigma^2\delta_i^2)$. The variance function (δ_i) allowed for the larger spread at WGP and DMI_PR, and the small variance of SI at JC, while DMI_HC and SRD were pooled. The errors did not show systematic bias and were normally distributed, confirmed by Q-Q plots and the Kolmogorov-Smirnov test ($P = 0.5284$, Fig. 4.4). The plot of observed versus fitted values further indicated that the model provided an unbiased representation of the data (Fig. 4.4).

Table 4.2. Log-likelihood, residual standard deviation (SD) and *P*-value for parameter *b* for the linear and nonlinear model fits for trembling aspen site index as a function of soil attributes and topographic indices (Eq. 4.1). Lowest negative log-likelihood and residual SD indicate the best explanatory variables. The null model is the mean, to which random effects for the intercept or parameter *a* were added. Residual SD is conditional on the random effects and variance function used. The dataset used for the analysis of soil properties is a subset of the full dataset.

	Negative log-likelihood	*P*-value for *b*	Residual SD, m
Site and soil properties (N = 115)			
Null model	226.90		1.740
Null model with random effects	204.03		1.343
Nutrient regime	190.34	0.0008	1.218
Moisture regime	191.08	0.0079	1.141
Depth to mottles	112.09*	0.0284	1.280*
Drainage regime	192.45	0.1298	1.187
Effective texture	193.23	0.7915	1.207
Coarse fragments	194.53	0.4353	1.208
Organic matter	194.82	0.8563	1.204
Topographic indices (N = 150)			
Null model	303.27		1.827
Null model with random effects	272.10		1.412
Depth-to-water:			
0.5 ha	256.01	0.0291	1.132
1 ha	257.88	0.1996	1.166
2 ha	255.79	0.0143	1.154
4 ha	**255.18**	**0.0138**	**1.158**
8 ha	257.85	0.4133	1.176
12 ha	258.05	0.6967	1.175
16 ha	258.05	0.7007	1.175
$\log_{10}$(FA)	258.22	0.7256	1.175
Slope	257.89	0.3732	1.179

*log-likelihood for the null model with random effects is −118.72, and residual SD is 1.441 m (N = 64).

3.2. Optimal flow initiation area

A flow initiation area of 4 ha yielded the highest log-likelihood (l = −255.18, Table 4.2), although the value was not much larger than obtained with an area of 2 ha (l = −255.79).

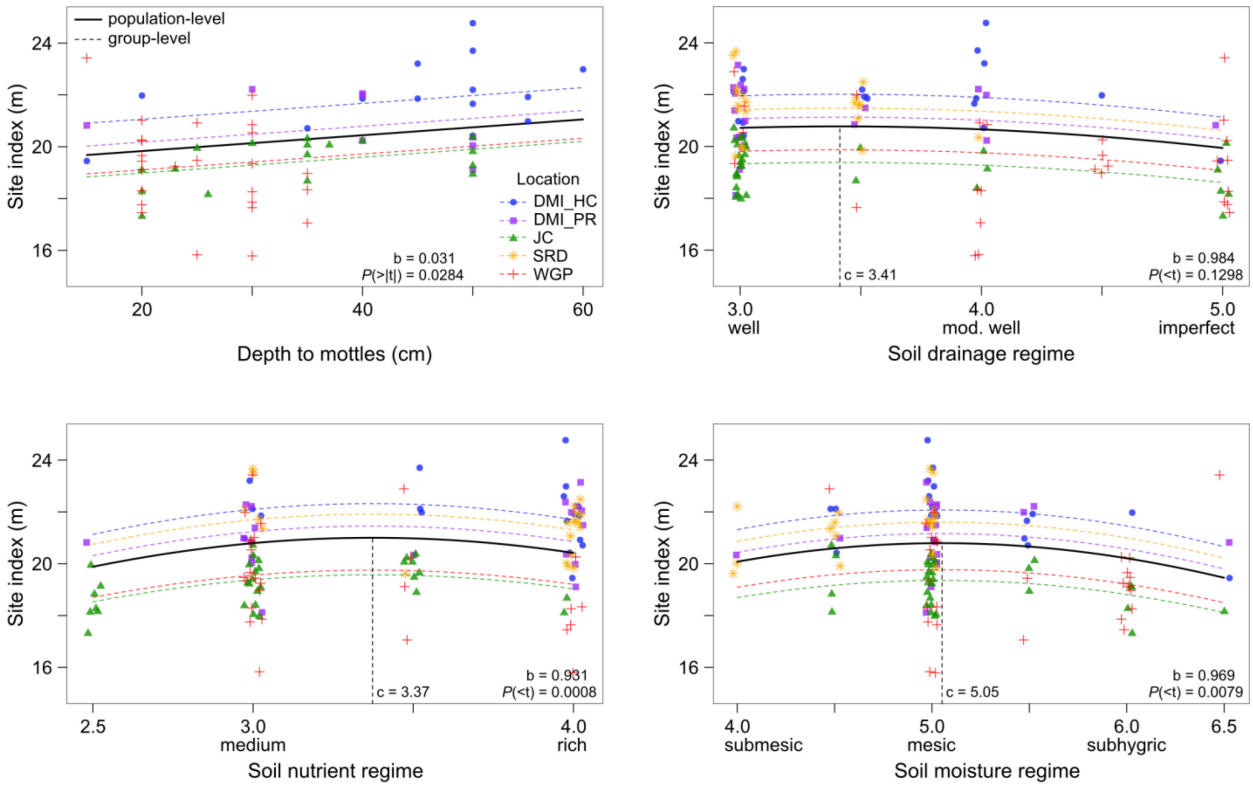

Figure 4.3. Relationship between site index of trembling aspen and depth-to-mottles, soil drainage, nutrient and moisture regime. The solid lines show the population average response from the mixed-effects models used to account for location differences, indicated by the dashed lines. A linear model was fit for DtMot, with its slope and two-sided *P*-value printed, while the normal function was used with the other predictors, for which parameters *c* and *b* with its one-sided *P*-value are printed (see section 2.4 for details). Different symbols and colors show the locations. Note that jitter was added to show all points.

Parameter *b* of the normal function was significantly less than 1 for DTW obtained at 4 ha (b = 0.997, P = 0.0138) and 2 ha (b = 0.994, P = 0.0143). Smaller flow initiation areas (0.5, 1 ha) produced models with lower log-likelihoods, of which only DTW at 0.5 ha contributed significantly (P = 0.0291). Larger areas (i.e., 8, 12 and 16 ha) gradually reduced the explanatory power of DTW, while none of them was significant. In fact, at 12 and 16 ha the estimates of parameter *b* were greater than 1 (b = 1.0001). Increasing the flow initiation area also resulted in a progressive increment of the DTW value at which maximum SI is realized, from 1.9 m at 0.5 ha to 6.9 m at 16 ha (Fig. 4.5). The curve for the 8 ha catchment area in Fig. 4.5 was obtained from a model without a variance function in order to have a stable estimate for parameter *c*.

Table 4.3. Estimates of fixed-effects, variance components (standard deviation scale, SD), variance parameters and residual standard error with the associated 95% confidence intervals (CI) for equations 4.2 and 4.3 which model trembling aspen site index (SI) as a function of soil moisture (SMR) and nutrient regime (SNR), and depth to water (DTW) calculated at flow initiation area of 4 ha. Results from conditional significance tests of the fixed-effects are shown—parameters β_2 and β_4 are tested if less than 1. A generalized R^2 was calculated based on the log-likelihood (l) ratio against the null model.

Fixed effect	Estimated coefficient	(95% CI)	*P*-value	Variance parameter / Random effect	Estimated parameter (95% CI)
SI = *f* (SMR, SNR): $l = -187.871$; null model: $l = -226.904$; ($\overline{R}^2_{LR} = 0.50$, N = 115)					
β_1	21.103	(19.983 – 22.223)	<.0001	δ_1 (JC)	1 (set value)
β_2 (SMR)	0.972	(0.947 – 0.998)	0.0180	$\delta_{2,3}$ (DMI_HC, SRD)	1.348 (0.938 – 1.937)
β_3	5.095	(4.680 – 5.509)	<.0001	δ_4 (DMI_PR)	1.782 (1.162 – 2.734)
β_4 (SNR)	0.946	(0.900 – 0.991)	0.0114	δ_5 (WGP)	2.542 (1.751 – 3.692)
β_5	3.297	(3.082 – 3.512)	<.0001	Random effects SD (σ_b)	1.192 (0.617 – 2.304)
				Residual SD (σ)	0.766 (0.592 – 0.991)
SI = *f* (DTW): $l = -254.809$; null model: $l = -303.266$; ($\overline{R}^2_{LR} = 0.48$, N = 150)					
β_1	20.972	(19.961 – 21.984)	<.0001	$\delta_{1,2,3}$ (DMI_HC, SRD, JC)	1 (set value)
β_2 (DTW)	0.997	(0.993 – 0.999)	0.0122	δ_4 (DMI_PR)	1.334 (0.972 – 1.829)
β_3	4.159	(3.132 – 5.187)	<.0001	δ_5 (WGP)	2.033 (1.544 – 2.677)
				Random effects SD (σ_b)	1.073 (0.477 – 2.417)
				Residual SD (σ)	0.998 (0.856 – 1.163)

3.3. Site index in relation to topographic indices

Flow accumulation and slope calculated from the DEM were not related (linearly or nonlinearly) with SI ($P = 0.7256$ and $P = 0.3732$, Table 4.2). To further reduce the error and increase the stability of the estimates, the model fit with DTW at 4 ha from Table 4.2 was modified by pooling the variance parameter for DMI_HC, SRD and JC and setting to 1 while DMI_PR and WGP were allowed a larger variance (Table 4.3, Fig. 4.6). However, DTW was significant with parameter b significantly lower than 1 ($P = 0.0122$) suggesting that maximum SI

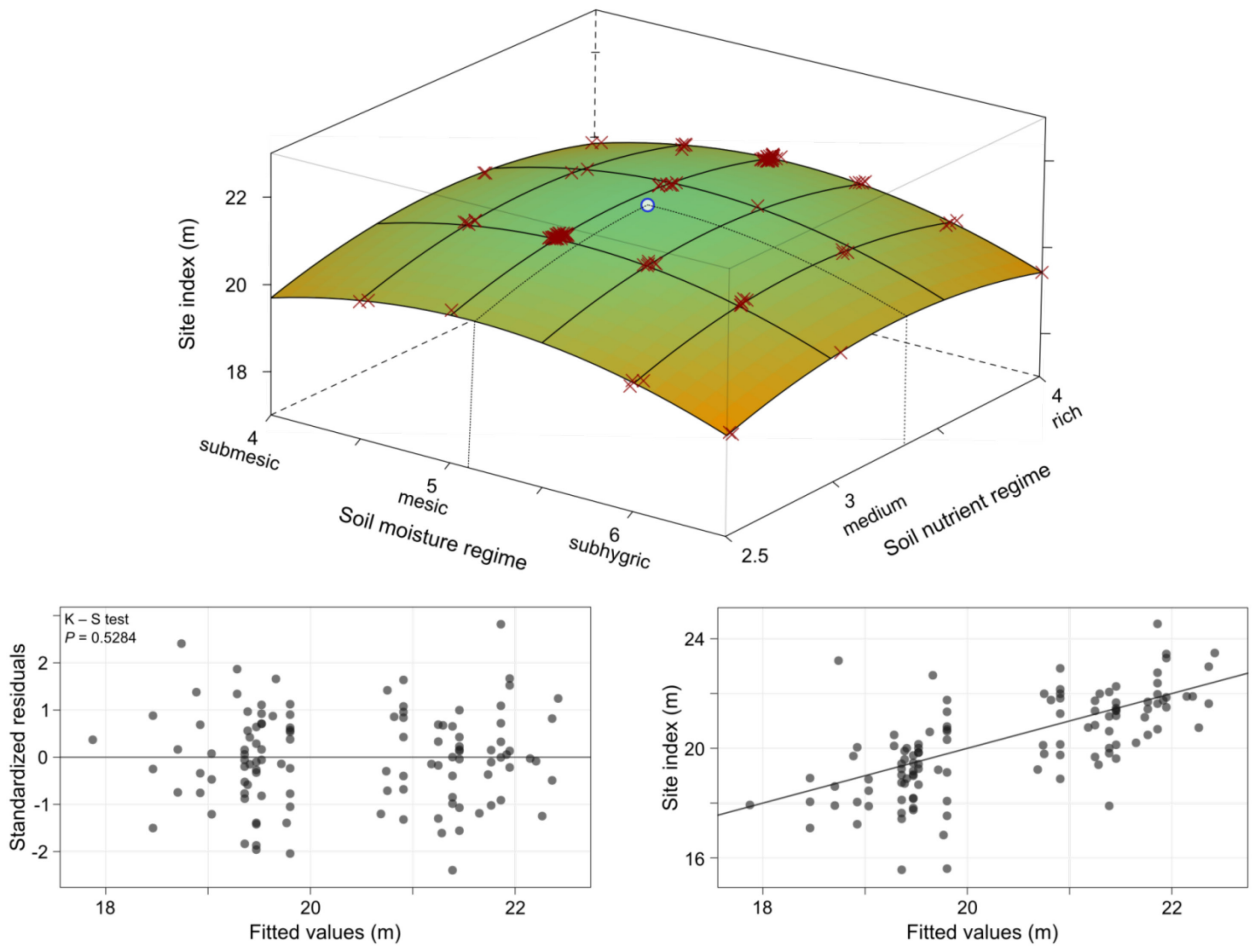

Figure 4.4. The model surface determined by Eq. 4.2 showing the relationship between trembling aspen site index, soil moisture and nutrient regime. Residual plot with the result of the Kolmogorov-Smirnov (K-S) normality test (bottom-left) and the observed versus fitted values (bottom-right) are displayed. Note that the points on the model surface are the fitted values and jitter was added to avoid overlap of points.

of 20.97 m was attained at DTW of 4.16 m (Table 4.3). The form of this model (Fig. 4.6) is

$$SI_{ij} = (\beta_1 + b_i)\beta_2^{(DTW_{ij}-\beta_3)^2} + \varepsilon_{j(i)}, \qquad \text{(Eq. 4.3)}$$

where SI_{ij} was the jth observation on the ith location, and β_1, β_2, β_3 were the parameters of the normal function. The random effects allowed maximum SI to shift between locations and were considered i.i.d. as $b_i \sim N(0, \sigma_b^2)$, while the within-group errors were nested in the locations and i.i.d. as $\varepsilon_{j(i)} \sim N(0, \sigma^2\delta_i^2)$—confirmed with Q-Q plots and the Kolmogorov-Smirnov test (Fig. 4.6). Diagnostic plots showed that the model is unbiased (Fig. 4.6), but a location-level error of

(0.99 m) compounded by that between-locations (1.07 m) indicated the low precision of the model. The strong spatial structure present in the errors of the null model was removed with Eq. 4.3. This model was used to calculate the map in Fig. 4.7 which shows the effect DTW on SI as controlled by the topography of the site (e.g., raised and low areas).

The variability between locations—accounted for by the random effects—could not be explained by climate variables retrieved from ClimateWNA (Wang et al. 2011) for the period 1981 – 2010. Mean annual temperature and precipitation were negatively correlated with the conditional modes of the random effects, while mean summer temperature showed the expected positive relationship but was weak ($P = 0.2918$) and could not be included in the model. We also calculated the climate moisture index (Hogg 1997) which balances evapotranspiration and precipitation, but this index had a weak negative association with the conditional modes.

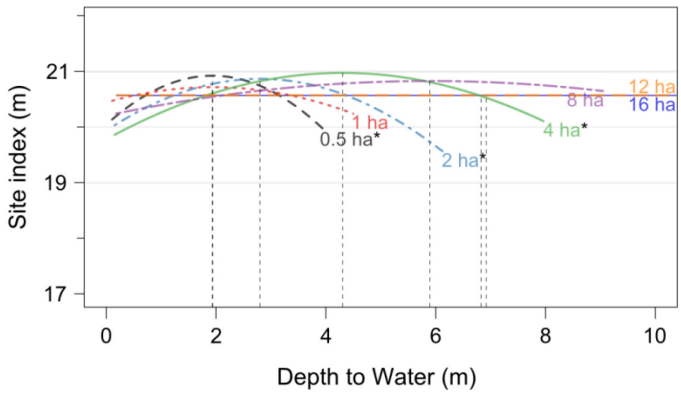

Figure 4.5. Population average relationship between trembling aspen site index (SI) and depth to water (DTW) calculated at flow initiation areas of 0.5, 1, 2, 4, 8, 12 and 16 ha. Asterisks specify that parameter *b* of the normal function is significantly less than 1. The vertical dashed lines show the DTW value at which peak SI is reached for each flow initiation area.

4. Discussion

4.1. Site index in relation to site and soil properties

Site index of trembling aspen was associated with soil moisture and nutrient regime.

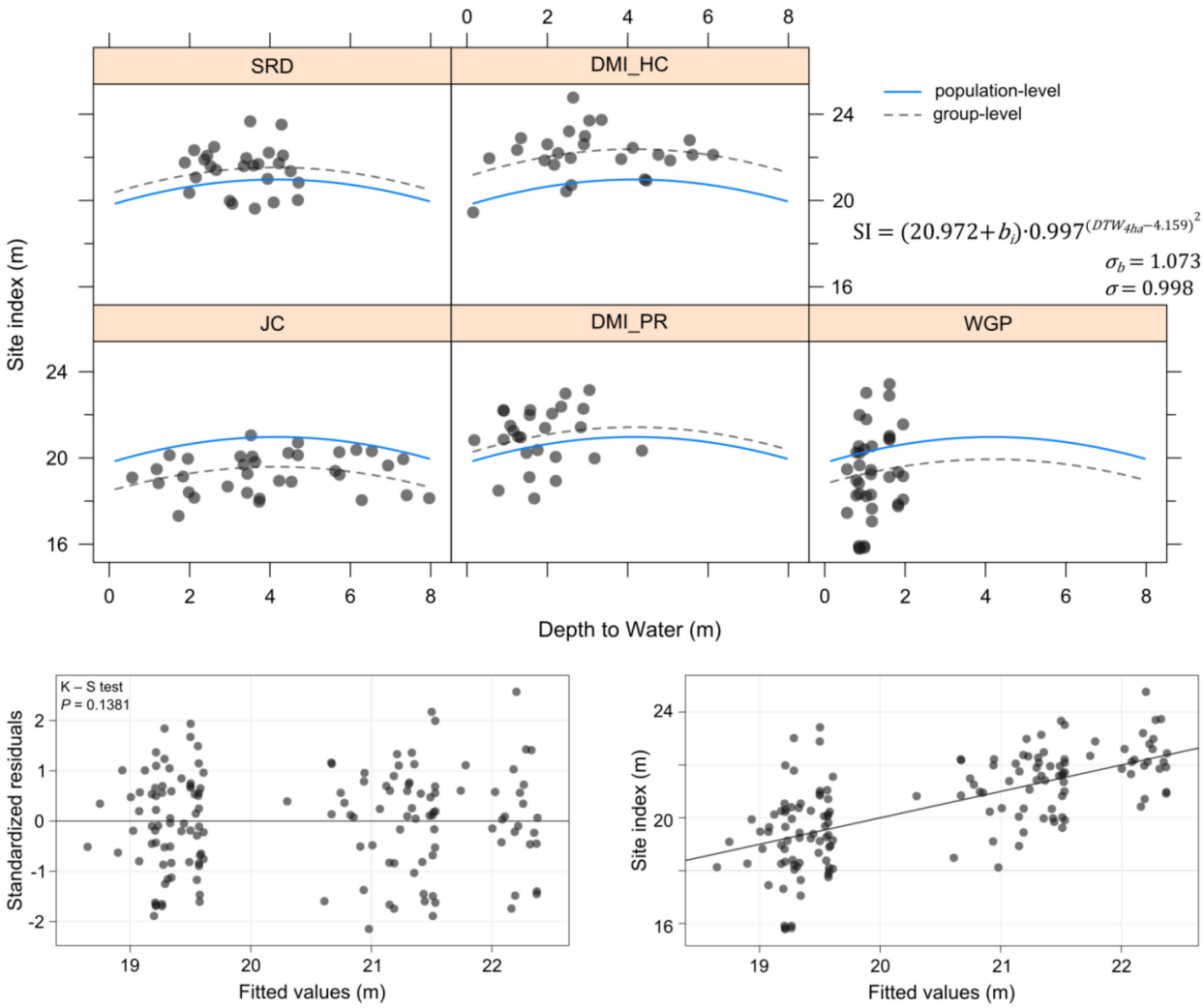

Figure 4.6. Relationship between trembling aspen site index and the depth-to-water index calculated at flow initiation area of 4 ha as defined by Eq. 4.3. The solid line represents the population-average model while the dashed line represents the shift in parameter *a* between locations, which are shown in different panels. Standardized residuals against fitted values (left) and observed versus fitted values (right) show an unbiased model with residual standard error (σ) and variance component (σ_b) printed, along with the parameter estimates. The Kolmogorov-Smirnov (K-S) test indicates normality of the residuals.

These models suggest that mesic sites (SMR = 5.05) with medium to rich nutrient regime (SNR = 3.37) yield maximum SI—SMR: a = 20.79 m; SNR: a = 21 m (Fig. 4.3). These findings are in agreement with the autoecology of aspen and previous site-growth studies. Perala D.A. in Burns and Honkala (1990) reports that aspen attains maximum SI (i.e., 23 – 25 m) on well drained mesic sites with silty-loam texture and water table between 0.6 – 2.5 m, which do not create

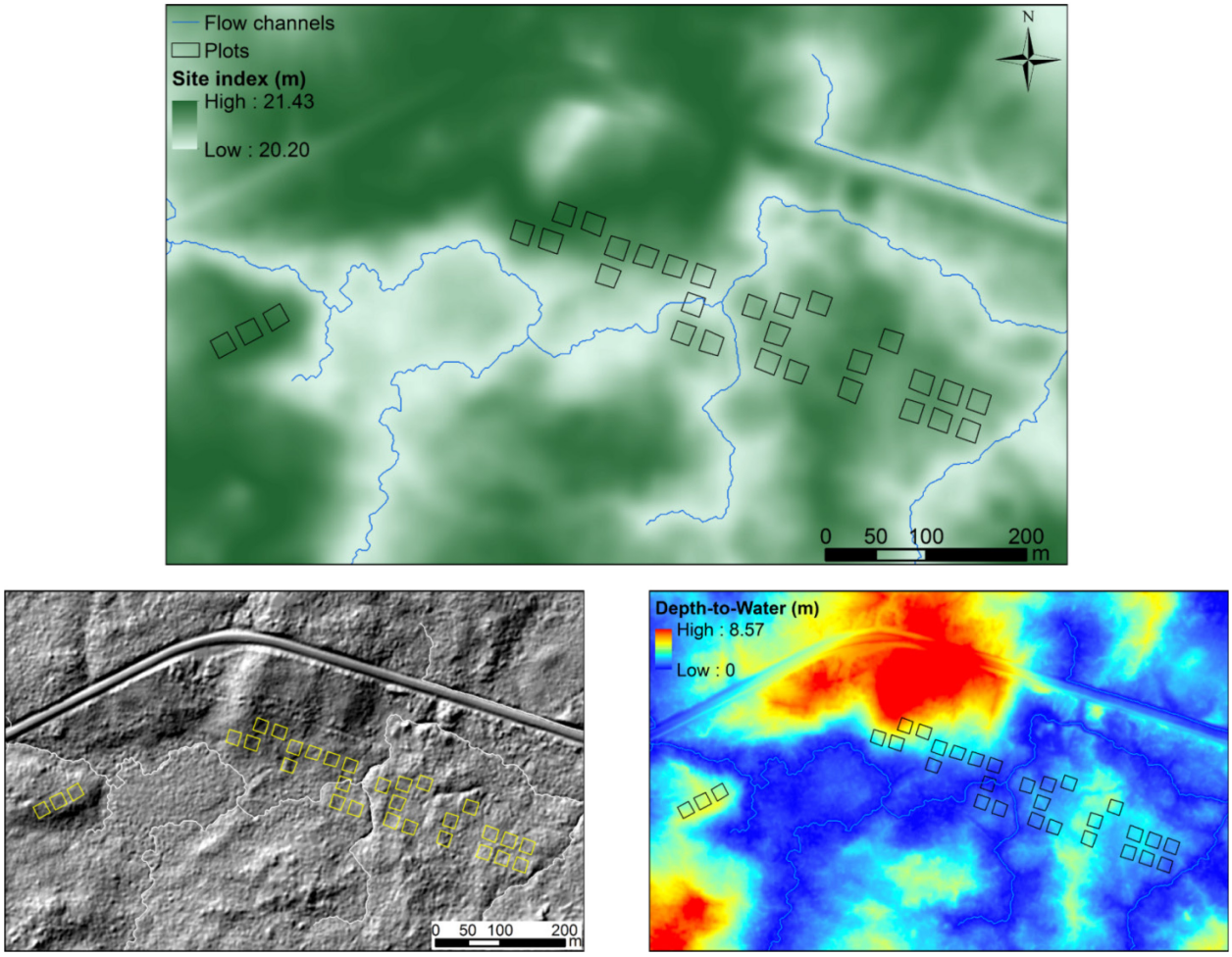

Figure 4.7. Trembling aspen site index map (top) obtained using Eq. 4.3 for the DMI_PR location. The hillshade (left) shows the topography of the area which determines the depth to water raster (right).

droughty or hypoxic conditions that aspen does not tolerate. In Alberta, Beckingham and Archibald (1996) state that dogwood ecosites (i.e., e) with slightly wet and nutrient rich soils provide best growing conditions for aspen, with SI values of 21.4 m. The normal function used to model the influence of SNR on aspen SI predicts that richer sites will grow stands of lower productivity (Fig. 4.3). This can be explained because nutrient rich soils also tend to be wetter (Beckingham and Archibald 1996), which favours development of the grass *Calamagrostis canadensis* (Michx.) Beauv. (Mueller-Dombois and Sims 1966) and organic matter accumulation leading to colder soils and shorter growing seasons (Hauessler and Coates 1986; Hogg and

Lieffers 1991). Both low soil temperatures and wet soils limit root growth, leaf area and shoot mass of aspen seedlings by reducing gas exchange and water use (Landhausser et al. 2001; Landhausser et al. 2003). This effect was also reflected in mature stands which are more productive on warmer soils with faster decomposition rates of high quality organic matter (Van Cleve et al. 1983).

Combining SMR and SNR into a single model (Eq. 4.2) provides an opportunity to assess the interaction between these two site factors. Consistent with the separate models, parameter estimates of Eq. 4.2 indicate that a maximum population-average SI of 21.1 m (up to 22.5 m at DMI_HC) is reached on mesic sites that are slightly rich in nutrients (Table 4.3). The generalized R^2 based on the likelihood ratio of the candidate model compared to the null model (Cox and Snell 1989; Nagelkerke 1991) was 0.50 when compared against the null model but dropped to 0.25 if random effects were added to the null. This value decreased to 0.12 when both random effects and the variance function were incorporated into the null model used for calculation. Based on this our model is much weaker than that of Chen et al. (1998) who found that aspen SI was strongly related with SMR and SNR ($R^2 = 0.63$), or more detailed attributes such as depth, pH, total nitrogen and potassium of the forest floor ($R^2 = 0.73$). Further, aspen SI was strongly associated with C:N ratio and electrical conductivity of the forest floor, percentage of very fine sand, conifer cover and elevation to produce an R^2 of 0.62 (Pinno et al. 2009). This model was much stronger on fluvial than on till sites. Large R^2 values were reported by Chen et al. (2002) from models that included SMR, SNR, topographic position and elevation ($R^2 = 0.82$), while variables reflecting moisture conditions (i.e., water-holding capacity, aridity index, degree-days) explained 69% of the variation in aspen SI (Ung et al. 2001). These studies emphasize the association, which can be considered causal, between productivity of sites growing aspen in the

boreal forest and various factors representing moisture and nutrient availability in soils.

One reason for which the presented studies report such large R^2 values might be related to the detailed soil measurements (e.g., pH, electrical conductivity, C:N ratio, total nitrogen) which could reveal the specific factors influencing aspen SI. We focused on assessing the overall soil moisture and nutrient regimes which are more commonly used in forestry and can be readily available in some areas (AESRD 2011) but did not collect soil samples for further analysis. Also, we used model estimates of SI based on top height of young stands (i.e., 17 yrs) which further increase the variability in the data. On the other hand, the generalized R^2 we calculated, while it reflects goodness of fit, does not have all the properties inherent in the R^2 of linear regression and we suggest caution in its interpretation and comparison with other studies. Despite this drawback, our modeling approach (i.e., mixed-effects models) accounted for variability between locations (e.g., parameter *a* for JC was lower by 1.5 m whereas that of DMI_HC greater by 1.4 m). Once the functional relationship given by the normal curve was established the location effects can be accounted for by covariates (Pinheiro and Bates 1995).

Climate controls the large scale variation in forest productivity, thus accurate prediction of SI under future climate scenarios requires a climate component in models. Furthermore, current height-age curves used to produce SI estimates may not be suitable to predict future site productivity, particularly in the boreal which will experience the largest changes (Hansen et al. 2006) Although we sampled sites across two degrees in latitude (Table 4.1), climate variables (e.g. mean annual and summer temperature or precipitation) were not related with the conditional modes of the random effects. In fact, the lower SI at JC and WGP created a negative relationship with temperature or precipitation. This is likely due to the generally wet nature of the WGP site which reduces aspen SI and to the high elevation of JC where summers are colder as indicated by

a positive but not significant relation between the conditional modes and mean summer temperature. However, the small number of random effects (n = 5) would not support strong inferences on climatic influence s on aspen SI. The large amount of unexplained variation in aspen SI could also be due to the within-population genetic diversity in these continuous aspen stands (Yeh et al. 1995) as was found for inland Douglas-fir where it accounted for approximately 40% of the variation in SI (Monserud and Rehfeldt 1990), as well as to other factors which were not measured.

Depth to mottles reflects the level at which the water table fluctuates to create reduction and oxidation conditions. Consistent with aspen autoecology we found that SI increases on sites where mottling occurs at greater depths (Fig. 4.3). However, water tables deeper than 2.5 m create drier conditions which tend to reduce aspen SI (Burns and Honkala 1990), making the relationship reach an asymptote or even decrease. Soil drainage regime was not significantly related with aspen SI (Fig. 4.3) but parameter estimates suggest that well to moderately-well drained soils (c = 3.41) yield maximum SI (a = 20.78 m), consistent with the silvics of aspen. Perhaps a wider range of drainage conditions would have given a stronger significant signal. Similarly, 90% of our plots had silty clay or silty clay loam texture making it difficult to find significant differences between textural classes. Some studies reported that greater height growth of aspen occurs on soils with higher content of clay because it increases water holding capacity (Martin and Gower 2006; Pare et al. 2001) but it can also increase water tension leading to reduced availability to plants. However, Johansson (2002) did not find an effect of soil texture on SI of *Populus tremula* L. Content of coarse fragments influences water holding capacity while thick layers of organic matter can decrease soil temperature, but we did not find significant associations between these and aspen SI. The lower SI at JC could be explained by the large

proportion of coarse fragments, 20%, while the other locations had an average of 3%.

4.2. Optimal flow initiation area

The depth-to-water algorithm depends on the flow channel network defined by the flow initiation area. A lower threshold area extends flow channels further into the headwaters of the watershed while setting a greater value will only identify the major streams, which collect water drained from a large area. The DTW algorithm integrates both horizontal and vertical distance from any cell in the landscape to the nearest flow channel (see section 2.3), therefore low catchment areas create a dense channel network which yields generally low DTW values whereas DTW values tend to increase when only the major streams are used in its calculation. In some situations two flow initiation areas can start in the same point (e.g., 12 and 16 ha in Fig. 4.1) as a result of convergence of two channels. To illustrate the effect of changing flow initiation area we calculated the length of the channels and the area with DTW < 1 m for the DMI_PR location shown in Fig. 4.7. A channel network of 6445.70 m was produced at 0.5 ha with 29.30 ha (of the 47.50 ha) under 1m of DTW, whereas increasing the threshold area to 16 ha identified a channel network of only 1857.38 m generating a DTW raster with 12.49 ha under 1 m. An intermediate flow initiation area of 4 ha produced 3097.66 m of channels and 18.66 ha of the area was classified below 1 m of DTW, values not very different from a 2 ha threshold (3458.38 m, 19.69 ha). The general consensus is that a flow initiation area of 4 ha represents flow conditions occurring late in the growing season (White et al. 2012) generating a channel network corresponding to ephemeral water bodies identified in the field (Murphy et al. 2011).

Our results suggest that an intermediate flow initiation area of 4 or 2 ha would best reflect the effects of soil moisture conditions on aspen SI in the boreal forest characterized by a gentle rolling topography which does not strongly direct water movement. Capturing the spatial

variation of soil wetness in the boreal landscape of Sweden was best realized with a catchment area of 1 – 2 ha (Ågren et al. 2014). However, this was only valid in landscapes with glacial till deposits defined by low permeability which become saturated very quickly after precipitation events. In an area with high hydraulic conductivity given by the coarse nature of the ice-river alluvium a large flow initiation threshold (e.g., 10 or 16 ha) performed better. The geology of our study locations is indeed formed by glacial till deposits, and only JC presents a layer of rounded cobble at 25 – 40 cm depth but exhibiting the same geomorphology. Murphy et al. (2011) tested flow initiation areas of 4, 5 and 6 ha recommending that the 4 ha threshold be used to predict drainage and vegetation class. In a different application, predicting rut location in the boreal forest was more reliable using DTW calculated at a threshold of 1 ha than 4 ha (Campbell et al. 2013). Larger flow initiation areas result in a shift to the right of parameter *c* (Fig. 4.5) indicating that the entire landscape receives larger DTW values since the channel network is sparser. Field observations and fitted models (Table 4.2) suggest that in the boreal landscape flow initiation areas of 12 and 16 ha describe the gravitational movement of water in a very similar fashion, whereas low thresholds (e.g., 0.5 and 1 ha) create a very dense channel network generating an overly wet landscape which persists for only a brief period of time early in the season after snowmelt.

4.3. Site index in relation to topographic indices

Topography controls soil formation processes at the hillslope level and thus topographic indices, simple or complex, can be used to capture small scale variability in site productivity given by variation in soil characteristics. The depth-to-water index calculated at a flow initiation area of 4 ha was associated with aspen site index, while simpler indices (e.g., flow accumulation, slope, aspect) were not related to aspen SI. The model in Eq. 4.1 (Table 4.2) was further

improved to increase the precision of the parameter estimates by using a different structure for the variance model, as shown in Eq. 4.3 (Table 4.3). Model estimates predict that a DTW value of 4.16 m yields the maximum SI of 20.97 m, which can vary from 19.59 m at JC to 22.38 m at DMI_HC. We applied Eq. 4.3 to the DMI_PR location shown in Fig. 4.7 where it can be noticed that raised areas have larger DTW values (>7 m) and are assigned lower SI similar to the wetter zones, according to the normal curve. We do not assume that DTW values indicate the actual depth to the water table but provide a measure of the hydrological connectivity between a cell in the landscape and a source of gravitational water (i.e., flow channel). This model gave a generalized R^2 of 0.48, dropping to 0.21 when the random effects were added and further to 0.04 when both random effects and variance function were included in the null model.

Several studies have shown that DTW is associated with soil physical and chemical properties and vegetation. Soil wetness—defined similarly to SMR—was predicted using DTW (Ågren et al. 2014), who emphasized that DTW, unlike TWI, is independent of the scale of the DEM used to compute it. Vegetation type ranked from hydric to xeric was linked with DTW (Murphy et al. 2011), while Hiltz et al. (2012) defined a vegetation index (i.e., linear function of $\log_{10}$DTW) adjusted for slope and aspect. Murphy et al. (2011) also reported that DTW was associated with soil drainage, percentage of water-filled pore space, forest floor depth, soil pH and total Mn. Using a 4 ha catchment area Murphy et al. (2009) found that a threshold DTW value of 1.5 m accounted for 71% of the variation in field-mapped areas with very poor to imperfectly drained soils (i.e., hydric SMR), suggesting that our DTW value of 4.16 m appears reasonable to define optimal growing conditions for aspen. In a companion study (see Chapter 2) we found that DTW was strongly related to SMR but that DTW failed to capture the spatial variation of SNR in the boreal forest. This deficiency could explain why the generalized R^2 for

the DTW model (Eq. 4.3, 0.04) is half of that for the combined SMR and SNR model (Eq. 4.2, 0.12). Furthermore, the errors induced by the growth projection system used to estimate SI values must be considered when interpreting the strength of this relationship, particularly given the young age at which SI was estimated.

To the best of our knowledge, this is the first work to investigate the relationship between the depth-to-water index and SI. An early study by Tom and Miller (1980) showed that Landsat-derived indices combined with topography (e.g., slope aspect, elevation) can successfully map SI, but the limited availability of highly accurate DEMs precluded advances in this area. Later, Holmgren (1994) found that catchment area to the plot determined remotely—similar to FA—was related with SI of Scots pine and Norway spruce but additional information measured in the field (e.g., soil texture, geochemistry) was necessary to obtain models with R^2 values of 0.41 and 0.19, respectively. The integrated moisture index of Iverson et al. (1997), which incorporates hillshade, FA, and curvature derived from DEMs and water holding capacity from soil maps, explained 64% of the variation in the SI of white oak (*Quercus alba*, L.). The topographic wetness index and an annual solar radiation index computed from a 12.5 m resolution DEM were used to predict SI of *Cryptomeria japonica* (L.f.) D.Don with a coefficient of determination of 0.65 (Mitsuda et al. 2007). These examples show how various topographic indices have been employed to map site productivity. The addition of soil data extracted from maps could potentially improve performance of these models. However, Pinno et al. (2009) reported that the low resolution of these maps did not provide data to account for variation in SI of aspen while McKenney and Pedlar (2003) showed that mapped soil data increased prediction error by 20 – 30% relative to data collected in the field. When higher resolution data (e.g., soil depth, available water storage capacity, and texture) was combined with interpolated precipitation, dryness and

elevation, a model was obtained to account for 35% of the variation in SI of loblolly pine (*Pinus taeda*, L.).

Interpolating climate variables has become a common practice and multiple studies have focused on trying to predict the effects of climate on site productivity. Monserud et al. (2006) found that growing degree days >5 °C was the best predictor of lodgepole pine SI and then used this model to predict that climate warming will increase its productivity but associated dryness will reduce its range to half of its current size by 2080. Productivity of the Pacific Northwest forests was predicted using mean annual temperature, precipitation and climate moisture index (Latta et al. 2009), whereas extending the study area farther south and east required only winter coldness and an index coupling precipitation and temperature in the growing season to predict gross primary productivity (Weiskittel et al. 2011). However, the coarse resolution of these climate data restricts predictions to large scale patterns but incorporating topographic indices would allow addressing hillslope and watershed level variation in forest site productivity. McKenney and Pedlar (2003) used regression trees to combine soil (i.e., depth of organic and mineral layer) and climate (i.e., temperature and precipitation) data to predict SI of jack pine (*Pinus banksiana* Lamb.) and black spruce across Ontario, Canada. Our modelling approach starts with a functional relationship between the small scale variation in SI and DTW giving the possibility to explain the inter-location (i.e., large scale) variability accounted for with the random effects on parameter *a* by making the conditional modes dependent on a climate factor. We tested mean annual and summer temperature and precipitation, as well as the climate moisture index of (Hogg 1997), but were not significant. Visual examination revealed that low aspen SI values were recorded at JC and WGP, locations with higher temperatures and higher precipitation (Table 4.1) as a result of their relative proximity to the foothills. The low SI at

WGP can be due to the severe coil compaction caused by traffic of heavy machinery during harvest in 1990 which eliminated aspen regeneration from some areas subsequently occupied by willow. Sampling from a larger number of locations across a wider range of climates is necessary to examine climate effects on aspen productivity.

Slope and aspect were not related with aspen SI as a result of the relatively flat relief which creates little difference between a north- or south-facing slope. Average slope per plot ranged between 2.7 and 11.1 with a mean of 4.9% indicating the small effect of topography on soil properties and, consequently, on site productivity. In terrain with an average slope of 22% ranging from 0 to 99%, both aspect and slope contributed significantly to a model predicting SI of Scots pine and Norway spruce (Sharma et al. 2012). Flow accumulation is the size of the area drained to each cell in the landscape, taking values from 1 to hundreds of thousands of m^2, and as such should represent the supply of gravitational water to the soil in that cell. However, FA was not related with aspen SI reflecting the small contribution of gravitational forces in the movement of water in and on the soil of the boreal landscape.

5. Conclusions

This study presents the first evaluation of the depth-to-water index in estimation of trembling aspen productivity, emphasizing the role of flow initiation area in the calculation of DTW. Aspen site index was successfully related with DTW calculated at a threshold area of 4 ha, peaking at a DTW value of 4.16 m. The use of such topographic indices is based on the functional connection that exists between soil formation processes and terrain morphology, thus allowing us to cover larger areas and greatly reduce the costs associated with field assessments. The DTW index is currently available for 80% of the forested land of the province of Alberta, as

well as for large areas in New Brunswick, Canada, making the potential application of these results immediate. However, we advise a conservative approach because both soil moisture and nutrient reserves were shown to control aspen SI while DTW has only been successfully related with SMR, thus reducing the accuracy of SI estimations. This weak association between SI and DTW can be attributed to the relatively flat relief of the boreal mixedwood forests where topography does not play a determinant role in water movement and thus soil properties. The low number of locations sampled did not allow us to successfully combine topographic indices with climate variables to give insight into both macro- and meso-scale variation of site productivity, but this represents a path that must be further explored. We recommend additional evaluations of DTW and other topographic indices in areas with varied topography dominated by different tree species to establish a working model to predict site productivity in the boreal forest.

Literature cited

AESRD. 2011. Alberta Vegetation Inventory (AVI) Crown Polygons. Alberta Environment and Sustainable Resource Development, Government of Alberta.

Ågren, A.M., Lidberg, W., Strömgren, M., Ogilvie, J., and Arp, P.A. 2014. Evaluating digital terrain indices for soil wetness mapping – a Swedish case study. Hydrol. Earth Syst. Sci. **18**(9): 3623-3634. doi: 10.5194/hess-18-3623-2014.

Assmann, E. 1970. The principles of forest yield study: studies in the organic production, structure, increment and yield of forest stands. Pergamon Press, Oxford.

Barnes, B.V., Zak, D.R., Denton, S.R., and Spurr, S.H. 1998. Forest ecology. 4th ed. John Wiley & Sons, Inc.

Beckingham, J.D., and Archibald, J.H. 1996. Field guide to ecosites of northern Alberta. North. For. Cent., Edmonton, AB.

Beven, K.J., and Kirkby, M.J. 1979. A physically based, variable contributing area model of basin hydrology. Hydrol. Sci. Bul. **24**(1): 43-69. doi: 10.1080/02626667909491834.

Bokalo, M., Comeau, P.G., and Titus, S.J. 2007. Early development of tended mixtures of aspen and spruce in western Canadian boreal forests. For. Ecol. Manag. **242**(2-3): 175-184. doi: 10.1016/j.foreco.2007.01.038.

Bokalo, M., Stadt, K.J., Comeau, P.G., and Titus, S.J. 2013. The validation of the Mixedwood Growth Model (MGM) for use in forest management decision making. Forests **4**(1): 1-27. doi: 10.3390/f4010001.

Bontemps, J.-D., and Bouriaud, O. 2014. Predictive approaches to forest site productivity: recent trends, challenges and future perspectives. Forestry **87**(1): 109-128. doi: 10.1093/forestry/cpt034.

Burns, R.M., and Honkala, B.H. 1990. Silvics of North America: 1. Conifers; 2. Hardwoods. U.S. Dept. of Agriculture, Forest Service, Washington, D.C.

Campbell, D.M.H., White, B., and Arp, P.A. 2013. Modeling and mapping soil resistance to penetration and rutting using LiDAR-derived digital elevation data. J. Soil Water Conserv. **68**(6): 460-473. doi: 10.2489/jswc.68.6.460.

Chen, H.Y.H., Klinka, K., and Kabzems, R.D. 1998. Site index, site quality, and foliar nutrients of trembling aspen: relationships and predictions. Can. J. For. Res. **28**(12): 1743-1755. doi: 10.1139/cjfr-28-12-1743.

Chen, H.Y.H., Krestov, P.V., and Klinka, K. 2002. Trembling aspen site index in relation to environmental measures of site quality at two spatial scales. Can. J. For. Res. **32**(1): 112-119. doi: 10.1139/x01-179.

Chen, H.Y.H., and Popadiouk, R.V. 2002. Dynamics of North American boreal mixedwoods. Environmental Reviews **10**(3): 137-166. doi: 10.1139/a02-007.

Cox, D.R., and Snell, E.J. 1989. The analysis of binary data. 2nd ed. Chapman and Hall, London. pp. 208-209.

Daniel, T.W., Helms, J.A., and Baker, F.S. 1979. Principles of Silviculture. 2nd ed. ed. McGraw-Hill, New York, N.Y. pp. 186-187.

Hansen, J., Sato, M., Ruedy, R., Lo, K., Lea, D.W., and Medina-Elizade, M. 2006. Global temperature change. Proceedings of the National Academy of Sciences **103**(39): 14288-14293. doi: 10.1073/pnas.0606291103.

Hauessler, S., and Coates, K.D. 1986. Autecological characteristics of selected species that compete with conifers in British Columbia: a literature review. Land management report no. 33, Ministry of Forests, Victoria, B.C. p. 181.

Hiltz, D., Gould, J., White, B., Ogilvie, J., and Arp, P. 2012. Modeling and mapping vegetation type by soil moisture regime across boreal landscapes. *In* Restoration and reclamation of boreal ecosystems: Attaining sustainable development. Cambridge Univ. Press, New York, NY. pp. 56-75.

Hodgson, M.E., Jensen, J.R., Schmidt, L., Schill, S., and Davis, B. 2003. An evaluation of LIDAR- and IFSAR-derived digital elevation models in leaf-on conditions with USGS Level 1 and Level 2 DEMs. Remote Sens. Environ. **84**(2): 295-308. doi: 10.1016/s0034-4257(02)00114-1.

Hogg, E.H. 1997. Temporal scaling of moisture and the forest-grassland boundary in western Canada. Agric. For. Meteorol. **84**(1-2): 115-122. doi: 10.1016/s0168-1923(96)02380-5.

Hogg, E.H., and Lieffers, V.J. 1991. The impact of *Calamagrostis canadensis* on soil thermal regimes after logging in northern Alberta. Can. J. For. Res. **21**(3): 387-394. doi: 10.1139/x91-048.

Holmgren, P. 1994. Topographic and geochemical influence on the forest site quality, with respect to *Pinus sylvestrys* and *Picea abies* in Sweden. Scand. J. For. Res. **9**(1): 75-82. doi: 10.1080/02827589409382815.

Huang, S.M., Meng, S.X., and Yang, Y.Q. 2009. A growth and yield projection system (GYPSY) for natural and post-harvest stands in Alberta. Alberta Sustainable Resource Development.

Iverson, L.R., Dale, M.E., Scott, C.T., and Prasad, A. 1997. A GIS-derived integrated moisture index to predict forest composition and productivity of Ohio forests (USA). Landsc. Ecol. **12**(5): 331-348. doi: 10.1023/a:1007989813501.

Johansson, T. 2002. Increment and biomass in 26-to 91-year-old European aspen and some practical implications. Biomass Bioenerg. **23**(4): 245-255. doi: 10.1016/s0961-9534(02)00056-9.

Klinka, K., and Carter, R.E. 1990. Relationships between site index and synoptic environmental-factors in immature coastal Douglas-fir stands. For. Sci. **36**(3): 815-830.

Landhausser, S.M., DesRochers, A., and Lieffers, V.J. 2001. A comparison of growth and physiology in *Picea glauca* and *Populus tremuloides* at different soil temperatures. Can. J. For. Res. **31**(11): 1922.

Landhausser, S.M., Silins, U., Lieffers, V., and Liu, W. 2003. Response of *Populus tremuloides*, *Populus balsamifera*, *Betula papyrifera* and *Picea glauca* seedlings to low soil temperature and water-logged soil conditions. Scand. J. For. Res. **18**(5): 391. doi: 10.1080/02827580310015044.

Lanner, R.M. 1985. On the insensitivity of height growth to spacing. For. Ecol. Manag. **13**(3-4): 143-148. doi: 10.1016/0378-1127(85)90030-1.

Latta, G., Temesgen, H., and Barrett, T.M. 2009. Mapping and imputing potential productivity of Pacific Northwest forests using climate variables. Can. J. For. Res. **39**(6): 1197-1207. doi: 10.1139/x09-046.

Maillard, P., and Alencar-Silva, T. 2013. A method for delineating riparian forests using region-based image classification and depth-to-water analysis. Int. J. Remote Sens. **34**(22): 7991-8010. doi: 10.1080/01431161.2013.827847.

Martin, J.L., and Gower, S.T. 2006. Boreal mixedwood tree growth on contrasting soils and disturbance types. Can. J. For. Res. **36**(4): 986-995. doi: 10.1139/x05-306.

McKenney, D.W., and Pedlar, J.H. 2003. Spatial models of site index based on climate and soil properties for two boreal tree species in Ontario, Canada. For. Ecol. Manag. **175**(1–3): 497-507. doi: http://dx.doi.org/10.1016/S0378-1127(02)00186-X.

Mitsuda, Y., Ito, S., and Sakamoto, S. 2007. Predicting the site index of sugi plantations from GIS-derived environmental factors in Miyazaki Prefecture. J. For. Res.-Jpn. **12**(3): 177-186. doi: 10.1007/s10310-007-0004-1.

Monserud, R.A., Huang, S.M., and Yang, Y.Q. 2006. Predicting lodgepole pine site index from climatic parameters in Alberta. For. Chron. **82**(4): 562-571.

Monserud, R.A., and Rehfeldt, G.E. 1990. Genetic and environmental components of variation of site index in inland Douglas-fir. For. Sci. **36**(1): 1-9.

Moore, I.D., Gessler, P.E., Nielsen, G.A., and Peterson, G.A. 1993. Soil attribute prediction using terrain analysis. Soil Sci. Soc. Am. J. **57**(2): 443-452. doi: 10.2136/sssaj1993.03615995005700020026x.

Mueller-Dombois, D., and Sims, H.P. 1966. Response of three grasses to two soils and a water table depth gradient. Ecology **47**(4): 644-648. doi: 10.2307/1933946.

Murphy, P.N.C., Ogilvie, J., and Arp, P. 2009. Topographic modelling of soil moisture conditions: a comparison and verification of two models. Eur. J. Soil Sci. **60**(1): 94-109. doi: 10.1111/j.1365-2389.2008.01094.x.

Murphy, P.N.C., Ogilvie, J., Connor, K., and Arpl, P.A. 2007. Mapping wetlands: A comparison of two different approaches for New Brunswick, Canada. Wetlands **27**(4): 846-854. doi: 10.1672/0277-5212(2007)27[846:mwacot]2.0.co;2.

Murphy, P.N.C., Ogilvie, J., Meng, F.R., White, B., Bhatti, J.S., and Arp, P.A. 2011. Modelling and mapping topographic variations in forest soils at high resolution: A case study. Ecol. Model. **222**(14): 2314-2332. doi: 10.1016/j.ecolmodel.2011.01.003.

Nagelkerke, N.J.D. 1991. A note on a general definition of the coefficient of determination. Biometrika **78**(3): 691-692. doi: 10.1093/biomet/78.3.691.

Osika, D.E., Stadt, K.J., Comeau, P.G., and MacIsaac, D.A. 2013. Sixty-year effects of deciduous removal on white spruce height growth and site index in the Western Boreal. Can. J. For. Res. **43**(2): 139-148. doi: 10.1139/cjfr-2012-0169.

Pare, D., Bergeron, Y., and Longpre, M.H. 2001. Potential productivity of aspen cohorts originating from fire, harvesting, and tree-fall gaps on two deposit types in northwestern Quebec. Can. J. For. Res. **31**(6): 1067-1073. doi: 10.1139/cjfr-31-6-1067.

Pinheiro, J.C., and Bates, D.M. 1995. Model building for nonlinear mixed-effects models. University of Wisconsin–Madison. 91.

Pinheiro, J.C., and Bates, D.M. 2000. Mixed-effects models in S and S-PLUS. Springer-Verlag, New York, NY. pp. 57-96; 201-225; 305-336.

Pinheiro, J.C., Bates, D.M., DebRoy, S., Sarkar, D., and Team, R.C. 2015. nlme: Linear and nonlinear mixed effects models. *In* http://CRAN.R-project.org/package=nlme.

Pinno, B.D., Pare, D., Guindon, L., and Belanger, N. 2009. Predicting productivity of trembling aspen in the Boreal Shield ecozone of Quebec using different sources of soil and site information. For. Ecol. Manag. **257**(3): 782-789. doi: 10.1016/j.foreco.2008.09.058.

Pitt, D.G., Comeau, P.G., Parker, W.C., MacIsaac, D., McPherson, S., Hoepting, M.K., Stinson, A., and Mihajlovich, M. 2010. Early vegetation control for the regeneration of a single-cohort, intimate mixture of white spruce and trembling aspen on upland boreal sites. Can. J. For. Res. **40**(3): 549-564. doi: 10.1139/x10-012.

R Core Team. 2015. *R: A language and environment for statistical computing*. R Foundation for Statistical Computing, Vienna, Austria.

Sharma, R.P., Brunner, A., and Eid, T. 2012. Site index prediction from site and climate variables for Norway spruce and Scots pine in Norway. Scand. J. For. Res. **27**(7): 619-636. doi: 10.1080/02827581.2012.685749.

Skovsgaard, J.P., and Vanclay, J.K. 2008. Forest site productivity: a review of the evolution of dendrometric concepts for even-aged stands. Forestry **81**(1): 13-31. doi: 10.1093/forestry/cpm041.

Smith, D.M., Larson, B.C., Kelty, M.J., and Ashton, P.M.S. 1997. The practice of silviculture: Applied forest ecology. Ninth edition ed. John Wiley & Sons, Inc., New York.

Sorensen, R., Zinko, U., and Seibert, J. 2006. On the calculation of the topographic wetness index: evaluation of different methods based on field observations. Hydrol. Earth Syst. Sci. **10**(1): 101-112.

Tarboton, D.G. 1997. A new method for the determination of flow directions and upslope areas in grid digital elevation models. Water Resour. Res. **33**(2): 309-319. doi: 10.1029/96wr03137.

Tom, C.H., and Miller, L.D. 1980. Forest site index mapping and modeling. Photogrammetric Engineering and Remote Sensing **46**(12): 1585-1596.

Ung, C.H., Bernier, P.Y., Raulier, F., Fournier, R.A., Lambert, M.C., and Regniere, J. 2001. Biophysical site indices for shade tolerant and intolerant boreal species. For. Sci. **47**(1): 83-95.

Van Cleve, K., Dyrness, C.T., Viereck, L.A., Fox, J., Chapin, F.S., and Oechel, W. 1983. Taiga ecosystems in interior Alaska. Bioscience **33**(1): 39-44. doi: 10.2307/1309243.

Wang, G.G., and Klinka, K. 1996. Use of synoptic variables in predicting white spruce site index. For. Ecol. Manag. **80**(1-3): 95-105. doi: 10.1016/0378-1127(95)03630-x.

Wang, T., Hamann, A., Spittlehouse, D.L., and Murdock, T.Q. 2011. ClimateWNA—High-Resolution Spatial Climate Data for Western North America. Journal of Applied Meteorology and Climatology **51**(1): 16-29. doi: 10.1175/jamc-d-11-043.1.

Weiskittel, A.R., Crookston, N.L., and Radtke, P.J. 2011. Linking climate, gross primary productivity, and site index across forests of the western United States. Can. J. For. Res. **41**(8): 1710-1721. doi: 10.1139/x11-086.

White, B., Ogilvie, J., Campbell, D.M.H., Hiltz, D., Gauthier, B., Chisholm, H.K., Wen, H.K., Murphy, P.N.C., and Arp, P.A. 2012. Using the cartographic depth-to-water index to locate small streams and associated wet areas across landscapes. Can. Water Resour. J. **37**(4): 333-347. doi: 10.4296/cwrj2011-909.

Yeh, F.C., Chong, D.K.X., and Yang, R.-C. 1995. RAPD variation within and among natural populations of trembling aspen (*Populus tremuloides* Michx.) from Alberta. Journal of Heredity **86**(6): 454-460.

Chapter 5

Synthesis and conclusions

This thesis has focused on exploring the capabilities and limitations of the topographic depth-to-water (DTW; Murphy et al. 2007) index to be used in ecological applications. My central objective was to evaluate the potential to use the DTW index to predict site productivity of trembling aspen growing on boreal mixedwood sites in Alberta. Before attempting to address this objective, I first wanted to investigate if site and soil properties defining site quality can be mapped by the DTW index and other topographic factors (i.e., flow accumulation – FA, slope), as well as if individual tree characteristics revealing tree physiology can be predicted by these topographic indices. Analysing these two components first, I was able to understand the limitations of the DTW index and provide support for a relationship between site index of trembling aspen and the DTW index, and the other terrain attributes. Throughout my thesis, I also examined the DTW algorithm to find the optimal flow initiation area to define flow channels, which are critical to the calculation of the DTW raster.

In Chapter 2, I explored the capability of the DTW index and other terrain attributes to predict site and soil properties. Soil moisture regime, drainage capacity and depth to mottles were the site and soil characteristics meaningfully and significantly related with the topographic indices. Low DTW values indicated soils with shallow depth to mottles and poor drainage, leading to wetter site conditions (i.e., subhygric). Other important site and soil properties (e.g.,

nutrient regime, texture, thickness of organic horizon) were not related with DTW, FA and slope. Model fit statistics indicated that the optimal flow initiation area for the relatively flat landscape of the boreal forest was 2 ha. The three topographic indices were then combined into a model to map soil moisture, while only DTW and FA significantly contributed to the models for drainage and depth to mottles. The model for depth to mottles was the strongest without any bias, whereas the other two had a weaker fit and showed some bias toward the extreme values. Efforts were devoted to preparing expressive figures to help understand the relationship between terrain morphology and the DTW index, as well as the effect of changing flow initiation area.

In Chapter 3, I presented the relationship between individual tree traits and the topographic indices. Carbon isotope ratio in wood of both trembling aspen and white spruce increased with DTW until a certain DTW threshold after which it levelled off. Larger amounts of annual precipitation led to lower carbon isotope ratios, with a stronger effect for trembling aspen than for white spruce. DTW and mean annual precipitation were then used together to explain variation in carbon isotope ratio, showing how a climate factor can be combined with a topographic index to assess water stress in trees. The topography of the aspen site was similar to that of the study areas from Chapter 1, thus a smaller threshold of 1 ha was the optimal flow initiation area. However, a larger catchment of 16 ha was the optimal flow initiation area for the spruce site since it was closer to the foothills and had a steeper slope. Individual tree height and diameter were also related with DTW, following a similar pattern to that of carbon isotope ratio. Since diameter is more strongly influenced by stand structure, its relationship with DTW was weaker than that of height. Slope and FA were not related with carbon isotope ratio, and only height of spruce showed a positive association with terrain slope.

In Chapter 4, I focused on evaluating the potential to use DTW and the other topographic

indices to predict site index of trembling aspen, but first I identified which site and soil attributes control site productivity. Soil moisture and nutrient regime were the strongest factors to predict aspen site index, which combined with a random effect for location accounted for about half of the variation in the data. DTW was the only topographic index to be significantly related with aspen site index, although the model fit was much poorer since the findings from Chapter 2 showed that DTW cannot predict nutrient availability. The optimal flow initiation area to calculate DTW was either 2 or 4 ha, which is consistent with the findings from Chapter 2 and aligns well with the operational choice of 4 ha made by the Government of Alberta. The limited number of locations did not allow us to successfully incorporate climate variables into the model, but this statistical approach easily lends itself to developing a prediction model integrating large scale (i.e., climate) and small scale (i.e., topography) processes.

This research has revealed four important messages:

1) The DTW index is related with soil properties (i.e., depth to mottles, soil moisture regime) directly controlled by water movement in the soil.

2) Site and soil properties (e.g., soil nutrient regime) which are not under direct influence of water movement in the soil cannot be predicted by the DTW index. This might be due to the weak topographic effect on soil formation processes in the boreal landscape and due to the stronger influence of other soil formation factors (e.g., parent material, climate, biota, history).

3) The DTW index captures variation in site conditions responsible for individual tree attributes (i.e., height, carbon isotope ratio). The important limitation is that DTW does not reflect mineral nutrient content, which is as essential as water supply to tree development.

4) Site index is correlated with the DTW index, but the complex interaction of factors and processes defining site quality does not allow prediction of site index solely based on DTW.

Other edaphic, topographic and climatic variables must be considered in order to develop robust models.

5) Optimal flow initiation area to start the flow channels necessary to calculate the DTW index depends on the topography of the area of interest. A smaller catchment area (i.e., 2 or 4 ha) is better suited for the relatively flat boreal landscape, whereas the stronger topographic gradients in the foothills require the use of larger threshold areas (i.e., 12 or 16 ha).

The importance of these results can be emphasized by simply stating that the DTW index is currently available for approximately 30 million ha (over 80%) of forested land in Alberta alone. Moreover, the flow initiation area of 4 ha adopted by the province is very close to what I found in terms of optimal flow initiation area. The province of New Brunswick (Murphy et al. 2007) as well as Sweden (Ågren et al. 2014) have also experimented with this topographic index, increasing its relevance in the context of remotely sensed modelling of the environment. This is another perspective that highlights the significance of this study, particularly considering the vast extent of the boreal forest in Canada and in the world. The remarkable progress of remote sensing technologies has improved the accuracy and availability of topographic and vegetation information, enabling us to develop new ways to harness this rich data in order to augment our capacity to model and predict forest ecosystem processes, especially in light of the highly uncertain future we have managed to bring upon ourselves by deeply impacting the environment of our planet.

The findings presented in this thesis could be applicable to other areas with a similar topography to that of the boreal forest, although the effect of different climate, parent material and vegetation structure on pedogenesis will slightly reduce the relevance of my results. This leads me to suggest a number of areas that require further research. One path would be to explore

the ecological applications of the DTW index in areas with different terrain morphology, or test it in areas with similar topography but contrasting climate and vegetation. I consider that some more work is necessary to fully understand to what extent the DTW index predicts physiological processes in trees. Instantaneous physiological traits (e.g., photosynthesis and transpiration rate, stomatal conductance) and long-term measurements (e.g., chlorophyll fluorescence) can be collected, or anatomical and morphological features of leaves that integrate an entire season can be used to reveal what aspect of tree physiology the DTW index influences. This would allow a more sound extension of the DTW index applications into analysing vegetation composition change under topographic gradients or identifying the ecological niche of tree species, as was shown with the topographic wetness index (Petroselli et al. 2013).

Another research path could be focused on how the DTW index can be employed to predict stand level characteristics (e.g., density, height, composition, productivity, leaf area index). However, this is, as this study has suggested, a difficult task to accomplish since the DTW index does not integrate all the environmental and other factors influencing stand structure and development. Additional edaphic—from soil maps as in Iverson et al. (1997)—and climate variables must be incorporated in order for these models to make accurate predictions at relevant scales, both small (i.e., stand) and large (i.e., regional).

Topographic indices determined from accurate digital elevation models represent the most cost effective method to obtain information about soil properties and characteristics of the vegetation for extensive areas. However, I agree with Moore et al. (1993) when they state that such topographic indices cannot be expected to entirely capture the complex and highly variable nature of soil properties, which together with climate, species autoecology, and stand history control the even more complex and variable structure of the forest.

Literature cited

Ågren, A.M., Lidberg, W., Strömgren, M., Ogilvie, J., and Arp, P.A. 2014. Evaluating digital terrain indices for soil wetness mapping – a Swedish case study. Hydrol. Earth Syst. Sci. **18**(9): 3623-3634. doi: 10.5194/hess-18-3623-2014.

Iverson, L.R., Dale, M.E., Scott, C.T., and Prasad, A. 1997. A GIS-derived integrated moisture index to predict forest composition and productivity of Ohio forests (USA). Landsc. Ecol. **12**(5): 331-348. doi: 10.1023/a:1007989813501.

Moore, I.D., Gessler, P.E., Nielsen, G.A., and Peterson, G.A. 1993. Soil attribute prediction using terrain analysis. Soil Sci. Soc. Am. J. **57**(2): 443-452. doi: 10.2136/sssaj1993.03615995005700020026x.

Murphy, P.N.C., Ogilvie, J., Connor, K., and Arpl, P.A. 2007. Mapping wetlands: A comparison of two different approaches for New Brunswick, Canada. Wetlands **27**(4): 846-854. doi: 10.1672/0277-5212(2007)27[846:mwacot]2.0.co;2.

Petroselli, A., Vessella, F., Cavagnuolo, L., Piovesan, G., and Schirone, B. 2013. Ecological behavior of *Quercus suber* and *Quercus ilex* inferred by topographic wetness index (TWI). Trees-Struct. Funct. **27**(5): 1201-1215. doi: 10.1007/s00468-013-0869-x.

Bibliography

Adams, H.R., Barnard, H.R., and Loomis, A.K. 2014. Topography alters tree growth-climate relationships in a semi-arid forested catchment. Ecosphere **5**(11). doi: 10.1890/es14-00296.1.

AESRD. 2005. Natural regions and subregions of Alberta. Alberta Sustainable Resource Development http://www.albertaparks.ca/albertaparksca/library/downloadable-data-sets.aspx, Edmonton, AB.

AESRD. 2011. Alberta Vegetation Inventory (AVI) Crown Polygons. Alberta Environment and Sustainable Resource Development, Government of Alberta.

Ågren, A.M., Lidberg, W., Strömgren, M., Ogilvie, J., and Arp, P.A. 2014. Evaluating digital terrain indices for soil wetness mapping – a Swedish case study. Hydrol. Earth Syst. Sci. **18**(9): 3623-3634. doi: 10.5194/hess-18-3623-2014.

Allen, R.B., Peet, R.K., and Baker, W.L. 1991. Gradient analysis of latitudinal variation in Southern Rocky Mountain forests. J. Biogeogr. **18**(2): 123-139. doi: 10.2307/2845287.

Assmann, E. 1970. The principles of forest yield study: studies in the organic production, structure, increment and yield of forest stands. Pergamon Press, Oxford.

Barnes, B.V., Zak, D.R., Denton, S.R., and Spurr, S.H. 1998. Forest ecology. 4th ed. John Wiley & Sons, Inc.

Beckingham, J.D., and Archibald, J.H. 1996. Field guide to ecosites of northern Alberta. North. For. Cent., Edmonton, AB.

Berry, J.A. 1988. Studies of mechanisms affecting the fractionation of carbon isotopes in photosynthesis. *In* Stable isotopes in ecological research. *Edited by* P.W. Rundel, J. R. Ehleringer and K. A. Nagy. pp. 82-94.

Beven, K.J., and Kirkby, M.J. 1979. A physically based, variable contributing area model of

basin hydrology. Hydrol. Sci. Bul. **24**(1): 43-69. doi: 10.1080/02626667909491834.

Bigras, F.J. 2005. Photosynthetic response of white spruce families to drought stress. New For. **29**(2): 135-148. doi: 10.1007/s11056-005-0245-9.

Bladon, K.D., Silins, U., Landhausser, S.M., Messier, C., and Lieffers, V.J. 2007. Carbon isotope discrimination and water stress in trembling aspen following variable retention harvesting. Tree Physiol. **27**(7): 1065-1071.

Bokalo, M., Comeau, P.G., and Titus, S.J. 2007. Early development of tended mixtures of aspen and spruce in western Canadian boreal forests. For. Ecol. Manag. **242**(2-3): 175-184. doi: 10.1016/j.foreco.2007.01.038.

Bokalo, M., Stadt, K.J., Comeau, P.G., and Titus, S.J. 2013. The validation of the Mixedwood Growth Model (MGM) for use in forest management decision making. Forests **4**(1): 1-27. doi: 10.3390/f4010001.

Bontemps, J.-D., and Bouriaud, O. 2014. Predictive approaches to forest site productivity: recent trends, challenges and future perspectives. Forestry **87**(1): 109-128. doi: 10.1093/forestry/cpt034.

Brubaker, S.C., Jones, A.J., Lewis, D.T., and Frank, K. 1993. Soil properties associated with landscape position. Soil Sci. Soc. Am. J. **57**(1): 235-239.

Buchmann, N., Kao, W.Y., and Ehleringer, J. 1997. Influence of stand structure on carbon-13 of vegetation, soils, and canopy air within deciduous and evergreen forests in Utah, United States. Oecologia **110**(1): 109-119. doi: 10.1007/s004420050139.

Burger, J.A. 2009. Management effects on growth, production and sustainability of managed forest ecosystems: Past trends and future directions. For. Ecol. Manag. **258**(10): 2335-2346. doi: 10.1016/j.foreco.2009.03.015.

Burgess, S.S.O., Adams, M.A., Turner, N.C., and Ong, C.K. 1998. The redistribution of soil water by tree root systems. Oecologia **115**(3): 306-311. doi: 10.1007/s004420050521.

Burns, R.M., and Honkala, B.H. 1990. Silvics of North America: 1. Conifers; 2. Hardwoods.

U.S. Dept. of Agriculture, Forest Service, Washington, D.C.

Burt, T.P., and Butcher, D.P. 1985. Topographic controls of soil moisture distributions. J. Soil Sci. **36**(3): 469-486.

Byun, J.G., Lee, W.K., Kim, M., Kwak, D.A., Kwak, H., Park, T., Byun, W.H., Son, Y., Choi, J.K., Lee, Y.J., Saborowski, J., Chung, D.J., and Jung, J.H. 2013. Radial growth response of Pinus densiflora and Quercus spp. to topographic and climatic factors in South Korea. Journal of Plant Ecology **6**(5): 380-392. doi: 10.1093/jpe/rtt001.

Campbell, D.M.H., White, B., and Arp, P.A. 2013. Modeling and mapping soil resistance to penetration and rutting using LiDAR-derived digital elevation data. J. Soil Water Conserv. **68**(6): 460-473. doi: 10.2489/jswc.68.6.460.

Chen, H.Y.H., Klinka, K., and Kabzems, R.D. 1998. Site index, site quality, and foliar nutrients of trembling aspen: relationships and predictions. Can. J. For. Res. **28**(12): 1743-1755. doi: 10.1139/cjfr-28-12-1743.

Chen, H.Y.H., Krestov, P.V., and Klinka, K. 2002. Trembling aspen site index in relation to environmental measures of site quality at two spatial scales. Can. J. For. Res. **32**(1): 112-119. doi: 10.1139/x01-179.

Chen, H.Y.H., and Popadiouk, R.V. 2002. Dynamics of North American boreal mixedwoods. Environmental Reviews **10**(3): 137-166. doi: 10.1139/a02-007.

Cox, D.R., and Snell, E.J. 1989. The analysis of binary data. 2nd ed. Chapman and Hall, London. pp. 208-209.

Daniel, T.W., Helms, J.A., and Baker, F.S. 1979. Principles of Silviculture. 2nd ed. ed. McGraw-Hill, New York, N.Y. pp. 186-187.

Ehara, H., Matsue, K., Shuin, Y., Aizawa, M., and Ohkubo, T. 2009. Validity of height estimation of Hinoki cypress using soil moisture indices based on the digital terrain model in Utsunomiya University Forests at Funyu. Bul. Utsunomiya Univ. For.(45): 9-16.

Farquhar, G.D., Ehleringer, J.R., and Hubick, K.T. 1989. Carbon isotope discrimination and photosyntehsis. Annu. Rev. Plant Physiol. Plant Molec. Biol. **40**: 503-537. doi: 10.1146/annurev.arplant.40.1.503.

Farquhar, G.D., Oleary, M.H., and Berry, J.A. 1982. On the relationship between carbon isotope discrimination and the inter-cellular carbon dioxide concentration in leaves. Aust. J. Plant Physiol. **9**(2): 121-137.

Francey, R.J., and Farquhar, G.D. 1982. An explanation of 13C/12C variations in tree rings. Nature **297**(5861): 28-31.

Gale, M.R., Grigal, D.F., and Harding, R.B. 1991. Soil productivity index: predictions of site quality for white spruce plantations. Soil Sci. Soc. Am. J. **55**(6): 1701-1708. doi: 10.2136/sssaj1991.03615995005500060033x.

Garten, C.T., and Taylor, G.E. 1992. Foliar delta C-13 within a temperate deciduous forest - spatial, temporal, and species sources of variation. Oecologia **90**(1): 1-7. doi: 10.1007/bf00317801.

Gessler, P.E., Chadwick, O.A., Chamran, F., Althouse, L., and Holmes, K. 2000. Modeling soil-landscape and ecosystem properties using terrain attributes. Soil Sci. Soc. Am. J. **64**(6): 2046-2056.

Guntner, A., Seibert, J., and Uhlenbrook, S. 2004. Modeling spatial patterns of saturated areas: An evaluation of different terrain indices. Water Resour. Res. **40**(5). doi: 10.1029/2003wr002864.

Hanba, Y.T., Noma, N., and Umeki, K. 2000. Relationship between leaf characteristics, tree sizes and species distribution along a slope in a warm temperate forest. Ecological Research **15**(4): 393-403. doi: 10.1046/j.1440-1703.2000.00360.x.

Hansen, J., Sato, M., Ruedy, R., Lo, K., Lea, D.W., and Medina-Elizade, M. 2006. Global temperature change. Proceedings of the National Academy of Sciences **103**(39): 14288-14293. doi: 10.1073/pnas.0606291103.

Hauessler, S., and Coates, K.D. 1986. Autecological characteristics of selected species that compete with conifers in British Columbia: a literature review. Land management report no. 33, Ministry of Forests, Victoria, B.C. p. 181.

Hiltz, D., Gould, J., White, B., Ogilvie, J., and Arp, P. 2012. Modeling and mapping vegetation type by soil moisture regime across boreal landscapes. *In* Restoration and reclamation of boreal ecosystems: Attaining sustainable development. Cambridge Univ. Press, New York, NY. pp. 56-75.

Hodgson, M.E., Jensen, J.R., Schmidt, L., Schill, S., and Davis, B. 2003. An evaluation of LIDAR- and IFSAR-derived digital elevation models in leaf-on conditions with USGS Level 1 and Level 2 DEMs. Remote Sens. Environ. **84**(2): 295-308. doi: 10.1016/s0034-4257(02)00114-1.

Hogg, E.H. 1997. Temporal scaling of moisture and the forest-grassland boundary in western Canada. Agric. For. Meteorol. **84**(1-2): 115-122. doi: 10.1016/s0168-1923(96)02380-5.

Hogg, E.H., Brandt, J.P., and Michaellian, M. 2008. Impacts of a regional drought on the productivity, dieback, and biomass of western Canadian aspen forests. Can. J. For. Res. **38**(6): 1373-1384. doi: 10.1139/x08-001.

Hogg, E.H., and Lieffers, V.J. 1991. The impact of *Calamagrostis canadensis* on soil thermal regimes after logging in northern Alberta. Can. J. For. Res. **21**(3): 387-394. doi: 10.1139/x91-048.

Holmgren, P. 1994. Topographic and geochemical influence on the forest site quality, with respect to *Pinus sylvestrys* and *Picea abies* in Sweden. Scand. J. For. Res. **9**(1): 75-82. doi: 10.1080/02827589409382815.

Huang, S.M., Meng, S.X., and Yang, Y.Q. 2009. A growth and yield projection system (GYPSY) for natural and post-harvest stands in Alberta. Alberta Sustainable Resource Development.

Husch, B., Beers, T.W., and Kershaw Jr., J.A. 2003. Forest mensuration. 4th ed. John Wiley & Sons, Inc., Hoboken, New Jersey.

Iverson, L.R., Dale, M.E., Scott, C.T., and Prasad, A. 1997. A GIS-derived integrated moisture index to predict forest composition and productivity of Ohio forests (USA). Landsc. Ecol. **12**(5): 331-348. doi: 10.1023/a:1007989813501.

Iverson, L.R., Prasad, A., and Rebbeck, J. 2004. A comparison of the integrated moisture index and the topographic wetness index as related to two years of soil moisture monitoring in Zalenski State Forest, Ohio. *In* 14th Central Hardwoods Forest Conference, Wooster, OH. pp. 515 - 517.

Jenny, H. 1941. Factors of soil formation: a system of quantitative pedology. McGraw-Hill, New York, NY. pp. 11-12.

Johansson, T. 2002. Increment and biomass in 26-to 91-year-old European aspen and some practical implications. Biomass Bioenerg. **23**(4): 245-255. doi: 10.1016/s0961-9534(02)00056-9.

Johnsen, K.H., Flanagan, L.B., Huber, D.A., and Major, J.E. 1999. Genetic variation in growth, carbon isotope discrimination, and foliar N concentration in *Picea mariana*: analyses from a half-diallel mating design using field-grown trees. Can. J. For. Res. **29**(11): 1727-1735. doi: 10.1139/cjfr-29-11-1727.

Kayahara, G.J., Carter, R.E., and Klinka, K. 1995. Site index of western hemlock (*Tsuga heterophylla*) in relation to soil nutrient and foliar chemical measures. For. Ecol. Manag. **74**(1-3): 161-169. doi: 10.1016/0378-1127(94)03493-g.

Kayahara, G.J., Klinka, K., and Schroff, A.C. 1997. The relationship of site index to synoptic estimates of soil moisture and nutrients for western redcedar (*Thuja plicata*) in southern coastal British Columbia. Northwest Sci. **71**(3): 167-173.

Kimmins, J.P. 2004. Forest ecology: a foundation for sustainable forest management and environmental ethics in forestry. 3rd ed. Prentice Hall, Upper Saddle River, NJ. pp. 291-292.

Klinka, K., and Carter, R.E. 1990. Relationships between site index and synoptic environmental-factors in immature coastal Douglas-fir stands. For. Sci. **36**(3): 815-830.

Kopecky, M., and Cizkova, S. 2010. Using topographic wetness index in vegetation ecology: does the algorithm matter? Appl. Veg. Sci. **13**(4): 450-459. doi: 10.1111/j.1654-

109X.2010.01083.x.

Landhausser, S.M., DesRochers, A., and Lieffers, V.J. 2001. A comparison of growth and physiology in *Picea glauca* and *Populus tremuloides* at different soil temperatures. Can. J. For. Res. **31**(11): 1922.

Landhausser, S.M., Silins, U., Lieffers, V., and Liu, W. 2003. Response of *Populus tremuloides*, *Populus balsamifera*, *Betula papyrifera* and *Picea glauca* seedlings to low soil temperature and water-logged soil conditions. Scand. J. For. Res. **18**(5): 391. doi: 10.1080/02827580310015044.

Lang, M., McCarty, G., Oesterling, R., and Yeo, I.Y. 2013. Topographic metrics for improved mapping of forested wetlands. Wetlands **33**(1): 141-155. doi: 10.1007/s13157-012-0359-8.

Lanner, R.M. 1985. On the insensitivity of height growth to spacing. For. Ecol. Manag. **13**(3-4): 143-148. doi: 10.1016/0378-1127(85)90030-1.

Latta, G., Temesgen, H., and Barrett, T.M. 2009. Mapping and imputing potential productivity of Pacific Northwest forests using climate variables. Can. J. For. Res. **39**(6): 1197-1207. doi: 10.1139/x09-046.

Leavitt, S.W. 1993. Seasonal C-13/C-12 changes in tree rings - species and site coherence, and a possible drought influence. Can. J. For. Res. **23**(2): 210-218. doi: 10.1139/x93-028.

Leavitt, S.W., and Long, A. 1984. Sampling strategy for stable carbon isotope analysis of tree rings in pine. Nature **311**(5982): 145-147. doi: 10.1038/311145a0.

Leavitt, S.W., and Long, A. 1986. Stable carbon isotope variability in tree foliage and wood. Ecology **67**(4): 1002-1010. doi: 10.2307/1939823.

Livingston, N.J., Guy, R.D., Sun, Z.J., and Ethier, G.J. 1999. The effects of nitrogen stress on the stable carbon isotope composition, productivity and water use efficiency of white spruce (Picea glauca (Moench) Voss) seedlings. Plant Cell and Environment **22**(3): 281-289. doi: 10.1046/j.1365-3040.1999.00400.x.

Lu, Y., Equiza, M.A., Deng, X., and Tyree, M.T. 2010. Recovery of *Populus tremuloides*

seedlings following severe drought causing total leaf mortality and extreme stem embolism. Physiologia Plantarum **140**(3): 246-257. doi: 10.1111/j.1399-3054.2010.01397.x.

MacCormack, K.E., Atkinson, N., and Lyster, S. 2015. Bedrock topography of Alberta, Canada. Alberta Geological Survey, Edmonton, AB.

Maclean, I.M.D., Bennie, J.J., Scott, A.J., and Wilson, R.J. 2012. A high-resolution model of soil and surface water conditions. Ecol. Model. **237–238**(0): 109-119. doi: 10.1016/j.ecolmodel.2012.03.029.

Maddala, G.S. 1983. Limited-dependent and qualitative variables in econometrics. Cambridge Univ. Press, Cambridge, UK.

Magee, L. 1990. R^2 measures based on wald and likelihood ratio joint significance tests. Am. Stat. **44**(3): 250-253. doi: 10.2307/2685352.

Maillard, P., and Alencar-Silva, T. 2013. A method for delineating riparian forests using region-based image classification and depth-to-water analysis. Int. J. Remote Sens. **34**(22): 7991-8010. doi: 10.1080/01431161.2013.827847.

Major, J. 1951. A functional, factorial approach to plant ecology. Ecology **32**(3): 392-412. doi: 10.2307/1931718.

Martin, J.L., and Gower, S.T. 2006. Boreal mixedwood tree growth on contrasting soils and disturbance types. Can. J. For. Res. **36**(4): 986-995. doi: 10.1139/x05-306.

McKenney, D.W., and Pedlar, J.H. 2003. Spatial models of site index based on climate and soil properties for two boreal tree species in Ontario, Canada. For. Ecol. Manag. **175**(1–3): 497-507. doi: http://dx.doi.org/10.1016/S0378-1127(02)00186-X.

Meinzer, F.C., Rundel, P.W., Goldstein, G., and Sharifi, M.R. 1992. Carbon isotope composition in relation to leaf gas-exchange and environmental conditions in Hawaiian *Metrosideros polymorpha* populations. Oecologia **91**(3): 305-311. doi: 10.1007/bf00317617.

Mitsuda, Y., Ito, S., and Sakamoto, S. 2007. Predicting the site index of sugi plantations from

GIS-derived environmental factors in Miyazaki Prefecture. J. For. Res.-Jpn. **12**(3): 177-186. doi: 10.1007/s10310-007-0004-1.

Monserud, R.A., Huang, S.M., and Yang, Y.Q. 2006. Predicting lodgepole pine site index from climatic parameters in Alberta. For. Chron. **82**(4): 562-571.

Monserud, R.A., and Marshall, J.D. 2001. Time-series analysis of delta C-13 from tree rings. I. Time trends and autocorrelation. Tree Physiol. **21**(15): 1087-1102.

Monserud, R.A., and Rehfeldt, G.E. 1990. Genetic and environmental components of variation of site index in inland Douglas-fir. For. Sci. **36**(1): 1-9.

Moore, I.D., Gessler, P.E., Nielsen, G.A., and Peterson, G.A. 1993. Soil attribute prediction using terrain analysis. Soil Sci. Soc. Am. J. **57**(2): 443-452. doi: 10.2136/sssaj1993.03615995005700020026x.

Moore, I.D., Grayson, R.B., and Ladson, A.R. 1991. Digital terrain modelling: a review of hydrological, geomorphological, and biological applications. Hydrol. Process. **5**(1): 3-30. doi: 10.1002/hyp.3360050103.

Mueller-Dombois, D., and Sims, H.P. 1966. Response of three grasses to two soils and a water table depth gradient. Ecology **47**(4): 644-648. doi: 10.2307/1933946.

Murphy, P.N.C., Ogilvie, J., and Arp, P. 2009. Topographic modelling of soil moisture conditions: a comparison and verification of two models. Eur. J. Soil Sci. **60**(1): 94-109. doi: 10.1111/j.1365-2389.2008.01094.x.

Murphy, P.N.C., Ogilvie, J., Connor, K., and Arpl, P.A. 2007. Mapping wetlands: A comparison of two different approaches for New Brunswick, Canada. Wetlands **27**(4): 846-854. doi: 10.1672/0277-5212(2007)27[846:mwacot]2.0.co;2.

Murphy, P.N.C., Ogilvie, J., Meng, F.R., White, B., Bhatti, J.S., and Arp, P.A. 2011. Modelling and mapping topographic variations in forest soils at high resolution: A case study. Ecol. Model. **222**(14): 2314-2332. doi: 10.1016/j.ecolmodel.2011.01.003.

Nagelkerke, N.J.D. 1991. A note on a general definition of the coefficient of determination. Biometrika **78**(3): 691-692. doi: 10.1093/biomet/78.3.691.

Niinemets, U., Cescatti, A., Lukjanova, A., Tobias, M., and Truus, L. 2002. Modification of light-acclimation of Pinus sylvestris shoot architecture by site fertility. Agric. For. Meteorol. **111**(2): 121-140. doi: 10.1016/s0168-1923(02)00011-4.

O'Callaghan, J.F., and Mark, D.M. 1984. The extraction of drainage networks from digital elevation data. Comput. Vision Graph. **28**(3): 323-344. doi: 10.1016/s0734-189x(84)80011-0.

Oliver, C.D., and Larson, B.C. 1996. Forest stand dynamics. Update edition ed. John Wiley & Sons, Inc., New York.

Osika, D.E., Stadt, K.J., Comeau, P.G., and MacIsaac, D.A. 2013. Sixty-year effects of deciduous removal on white spruce height growth and site index in the Western Boreal. Can. J. For. Res. **43**(2): 139-148. doi: 10.1139/cjfr-2012-0169.

Pare, D., Bergeron, Y., and Longpre, M.H. 2001. Potential productivity of aspen cohorts originating from fire, harvesting, and tree-fall gaps on two deposit types in northwestern Quebec. Can. J. For. Res. **31**(6): 1067-1073. doi: 10.1139/cjfr-31-6-1067.

Petroselli, A., Vessella, F., Cavagnuolo, L., Piovesan, G., and Schirone, B. 2013. Ecological behavior of *Quercus suber* and *Quercus ilex* inferred by topographic wetness index (TWI). Trees-Struct. Funct. **27**(5): 1201-1215. doi: 10.1007/s00468-013-0869-x.

Pinheiro, J.C., and Bates, D.M. 1995. Model building for nonlinear mixed-effects models. University of Wisconsin–Madison. 91.

Pinheiro, J.C., and Bates, D.M. 2000. Mixed-effects models in S and S-PLUS. Springer-Verlag, New York, NY. pp. 57-96; 201-225; 305-336.

Pinheiro, J.C., Bates, D.M., DebRoy, S., Sarkar, D., and Team, R.C. 2015. nlme: Linear and nonlinear mixed effects models. *In* http://CRAN.R-project.org/package=nlme.

Pinno, B.D., Pare, D., Guindon, L., and Belanger, N. 2009. Predicting productivity of trembling

aspen in the Boreal Shield ecozone of Quebec using different sources of soil and site information. For. Ecol. Manag. **257**(3): 782-789. doi: 10.1016/j.foreco.2008.09.058.

Pitt, D.G., Comeau, P.G., Parker, W.C., MacIsaac, D., McPherson, S., Hoepting, M.K., Stinson, A., and Mihajlovich, M. 2010. Early vegetation control for the regeneration of a single-cohort, intimate mixture of white spruce and trembling aspen on upland boreal sites. Can. J. For. Res. **40**(3): 549-564. doi: 10.1139/x10-012.

R Core Team. 2015. *R: A language and environment for statistical computing*. R Foundation for Statistical Computing, Vienna, Austria.

Roden, J.S., Johnstone, J.A., and Dawson, T.E. 2011. Regional and watershed-scale coherence in the stable-oxygen and cabon isotope ratio time series in tree rings of coast redwood (*Sequoia sempervirens*). Tree-Ring Research **67**(2): 71-86.

Schulze, E.D., Williams, R.J., Farquhar, G.D., Schulze, W., Langridge, J., Miller, J.M., and Walker, B.H. 1998. Carbon and nitrogen isotope discrimination and nitrogen nutrition of trees along a rainfall gradient in northern Australia. Aust. J. Plant Physiol. **25**(4): 413-425.

Seibert, J., Stendahl, J., and Sorensen, R. 2007. Topographical influences on soil properties in boreal forests. Geoderma **141**(1-2): 139-148. doi: 10.1016/j.geoderma.2007.05.013.

Sharma, R.P., Brunner, A., and Eid, T. 2012. Site index prediction from site and climate variables for Norway spruce and Scots pine in Norway. Scand. J. For. Res. **27**(7): 619-636. doi: 10.1080/02827581.2012.685749.

Silim, S.N., Guy, R.D., Patterson, T.B., and Livingston, N.J. 2001. Plasticity in water-use efficiency of *Picea sitchensis*, *Picea glauca* and their natural hybrids. Oecologia **128**(3): 317-325.

Skovsgaard, J.P., and Vanclay, J.K. 2008. Forest site productivity: a review of the evolution of dendrometric concepts for even-aged stands. Forestry **81**(1): 13-31. doi: 10.1093/forestry/cpm041.

Smith, D.M., Larson, B.C., Kelty, M.J., and Ashton, P.M.S. 1997. The practice of silviculture:

Applied forest ecology. Ninth edition ed. John Wiley & Sons, Inc., New York.

Sohn, J.A., Gebhardt, T., Ammer, C., Bauhus, J., Haeberle, K.-H., Matyssek, R., and Grams, T.E.E. 2013. Mitigation of drought by thinning: Short-term and long-term effects on growth and physiological performance of Norway spruce (Picea abies). For. Ecol. Manag. **308**: 188-197. doi: 10.1016/j.foreco.2013.07.048.

Sorensen, R., Zinko, U., and Seibert, J. 2006. On the calculation of the topographic wetness index: evaluation of different methods based on field observations. Hydrol. Earth Syst. Sci. **10**(1): 101-112.

Sun, Z.J., Livingston, N.J., Guy, R.D., and Ethier, G.J. 1996. Stable carbon isotopes as indicators of increased water use efficiency and productivity in white spruce (*Picea glauca* (Moench) Voss) seedlings. Plant Cell and Environment **19**(7): 887-894. doi: 10.1111/j.1365-3040.1996.tb00425.x.

Tarboton, D.G. 1997. A new method for the determination of flow directions and upslope areas in grid digital elevation models. Water Resour. Res. **33**(2): 309-319. doi: 10.1029/96wr03137.

Tom, C.H., and Miller, L.D. 1980. Forest site index mapping and modeling. Photogrammetric Engineering and Remote Sensing **46**(12): 1585-1596.

Ung, C.H., Bernier, P.Y., Raulier, F., Fournier, R.A., Lambert, M.C., and Regniere, J. 2001. Biophysical site indices for shade tolerant and intolerant boreal species. For. Sci. **47**(1): 83-95.

Van Cleve, K., Dyrness, C.T., Viereck, L.A., Fox, J., Chapin, F.S., and Oechel, W. 1983. Taiga ecosystems in interior Alaska. Bioscience **33**(1): 39-44. doi: 10.2307/1309243.

Walia, A., Guy, R.D., and White, B. 2010. Carbon isotope discrimination in western hemlock and its relationship to mineral nutrition and growth. Tree Physiol. **30**(6): 728-740. doi: 10.1093/treephys/tpq020.

Wang, G.G., and Klinka, K. 1996. Use of synoptic variables in predicting white spruce site index. For. Ecol. Manag. **80**(1-3): 95-105. doi: 10.1016/0378-1127(95)03630-x.

Wang, T., Hamann, A., Spittlehouse, D.L., and Murdock, T.Q. 2011. ClimateWNA—High-Resolution Spatial Climate Data for Western North America. Journal of Applied Meteorology and Climatology **51**(1): 16-29. doi: 10.1175/jamc-d-11-043.1.

Waring, R.H., and Silvester, W.B. 1994. Variation in foliar delta C-13 values within the crowns of *Pinus radiata* trees. Tree Physiol. **14**(11): 1203-1213.

Warren, C.R., McGrath, J.F., and Adams, M.A. 2001. Water availability and carbon isotope discrimination in conifers. Oecologia **127**(4): 476-486. doi: 10.1007/s004420000609.

Weiskittel, A.R., Crookston, N.L., and Radtke, P.J. 2011. Linking climate, gross primary productivity, and site index across forests of the western United States. Can. J. For. Res. **41**(8): 1710-1721. doi: 10.1139/x11-086.

White, B., Ogilvie, J., Campbell, D.M.H., Hiltz, D., Gauthier, B., Chisholm, H.K., Wen, H.K., Murphy, P.N.C., and Arp, P.A. 2012. Using the cartographic depth-to-water index to locate small streams and associated wet areas across landscapes. Can. Water Resour. J. **37**(4): 333-347. doi: 10.4296/cwrj2011-909.

Yeh, F.C., Chong, D.K.X., and Yang, R.-C. 1995. RAPD variation within and among natural populations of trembling aspen (*Populus tremuloides* Michx.) from Alberta. Journal of Heredity **86**(6): 454-460.

Ziadat, F.M. 2005. Analyzing digital terrain attributes to predict soil attributes for a relatively large area. Soil Sci. Soc. Am. J. **69**(5): 1590-1599. doi: 10.2136/sssaj2003.0264.

Appendices

A.1. R code for SI estimation using the GYPSY models of Huang et al. 2009.

Copy-paste this into R and run it. Play with different `topht` and `age` values. Try `age = 50`.

Aspen

```
SI_Aw <- function(topht,age){
  si0=10          # initial site index value to start the function
  b1=9.908888
  b2=-3.92451
  b3=-0.32778
  b4=0.134376
  repeat{
    x10=1+exp(b1+b2*sqrt(log(1+50))+b3*(log(si0))^2+b4*sqrt(50))
    x20=1+exp(b1+b2*sqrt(log(1+age))+b3*(log(si0))^2+b4*sqrt(50))
    si1=topht*x20/x10
    si0=(si0+si1)/2
    if(abs(si0-si1)<0.00000001){break}
  };si1
}

# Example:
SI_Aw(topht = 10.07500005, age = 21)
```

Spruce

```
SI_Sw <- function(topht,age){
  si0=10
  b1=12.14943
  b2=-3.77051
  b3=-0.28534
  b4=0.165483
  repeat{
    x10=1+exp(b1+b2*sqrt(log(1+50^2))+b3*(log(si0))^2+b4*sqrt(50))
    x20=1+exp(b1+b2*sqrt(log(1+age^2))+b3*(log(si0))^2+b4*sqrt(50))
    si1=topht*x20/x10
    si0=(si0+si1)/2
    if(abs(si0-si1)<0.00000001){break}
  };si1
}

# Example:
SI_Sw(topht = 10.07500005, age = 21)
```

A.2. R code for Eq. 3.3 (p. 58)

Aspen

```
fm5Aw.gnls = gnls(d13C~a1+(a2-a1)*exp(-exp(a3)*DTW_1_3mean)+b*PPT,
            d13CAwLc.dat, a1+a2+a3+b~1, start=c(a1=-24,a2=-25,a3=2,b=-0.01),
            corr=corSymm(form=~1|Tree), na.action=na.omit)
```

Spruce

```
fm5Sw.gnls = gnls(d13C~a1+(a2-a1)*exp(-exp(a3)*DTW_16_3mean)+b*PPT,
            d13CSwLc.dat, list(a1+a2+a3+b~1), start=c(-26,-27,-1,-0.01),
            corr=corSymm(form=~1|Tree), na.action=na.omit)
```

3D Graph (Fig. 3.5)

```
predAwd13C.dat = matrix(nrow=24,ncol=24)

for (i in 1:24) {
   newd13C.dat = data.frame(DTW_1_3mean=rep(0+0.1*(i-1),24),
                                          PPT=seq(330,490,length.out=24))
   predAwd13C.dat[i,] = as.vector(predict(fm5Aw.gnls, newdata=newd13C.dat))
}

nrz = nrow(predAwd13C.dat)
ncz = ncol(predAwd13C.dat)
color = colorRampPalette(c("lightgreen","orange"))(255)
zfacet = predAwd13C.dat[-1,-1] + predAwd13C.dat[-1,-ncz] + predAwd13C.dat[-
nrz,-1] + predAwd13C.dat[-nrz,-ncz]
facetcol = cut(zfacet, 255)

plot.persp = persp(seq(0,2.3,0.1), seq(330,490,length.out=24),
      predAwd13C.dat, xlim=c(0,2.3), ylim=c(330,490), zlim=c(-28.5,-25.5),
      xlab="Depth-to-water (m) at 1 ha", ylab="Mean annual precipitation
      (mm)", zlab="Carbon isotope ratio", theta=215, phi=15, expand=0.5,
      d=15, col=color[facetcol], border=NA, ltheta=35, shade=0.3,
      ticktype="detailed", nticks=4)

predd13C = trans3d(d13CAwLc.dat$DTW_1_3mean[-37], jitter(d13CAwLc.dat$PPT[-
      37],0.4), fitted(fm5Aw.gnls), plot.persp)

points(predd13C, col=rgb(139/255,0,0,0.6),  pch=16)
```

A.3. R code for Eqs. 4.2 and 4.3 (p. 85 and 89)

```
Loc2=SI.gdat$Loc

levels(Loc2)

fmSIsMrsNr.nlme = nlme(SI~a*b1^((SMR3-c1)^2)*b2^((SNR3-c2)^2), SIsmr.gdat,
      a+b1+b2+c1+c2~1, a~1|Loc, start=c(a=20,b1=0.98,b2=0.98,c1=5,c2=3),
      weights=varIdent(form=~1|Loc2))           # Eq. 4.2

fmSIDTW4.nlme = nlme(SI~a*b^((DTW_4_mean-c)^2), SI.gdat, a+b+c~1, a~1|Loc,
      start=c(a=19,b=0.89,c=3),weights=varIdent(form=~1|Loc2))    # Eq. 4.3
```

Graph with 95% CI and PI

```
ci = matrix(nrow=150,ncol=11)
ci[,1] = SI.dat$DTW_4_mean
ci[,2] = as.matrix(fitted(fmSIDTW4.nlme, level=0))
ci[,3] = 0.9966017^((ci[,1]-4.1591873)^2)
ci[,4] = 20.972019*((ci[,1]-4.159187)^2)*(0.9966017^((ci[,1]-4.1591873)^2-1))
ci[,5] = 2*20.9720196*log(0.9966017)*(4.1591873-ci[,1])*(0.9966017^((ci[,1]-
                                                          4.1591873)^2))
X = ci[,3:5]

#confidence interval for E(y)
VarG = diag(X %*% vcov(fmSIDTW4.nlme) %*% t(X))
ci[,6] = qt(0.975,147) * sqrt(VarG)
ci[,7] = ci[,2] - ci[,6]
ci[,8] = ci[,2] + ci[,6]

#prediction interval for y0
VarG = fmSIDTW4.nlme$sigma^2 + diag(X %*% vcov(fmSIDTW4.nlme) %*% t(X))
ci[,9] = qt(0.975,147) * sqrt(VarG)
ci[,10] = ci[,2] - ci[,9]
ci[,11] = ci[,2] + ci[,9]

plot(SI~DTW_4_mean, SI.dat, col=LocColors[Loc], xlab="Depth to water (m)",
ylab="Site index (m)", ylim=c(15,25), pch=c(16,15,17,8,3)[Loc], las=1)

id=order(SI.dat$DTW_4_mean)
lines(SI.dat$DTW_4_mean[id], fitted(fmSIDTW4.nlme,level=0)[id], lwd=2, col=3)
lines(SI.dat$DTW_4_mean[id], ci[,7][id], col=3, lty=2)
lines(SI.dat$DTW_4_mean[id], ci[,8][id], col=3, lty=2)
lines(SI.dat$DTW_4_mean[id], ci[,10][id], col=4, lty=2)
lines(SI.dat$DTW_4_mean[id], ci[,11][id], col=4, lty=2)

legend("bottomright", lty=2, pch=c(16,15,17,8,3),
c("DMI_HC","DMI_PR","JC","SRD","WGP"), col=LocColors, title="Location")
text(c(6,6), c(16.5,16), c(expression(b==0.997),expression(P==0.0122)))
abline(v=4.1591873, h=20.9720196, lty=2)
```